Methods for Determining Tidal Flows & Material Fluxes in Estuarine Cross-Sections

Methods for Determining Tidal Flows & Material Fluxes in Estuarine Cross-sections

Terry M. Hume and Robert G. Bell

Water Quality Centre, Ecosystems Division,
National Institute of Water and Atmospheric Research - NIWAR
(formerly Department of Scientific and Industrial Research -DSIR)
Hamilton, New Zealand

Water Quality Centre Publication No. 22
Hamilton, New Zealand
1993

ABSTRACT: This handbook presents methods for estimating tidal flows and material fluxes through estuarine cross-sections. It covers both theoretical determinations (based on existing data) and field measurements (tidal gaugings). Guidelines on choice of technique, planning surveys, and study site selection are presented. It reviews methods for processing the field data from a tidal gauging to derive estimates of flows, tidal prism, residual currents, material fluxes and tidal exchange ratio, and describes various approaches to presenting the data in plot format. The focus is on measurement techniques adapted for use in New Zealand estuaries. This handbook will be useful to scientists, engineers and technicians.

Keywords: currents; tides; tidal flow; tidal prism; salinity; fluxes; tidal gauging; field measurements; tidal inlets; estuaries; New Zealand

Acknowledgements: We thank Dr Murray Hicks, Allan Singleton, and Prof. Ed Herdendorf for their constructive reviews, and Val Hector for editing the manuscript.

Cover Photo: By Rod Budd

Cataloguing-in-Publication Data

Hume, Terry M.
Methods for determining tidal flows & material fluxes in estuarine cross-sections / by Terry M. Hume and Robert G. Bell - Hamilton, N. Z. : Water Quality Centre, DSIR, 1993.
ISSN 0112-689X; 22 (Water Quality Centre publication No. 22)
ISBN 0-477-02652-4
1. Estuaries - Handbook. I. Bell, Robert G. II. Water Quality Centre (Hamilton, N. Z.) III. Title. IV. Series.

Methods for determining tidal flows & material fluxes in estuarine cross-sections
Terry M. Hume and Robert G. Bell

Published in 1993 by:
Water Quality Centre, Ecosystems Division, National Institute of Water and Atmospheric Research - NIWAR (formerly Department of Scientific and Industrial Research - DSIR)
PO Box 11-115, Hamilton, New Zealand.

Printed by:
Waikato Print, Hamilton

CONTENTS

Chapter 1

INTRODUCTION

In many scientific, engineering and environmental monitoring programmes there is a need to determine tidal flows and material fluxes through estuarine cross-sections. For some studies estimates from existing data will suffice. Other studies will require detailed field measurements of tidal flows and material fluxes, or 'tidal gaugings' as they are commonly known in New Zealand. In many instances the tidal dynamics and transport of material through an estuary are best investigated using one-dimensional (cross-section averaged) or two dimensional (depth-averaged) numerical models. However, even these modelling studies require the collection of good quality data on water levels, tidal flows and material fluxes to calibrate and verify the models, or to provide model boundary conditions.

Field measurements of tidal flows and material fluxes in estuaries are most often carried out at the inlet (or entrance) of an estuary, because the constricted flow path at these locations simplifies the flow patterns. Tidal gaugings commonly use techniques adapted from river gauging methods, for which reliable procedures have been developed. However, estuaries, unlike rivers, typically experience large semi-diurnal or diurnal oscillations in water level, accompanied by reversing current velocities, flows and material fluxes. Furthermore, across an estuarine channel there can be marked lateral and vertical variability in flow speed and direction with change of the tide, as well as stratification (Kjerfve & Proehl 1979). Therefore a detailed understanding of the velocity distribution in the channel cross-section is essential when determining the tidal discharge and flux. Temporal or spatial changes in material concentrations are second order effects, especially in well-mixed estuaries, and these must also be accounted for. Deciding on the number of measurement stations across a channel needed to accurately estimate material fluxes, is a prime consideration (Kjerfve *et al.* 1981). Because the variability of some measured parameters (e.g., velocity) is inherently large, both spatially and/or temporally, the precision of any one observation is often less important than the number of measurement stations and the intensity of sampling.

Correctly selected procedures are a prerequisite for good results. It is also important to employ the best techniques for analysing and presenting the data to optimise its later use. Although reliable procedures for river gauging methods have been documented (e.g., Rantz *et al.* 1982; DVWK 1990), there is no similar comprehensive review or guide to executing these surveys in estuaries. The best review is by Dyer (1979), which focuses on sediment measurements.

This handbook reviews methods of estimating tidal flows and material fluxes through estuarine cross-sections. It combines theoretical knowledge with field experience to describe 'desk top' calculations, field methods and equipment requirements, and various techniques for analysing and presenting data. Scientists, engineers and technicians involved in estuarine field studies will benefit from using this manual.

Chapter 2

ESTUARINE PROCESSES AND THEIR IMPLICATIONS FOR TIDAL GAUGINGS

A basic understanding of the physical processes which operate in estuaries is of help when determining tidal flows and material fluxes in estuaries. This is very much the case in New Zealand where varied geology, oceanography and latitudinal zonation have produced a very diverse range of estuaries, and therefore a wide range of hydrological and sedimentological conditions (Hume & Herdendorf 1988). Because many New Zealand estuaries are shallow, tidal and sometimes wind-driven currents dominate, and the large tidal range to depth ratio results in significant variability in residual currents and in substantial intertidal areas being exposed at low water. Density currents can sometimes be significant, depending on the proximity and flow rate of rivers. With such a wide range of conditions, sampling strategies must be tailored to each individual situation.

What is an Estuary?

An *estuary* is generally defined as "a partially enclosed coastal body of water, which is either permanently or periodically open to the sea, and within which there is measurable variation of salinity due to the mixture of seawater and freshwater derived from land drainage" (Day 1981). The wide variety of estuaries in New Zealand are described and classified in Hume & Herdendorf (1988).

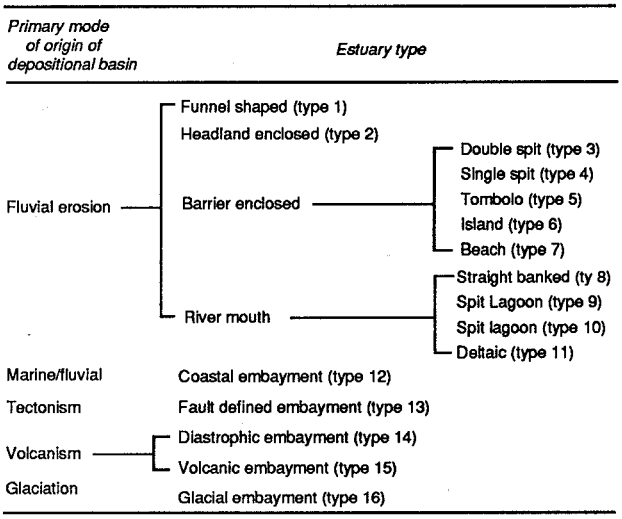

Figure 2.1 Various types of estuaries in New Zealand based on the classification by Hume & Herdendorf (1988).

Their classification (Fig. 2.1) groups estuaries into a variety of types that reflect basin morphology, and catchment and coastal sedimentological and hydrological processes. It is relevant to planning tidal gaugings because similar processes operate in each estuary type. Thus, for instance, measurement techniques found appropriate in a specific Type 1, should therefore be applicable in other Type 1 estuaries.

Tidal Theory and Definitions

The *tide* is a periodic rising and falling of the level of the surface of the sea, caused by the gravitational attraction of the sun and moon on the waters of the rotating earth. The motion depends on the relative positions of the earth, moon and sun at a particular time. *Tidal forcing* is the predominant process governing the dynamic behaviour of estuaries. In the seas around New Zealand the *lunar semi-diurnal (M_2) tide* (period 12.42 hours) is the dominant tide. The *solar semi-diurnal (S_2) tide* (period 12 hours) is much smaller in amplitude, but its movement in and out of phase with the M_2 tide produces the spring-neap tide sequence. *Spring tides* are those which rise highest and fall lowest from the mean level, generating the greatest tidal range. In theory, they occur when the earth, moon and sun are all in line, (i.e., at the time of the full moon and the new moon), when the tidal bulge of the earth's oceans is greatest. In practice, the time interval between the new or full moon, and the occurrence of spring tides around New Zealand, called the age of the tide, varies from 0 hours (at Timaru) to nearly 8 days (at Wellington), but mostly is in the range 1 to 2.5 days (Heath 1985). When the forces exerted by the moon and sun are 90 degrees out of phase and operating at right angles to each other, which occurs at the time of the first and last quarters of the moon, the minimum tidal ranges are produced and *neap tides* occur. Generally, in New Zealand, two spring tides and two neap tides occur each month. Normally, the height of two successive high (HW) or low (LW) tides differs during a lunar day (25 hours). This so-called "daily inequality" is caused by the moon's declination (i.e., the angle between the plane of moon's orbit and the plane of the earth's equator) and may cause the ebb and flood tidal prism to be different.

Tidal streams are a direct effect of the tides. Whereas tides are periodic vertical movements of the water, tidal streams or currents are horizontal movements. The *flood tide* is the period covering the incoming tide or rising water level, and the *ebb tide* the outgoing tide or falling water level. *Slack water* is the interval between the cessation of a tidal stream and its commencement in the opposite direction.

Comprehensive texts on tides include Godin (1972), Forrester (1983) and Pugh (1987), the latter two being the most practical and easily understood handbooks. Specific information on the main astronomical tides around New Zealand e.g., tide amplitude and phase, is published annually in the NZ Nautical Almanac (Marine Division, Ministry of Transport) and is discussed by Heath (1977, 1985).

After even a small amount of field experience it will be apparent that observed tides do not always follow the predictions of tidal theory, and are therefore different from those reported in the tide tables. For instance, high water may not occur at the predicted times and the tide range may differ from that reported in the tide tables, slack water seldom corresponds with HW and LW, and plots of water level against time do not always produce a sinusoidal tidal curve. The theory does not predict these deviations from the norm, which are due to a combination of effects, such as the shape or morphology of the estuary basin, wind stress on the water surface, freshwater inflow, atmospheric changes and outer ocean influences. These effects, which distort the tidal wave as it travels through an estuary, are described below with examples. (Note that the tidal waves we are referring to here are not tsunamis, or giant waves generated by earthquakes, but long period waves with a period corresponding to that of the tide-generating force).

Shallow Water Effects and Morphological Controls on Tides and Flows

When a tidal wave travels up an estuary it is distorted as it encounters shallow water, in a similar, but less dramatic, manner to shoaling swell waves approaching a beach. The distortion comes about because the range of the tide is no longer small compared to the average depth and thus the depth-dependent *celerity*, or speed of travel, of the wave crest is significantly faster than that of the trough.

Shallow water effects are well illustrated by the tides in Otago Harbour which has a narrow channel, flanked by extensive intertidal areas. The overall average depth is 4.5 m at mean high water springs with a 1.8 m tide range in the headwaters. Water level measurements for a spring tide at three sites (0, 12 and 22 km upstream from the entrance) in the harbour (Fig. 2.2) show:

(a) The tide range increasing by 0.3 m as one moves from the mouth to the head of the estuary, but with an accompanying set-up (or superelevation) in local mean tide level (Fig. 2.2). This effect generally increases towards the head of an estuary, until a point is reached where bed friction begins to dominate and then the tide range decreases.
(b) As the tidal wave travels upstream, the rise from LW to HW becomes more abrupt and short-lived i.e., progressively shorter flood tide and longer ebb tide periods upstream of the mouth (Fig. 2.2). In some funnel-shaped estuaries, this abruptness in the rising tide may lead to the creation of a tidal bore (Pugh 1987).
(c) Tides within the harbour no longer synchronising with the ocean tide, causing LW to lag significantly (by 40 minutes) (Fig. 2.2). HW also lags but to a lesser degree (by 15 minutes) due to the higher wave celerity.

Another shallow water effect that occurs in estuaries is the distortion of flows and current velocities resulting from the distortion of the tidal wave and the local set-up of mean tide level. The results of flow distortion can be seen in measurements made at the mouth of Tairua Estuary, Coromandel Peninsula (Fig. 2.3). There the ebb tide flow increases rapidly after HW, then decreases slowly during the latter part of the ebb tide. Another result of flow distortion is that slack tide rarely coincides with HW and LW. This is particularly true around LW when the change from ebb to flood flow can occur up to one or two hours later than LW. At Tairua, for example, slack water lagged LW by 1.2 hours.

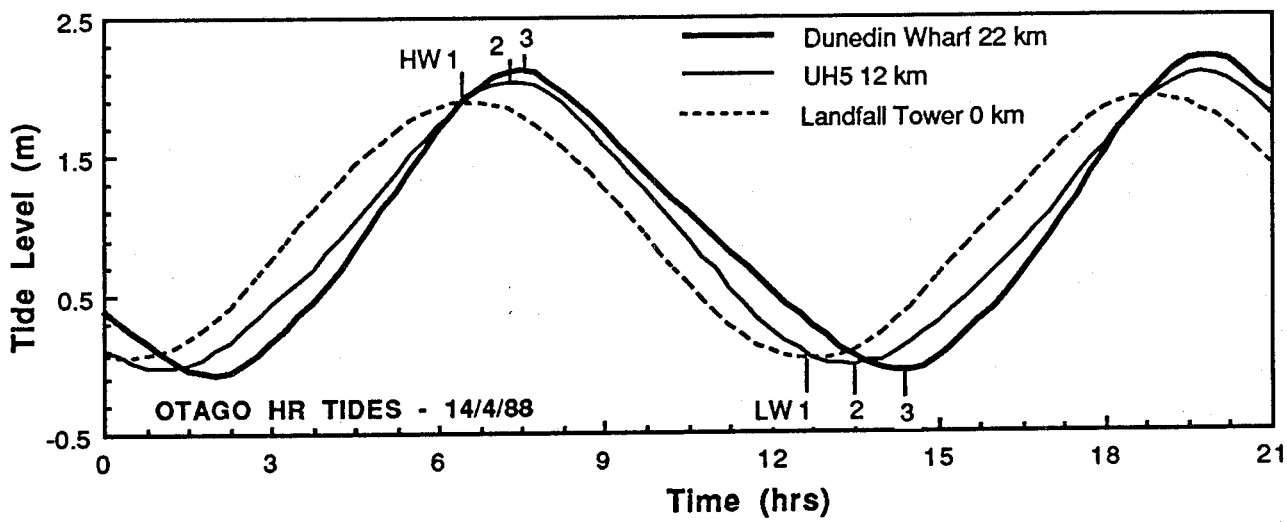

Figure 2.2 Distortion of a spring tide as it travels 22 km up Otago Harbour. Note that the curve is asymmetric and steeper on the leading edge and that the tidal range is greater in the estuary headwaters (Dunedin Wharf) than at the mouth (Landfall Tower).

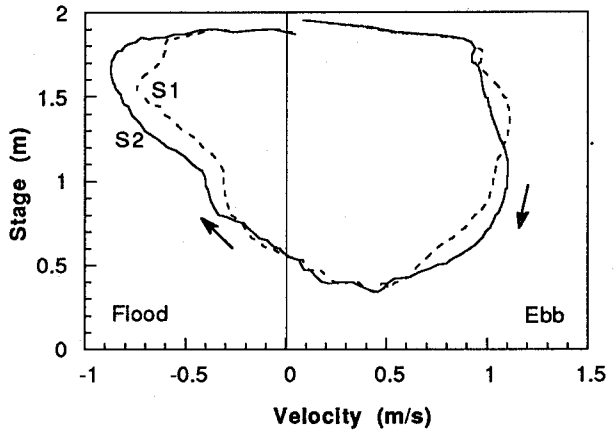

Figure 2.3 Stage height versus depth averaged velocity for two vertical profile sites (S1 and S2) at the entrance to Tairua Harbour, Coromandel.

In addition to the above effects, if the estuary narrows toward the head, the tidal wave energy is further compressed laterally. This effect, called *funnelling*, causes the tide height to increase (Forrester 1983).

Both shallow water and bed morphology effects are well illustrated by water level records from Lucas Creek, a 6 km long tidal creek in the headwaters of Waitemata Harbour (Fig. 2.4). Here, as in the Otago Harbour example, shallow water effects cause the tidal range to be 0.25 m greater at the entrance to Lucas Creek (L18), than it is 14 km downstream at Queen's Wharf at the mouth of the Waitemata Harbour. The most striking feature of the tide curves, however, is that while LW level does not fall as far in the headwaters as it does at the entrance to the creek, the level of high tide increases up Lucas Creek. This effect is caused by bedrock sills in the creek upstream of the water level measurement stations. These sills pond the waters at the lower stages of the tide, inhibiting the ebb tide drainage and resulting in a stationary water level for a period over low tide.

In estuaries basin morphometry can result in marked spatial and temporal variations in current velocity occurring throughout a tidal cycle. This occurs because, as the tide rises and falls, the wetted surface in the cross-section, and therefore the area of the flow cross-section, changes. Hence, a wide shallow tidal reach at HW may change to a narrow incised channel at LW, with an accompanying increase in current velocity. This effect can distort the discharge signature. For example, in the Tamaki Estuary, the neap tide inflow shows a bi-modal or double peak, in contrast to the spring tide inflow which shows a single peak (Fig. 2.5). The neap tide (tide range 1.9 m) bi-modal pattern, may occur as flows, peaking at lower water levels, are confined to the main channels. This is followed by a period of slower flow when inflow must overcome the increasing friction as the flood flow spills out of the channel and over the intertidal flats, followed by a further period of high discharge as the water over the intertidal area deepens. On spring tides (tide range 3.5 m) the bi-modal pattern is masked by the more rapid changes in tidal elevation and hence greater energy head differences.

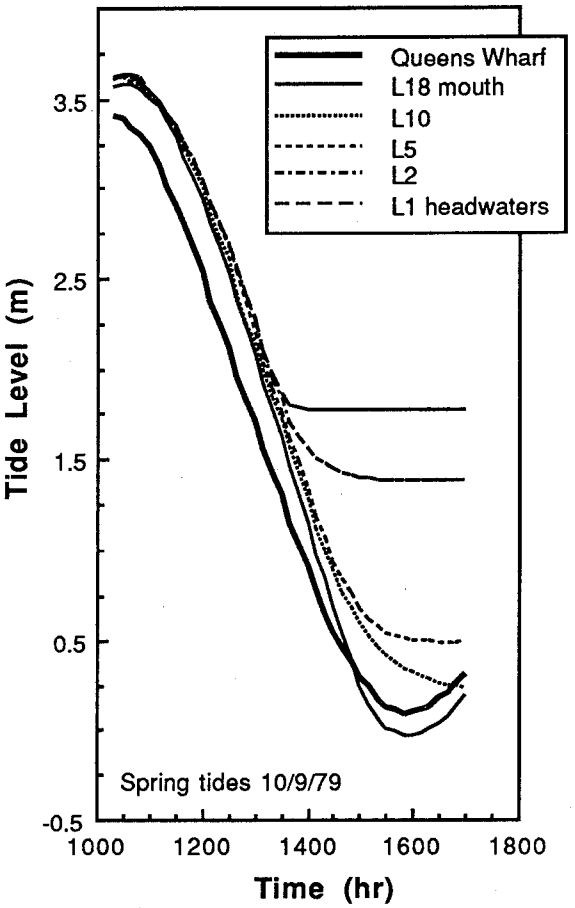

Figure 2.4 Tide levels (spring tide conditions) recorded at the entrance to Waitemata Harbour, and at various positions (L1-L18) along Lucas Creek in the upper harbour (after Johnston 1980).

The basin morphology of the lower part of an estuary can alter the flow patterns upstream. In the Outfall Channel of the Ahuriri Estuary at Napier, for instance, gravel bars downstream greatly modify the water levels and discharge in the Channel by ponding the ebb tide drainage (Fig. 2.6) (Hume *et al.* 1990). On the open coast the tidal range is 1.39 m and the tidal duration 6.25 hours (flood) and 6.3 hours (ebb). In comparison, 2.4 km upstream of the coast in the Outfall Channel, the tide range is only 0.48 m and the tide duration c.3 hour (flood) and c.9.5 hour (ebb), with most of the water level drop occurring in the first 3 hours after high tide. The substantial difference in tidal characteristics between the Outfall Channel and the open coast is a response to morphological factors and frictional dissipation. The estuary bed of the Channel is much higher than the sea bed at the mouth of Ahuriri Estuary.

Between the coast and the Channel a series of rapids formed in the old river gravel fan prevents flood tide flow into the Channel until the water level rises about 0.9 m above LW. When the incoming tide tops the

level of the gravel fan, about 3.5 hours after low tide on the open coast, the water level in the Outfall Channel rises about 4 cm in 0.5 hour, but there is no inflow due to a back-water effect on the ebb tide drainage.

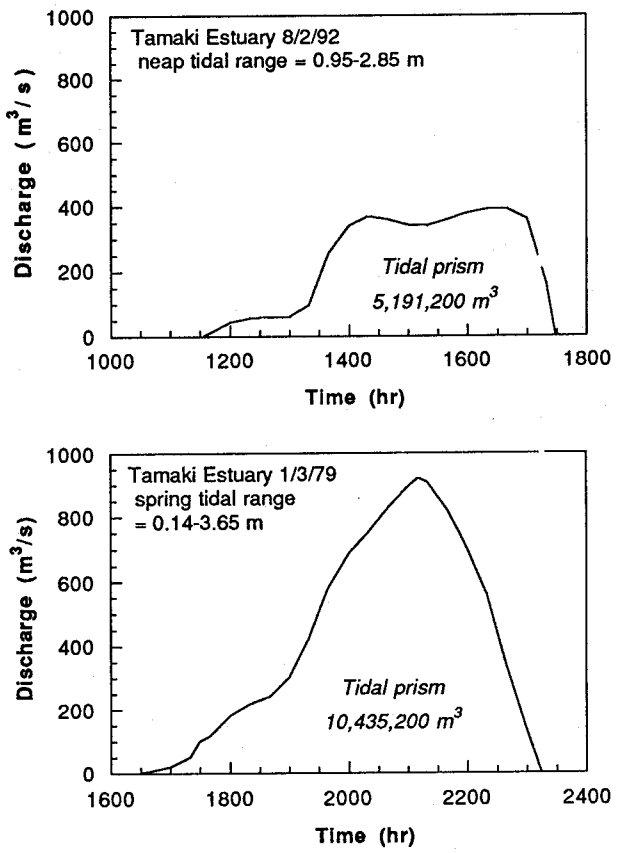

Figure 2.5 Comparison of neap and spring flood tide discharge curves in the Tamaki Estuary, Auckland (after Hume 1979a).

When inflow begins, it corresponds with mid tide on the open coast and the time when the rate of rise of water level on the open coast is greatest. Hence tide flow into the Channel is initially very swift. However the flow is short lived, and inflow stops about 2 hours after high tide on the open coast (Fig. 2.6).

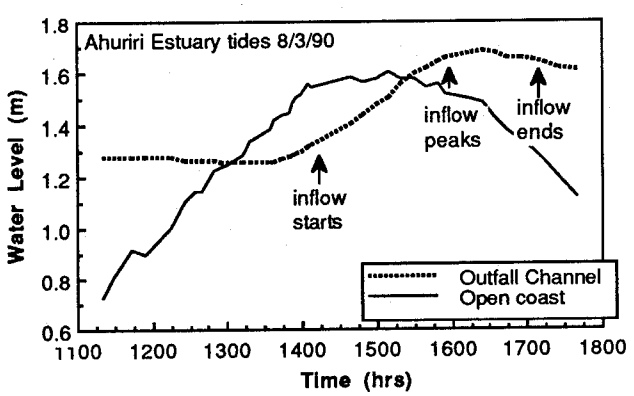

Figure 2.6 Comparison of tide levels and flood tide flow characteristics in the Outfall Channel, Ahuriri Estuary, Napier.

Basin morphometry can result in separation of tidal flow paths. Because tidal currents are cyclic and bi directional, the main flow path on the flood tide may be different to that on the ebb, particularly in the vicinity of the estuary mouth or at bends in the channel. In these situations flood and ebb channels are often separated by shoals.

The distortion or nonlinear interactions of astronomical tides in shallow water can be represented mathematically by *over tides*. Overtides are shallow water constituents for which the angular speeds are multiples, sums or differences of the main astronomical tide constituents. The main shallow water constituent is the quarter-diurnal M_4 tide (period 6.2 hours), which is the first overtide harmonic of the M_2 astronomical tide. Mathematical representation of overtides permits the water level fluctuations to be modelled and predicted.

The effects of shallow water, estuary morphology and freshwater runoff on tides and flows have the following implications for tidal measurement and computations:
(a) Tide times and ranges can vary from the predictions. Tidal discharge may begin earlier or later than expected. You must allow for this when planning field work.
(b) In the headwaters of estuaries shallow water effects distort the tidal wave over relatively short distances. Therefore it is important to have the water level measurement site in close proximity to the gauging site.
(c) Slack water does not always coincide with the times of high and low water, and needs to be recorded separately. It is important to know these times when planning the start/finish time of a gauging and also later for calculating the discharge.
(d) The tidal peak discharge for spring and neap tides may occur at different times. Therefore when measurements are made over a part tidal cycle only, be careful to ensure that the measurement period covers peak discharge.
(e) Marked spatial and temporal variations in current velocity occur throughout a tidal cycle in estuaries. Flow distribution across a channel may vary from the ebb to the flood tide as flow is directed along ebb- or flood-dominated channels. Studying bathymetric charts and aerial photographs taken at low tide will help decide whether this will happen and aid in planning measurement strategies. It is important to choose a measurement site that is representative of the situation.
(f) Water levels and current flows at a gauging site can be markedly influenced by estuary bed morphology up- and down-stream. This can result in sluggish flows, such as where the bed level drops rapidly and conversely rapid increases in flows may occur. It is useful if these effects can be anticipated because measurement strategies may need to be adjusted to account for them.
(g) The degree of asymmetry of tidal flows in estuaries has important consequences for sediment transport and net material fluxes through the tidal inlet. Any process which depends non-linearly on water speed, or has a threshold of operation (e.g., sediment transport), may have a non-zero mean (or net value) when averaged over

a tidal cycle, even though the mean flow through the cross-section is zero (Heath 1981).

River Inflow

In most New Zealand estuaries the river inflow is small and the hydrology is tidally dominated for most of the time. However, during floods it is common for water levels to increase dramatically for several hours and for river flows to dominate the hydrodynamics. This is clearly illustrated in Fig. 2.7 by the water level record measured 1 km upstream of the tidal inlet in Tairua Estuary (Coromandel). The record shows the normal spring-neap-spring tidal cycle. When a river flood elevated the daily mean water level by nearly 0.8 m on 12-13 April 1981, the tidal signal was markedly dampened and the residual or tidally-averaged current velocity became strongly directed seawards at the mouth of the estuary.

Appreciable freshwater input distorts the tidal wave and modifies its timing. This effect has been modelled in Maketu Estuary in the Bay of Plenty in order to assess the impact of diverting the Kaituna River into the estuary (Kingston Reynolds Thom & Allardice 1986). Fig. 2.8 shows the effect on the hydrograph of increasing the freshwater inflow from its existing <1 m^3/s to 30 m^3/s. The incoming tidal flow decreases from 82 to 59 m^3/s, and ebb flow increases from 62 to 75 m^3/s. In addition the duration of the flood tide is shortened, and the duration of the ebb tide increased.

Estuaries can be broadly classified into three hydrodynamic types on the basis of the relative magnitudes of river and tidal flow (Pritchard 1967): (a) highly stratified estuaries (river-dominated); (b) partially mixed estuaries; and (c) well mixed estuaries (tide-dominated). Of course, an estuary may change its character or 'type' for a short duration (as the Tairua estuary exhibited during a river flood, Fig. 2.7) or over longer seasonal periods (e.g., rainy seasons). Density gradients generated by vertical and longitudinal changes in salinity, and to a lesser extent temperature, have a major effect on current velocities both vertically and laterally, particularly for partially mixed estuaries (Fischer *et al.* 1979). Velocity and salinity profiles for the Wairau River, Marlborough, described in Hume & Williams (1981) show the effect of vertical stratification (Fig. 2.9). The graphs show that at half ebb tide (1325 hrs) the water column is stratified, with the more saline ocean water immobilised near the bed of the river under the less dense river outflow.

Later (1620 hrs) on the ebb tide the water column is less stratified and outflow increases near the bed as the tidal influence wanes. At the tidal inlet of well-mixed estuaries, it is quite common to observe a short period around LW when a degree of stratification occurs, with denser sea water creeping slowly upstream near the channel bed, while the less dense surface waters continue to flow seawards across the top. Brief periods of oppositely directed currents at each side of the cross-section may also occur at periods around both slack tides, particularly for wide mouthed estuaries.

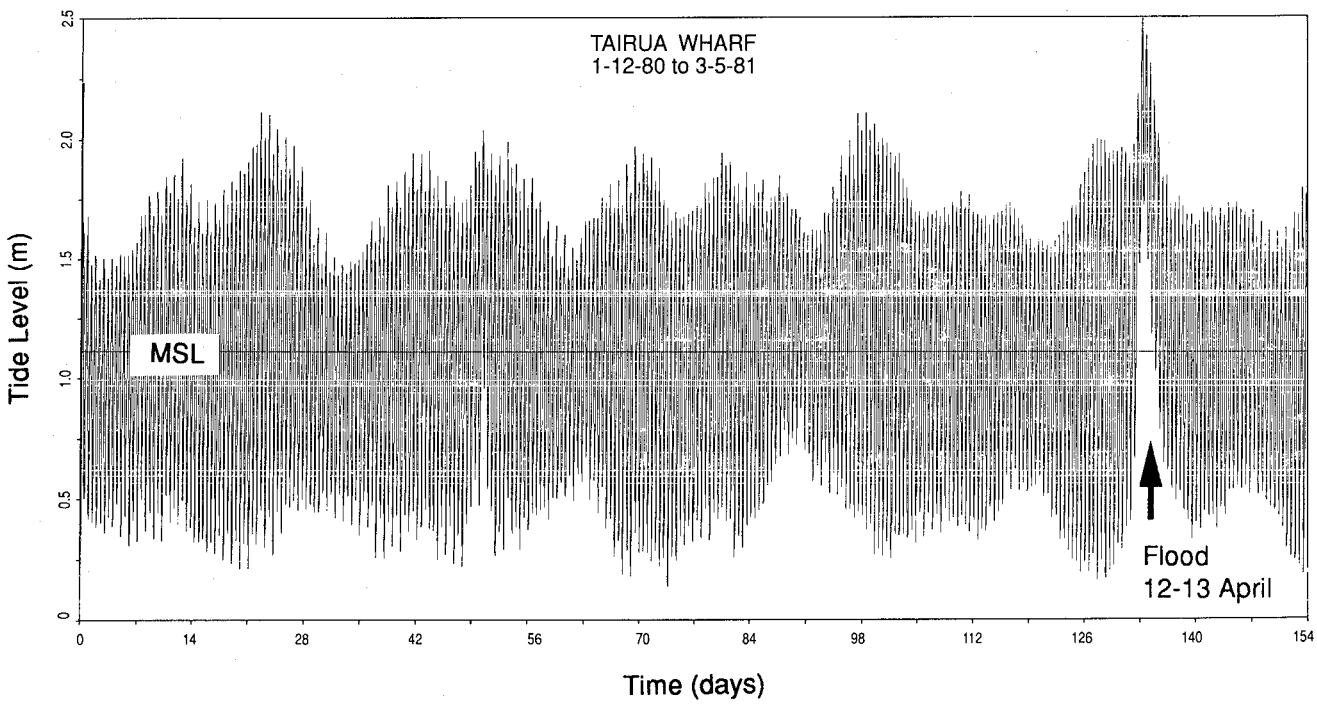

Figure 2.7 Water levels from December 1980-May 1991 at the Tairua Wharf, 1 km upstream of the entrance to Tairua Harbour (eastern Coromandel coast). Note the spring-neap cycles and how the water levels are elevated by a flood on the 12-13 April 1981.

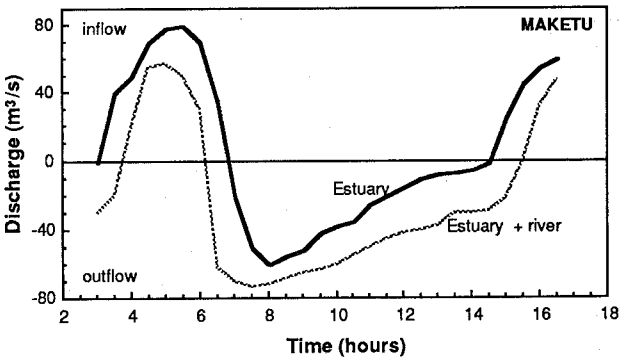

Figure 2.8 The discharge/time hydrograph for the entrance to Maketu Estuary, Bay of Plenty, modelled for existing river inflow (<1 m^3/s) and large river inflow of 30 m^3/s (after KRTA 1986, Fig. 6).

An appreciation of some of the complexities of flow within different types of estuaries is essential when planning tidal gaugings. The hydrodynamic character of the estuary has a direct bearing on the longitudinal siting of the gauging cross-sections, on the number of verticals and the number of velocity measurements needed to define the velocity profiles. The number will generally need to increase for partially or fully stratified estuaries. An understanding of the circulation 'type' is even more critical for estuarine surveys where fluxes of material are to be estimated. This is particularly so if the material is in particulate form such as suspended sediment, because most of the sediment load is concentrated in the bottom layer. Unless fresh water runoff is known to be negligible some preliminary *in-situ* salinity and temperature surveys should be carried out together with an estimation of freshwater runoff rates. This will determine the 'type' of estuarine circulation and so help optimise the field sampling programme.

Meteorological Processes

Meteorological processes can also have a marked effect on tide levels and flow. In fact any variations in tide level and flow remaining after the tidal forcing and freshwater input are subtracted from the record are generally assumed to be due to meteorological effects. Meteorological processes include wind-generated currents, hydrostatic changes in water level due to atmospheric pressure changes , and wind set-up and surges (which can increase local water levels by up to a metre or so).

As a general rule in the open ocean, low barometric pressure tends to raise sea level above predicted levels by about 1 cm for every millibar reduction in air pressure. This 'inverted barometer' effect can be seen in records from Marsden Point, at the entrance to Whangarei Harbour (Fig. 2.10). Here the drop in barometric pressure to 976 mb could account for 0.38 m of the maximum increase of about 0.8 m in sea level above the predicted spring tide HW's. In coastal and estuarine areas however, there is often some departure from the above rule e.g., at Moturiki in the Bay of Plenty the factor is ~ 0.6 cm per 1 mb reduction.

Wind set-up and surges increase local water levels by up to a metre or so on the New Zealand coast (e.g., Agnew 1966, Heath 1979, Hume 1979b). In the Marsden Point example (Fig. 2.10) for instance, the increase in water level not accounted for by the barometric pressure effect can largely be accounted for by wind set-up and surge which "stacks" water up against the coast.

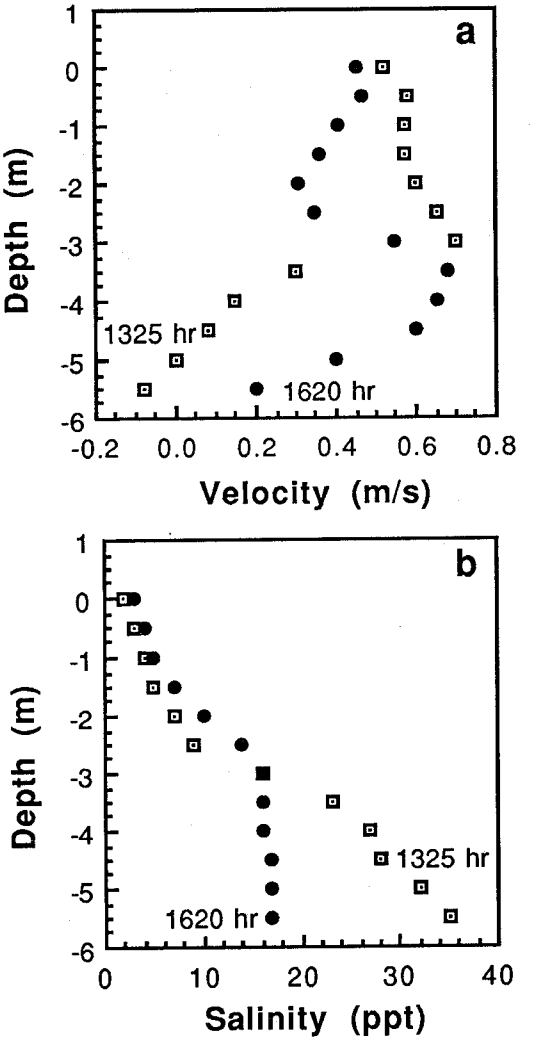

Figure 2.9 Velocity (a) and salinity (b) profiles upstream of the mouth of the Wairau Estuary (Cloudy Bay, South Island) showing stratification of flows. Note that the deeper saline waters have a stronger flow seawards at the later stages of the tide compared to the upper layer of fresh water (after Hume & Williams 1981).

Although in many estuaries the hydrodynamics are dominated near the mouth by tidal currents and in the headwaters by river inflow, wind-generated circulation may be relatively important in the wider middle reaches of large estuaries, where the river and tidal currents are damped by friction (Smith 1985). Wind-driven

circulation may also arise in wide, shallow embayments which are linked to deeper main channels (e.g., Fischer *et al.* 1979).

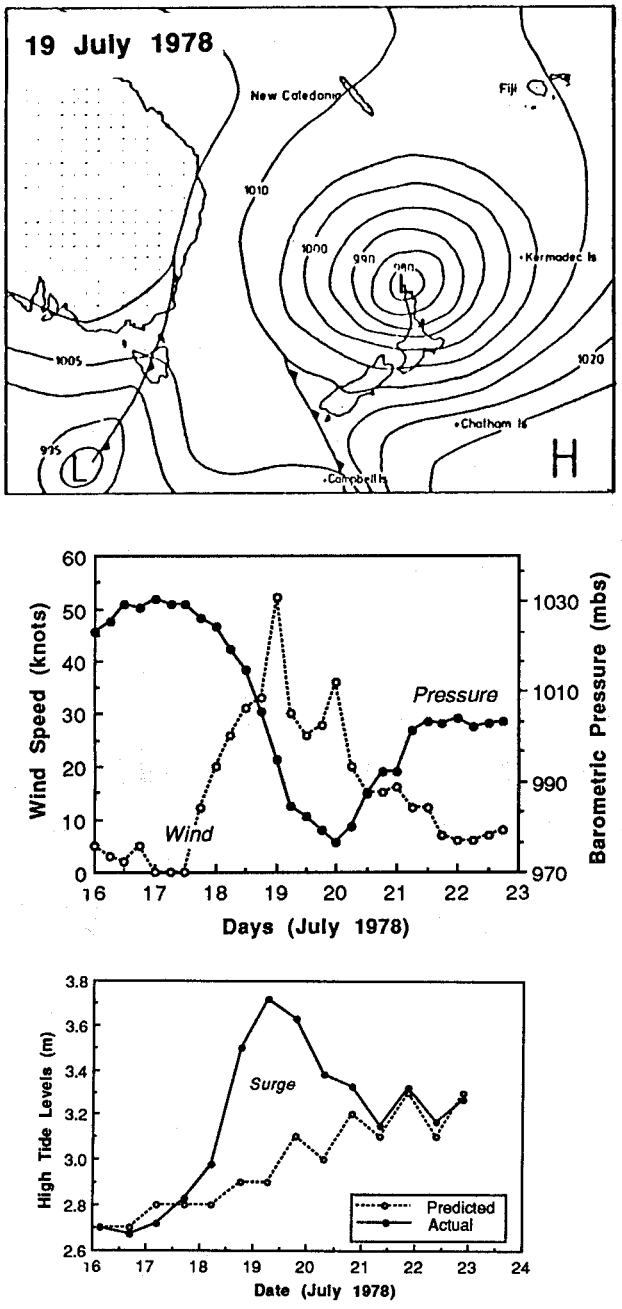

Figure 2.10 Meteorological factors influencing sea levels at Marsden Point, Northland, in July 1978 (after Hume 1979b).

Sea level fluctuations induced by pressure changes or wind-generated forcing (e.g., coastal alongshore winds), generally last for >1 day and can have a major effect on the residual flows and hence the tidal exchange of solutes and water volumes between an estuary and the adjacent coastal waters. Care is required therefore when using estimates of material fluxes and net or residual currents obtained from a gauging over a single tidal cycle, because the results will be biased by the conditions on that day. Indeed Weisberg (1976) argues that meaningful residual current or non-tidal flux estimates can not usually be obtained by averaging only a few tidal cycles. Tidal gaugings should be undertaken under average conditions, and short intensive tidal gaugings should be supplemented if possible with records from recording current meters moored over a longer period (1 to 2 months), and by numerical modelling.

Oceanic Processes

Water entering an estuary on the flood tide is a mixture of "new" ocean water and "old" estuary water, i.e., water that left the estuary on previous ebb tides. The influx of "new" ocean water is known as *tidal exchange*, and is an important component in determining the net (or residual) fluxes of material at the entrance. The process of tidal exchange, which is strongly influenced by longshore currents, the momentum of the ebb tidal jet (the outflowing water body at an estuary entrance), and meteorological effects, largely controls *net* material flux (e.g., nutrients, sediment) at an entrance. For example, in the presence of strong longshore currents the ebb tidal jet is directed along the coast away from the entrance so that only a small volume of "old" estuary water re-enters the estuary on the incoming tide. Generally this "old" estuary water is derived from the outflow during the latter stages of the ebb tide. In such a case replenishment by "new" ocean water predominates. Figure 2.11 shows this process in operation off the Tairua Estuary entrance.

A tidal exchange ratio, R_e, can be defined as the ratio of the tidal volume of "new" ocean water to tidal volume of water (i.e., "new" + "old" water) that enters the estuary during a flood tide (Fischer *et al.* 1979). Values of R_e can be readily computed from the results of tidal gaugings undertaken in an entrance, where velocities and one or more water-borne constituents such as salinity have been sampled.

Figure 2.11 Tairua Estuary entrance, showing the ebb tidal jet exiting the entrance and the resulting suspended sediment plume. Changes in longshore current, imprinted on the plume shape, have occurred early in the ebb tide phase, but generally the current to the left will ensure predominantly 'new' water will enter the estuary from the right. Photo taken by Whites Aviation in 1984.

Further Reading

Further reading is available in comprehensive texts on estuarine physical processes and behaviour such as those by McDowell & O'Connor (1977), Dyer (1973), Officer (1976) and Kjerfve (1988). The latter publication contains a good chapter on field measurements applicable to tidal gaugings.

Chapter 3

"DESK TOP" EVALUATIONS OF TIDAL FLOWS AND MATERIAL FLUXES

It is essential to define the objectives of a proposed survey because these will determine the data requirements and approach. In some cases estimates of flow and material fluxes may be obtained using existing data and "desk top calculation", rather than by field work which can be expensive or impractical (e.g., Morris 1983). These methods will usually be less accurate unless suitable field data has been gathered in the past at the site of interest. The methods described in this section have been developed mainly to estimate the tidal discharge and tidal prism, and should not generally be used to provide estimates of material fluxes (e.g., Boon 1975).

Locating Existing Data

Data on New Zealand estuaries is held in a wide variety of sources. Comprehensive reviews by Heath (1985) and Hume *et al.* (1992) describe coastal oceanographic work undertaken in New Zealand. Bibliographies covering more specific topics include those by Estcourt (1976) (scientific studies of New Zealand estuaries), Thompson (1981) (marine geology and physical oceanography of New Zealand's ports and harbours) and Hume & Harris (1981) (oceanographic and sedimentological studies for the Northland-Auckland coastline). A variety of bibliographies describe more site specific studies e.g., Bardsley (1976), Anderson (1977) and Hume (1984).

McLay (1976) and Hume & Herdendorf (1988) contain good background information on the characteristics and geological origin of estuaries. Heath (1985) contains tables of the physical characteristics of 32 New Zealand estuaries and embayments, including tidal prism and approximate residence times. Hume & Herdendorf (1992) present similar information for estuaries on the northeast coast of the North Island. University theses on coastal and estuarine topics usually contain raw data and good reviews of existing data. Some reports tabulate data and describe results of tidal gaugings e.g., Freestone (1978), Hume *et al.* (1986a, b, and c).

Agencies which gather and store data bases of information include: Regional Councils (hydrology, tidal gaugings, environmental investigations); National Institute of Water and Atmospheric Research - NIWAR (formerly called DSIR - Marine and Freshwater) (hydrology, tidal gaugings, tidal exchange and environmental studies); Royal New Zealand Navy and Port companies (bathymetric and tide data); Department of Conservation and Universities (scientific studies usually focussed on one area, for example in the region of marine laboratories and marine reserves). Unfortunately, because of extensive reorganisation within local and national government over the last few years some of this data is hard to track down, you may have to pay for the data, and some has been lost!

Bathymetric Charts

Estimates of tidal prism and other hydraulic parameters can be made using data from bathymetric charts. This approach has an advantage over a tidal gauging in that not only is it inexpensive, but it allows the parameters to be calculated for a variety of tidal situations (e.g., neap or spring tides). The accuracy of the estimates depends on the level of detail in the bathymetric data, so good estimates of tidal volume can be made, for instance, in the vicinity of major ports, where very detailed sounding data are generally available.

Tidal prism (Ω)(m^3) is calculated from a bathymetry chart by determining the volume of water between selected bed levels in the range from LW to HW (Fig. 3.1) using:

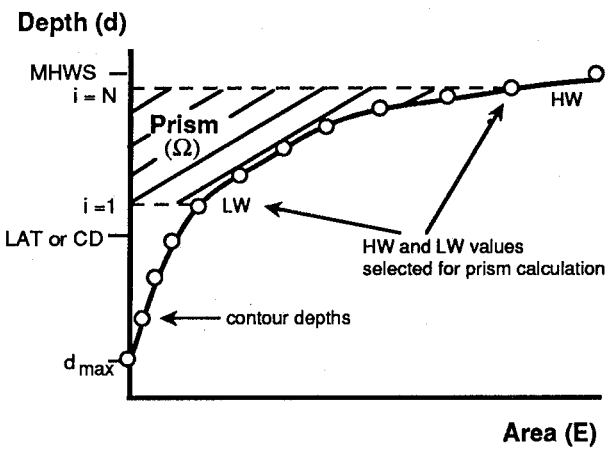

Figure 3.1 Calculating tidal prism from bathymetry charts.

(a) the general trapezoidal integration rule:

$$\Omega = \frac{1}{2}\sum_{i=1}^{N-1}[(E_i + E_{i+1}).|d_{i+1} - d_i|] \qquad (3.1)$$

where E_i = surface area at bed contour level d_i and E_{i+1} = surface area at bed contour level d_{i+1}, and d is positive above Chart Datum

or
(b) the formula of Hutchison (1975):

$$\Omega = \frac{1}{3}\sum_{i=1}^{N-1}[(E_i+E_{i+1})+\sqrt{E_i.E_{i+1}}\,].\,|\,d_{i+1}-d_i\,| \qquad (3.2)$$

which is more suitable than the former method for estuaries and lakes because it incorporates a better representation of a basin's shape.

The surface area at various stages of the tide can be determined from the chart by planimeter, cutting and weighing, or computer driven digitizer. Details of these techniques can be found in Maling (1989). When utilising bathymetric data for this purpose, care must be taken in sorting out levels, datums and chart projections, which can vary between charts and from place to place.

An estimate of the magnitude of the mean tidal velocity U_{mean} (m/s) can be calculated from:

$$U_{mean} = \frac{2\Omega}{AT} \qquad (3.3)$$

where Ω (m^3) is the tidal prism, A (m^2) is the channel cross-sectional area, and T (sec) is the tidal period (usually 12.42 hours, the semidiurnal period).

Another useful parameter is the sinusoidal maximum flow (Q_{max}) (m^3/s) through the channel cross-section which can be calculated from:

$$Q_{max} = \frac{\pi\Omega}{T} \qquad (3.4)$$

Empirical Formula

Unfortunately, many of New Zealand's small estuaries lie outside the major ports and are therefore uncharted. However although estimates of flow and flux from bathymetric data are not possible in these situations, tidal discharge and prism can still be readily *estimated* using various empirical formulae.

Hume (1991) describes relationships between the hydraulic and morphologic parameters for eleven tidal waterways inside estuaries in the Auckland region. For these waterways the maximum or peak tidal discharge (Q_p) and spring tidal prism (Ω_S) are related to either the channel cross-sectional area measured below mean tide level (A_{mtl}) or to the estuary free surface area (E) measured at HW:

$$\Omega_S = 1.547 \times 10^4\, A_{mtl}^{0.928} \quad (r^2 = 0.94, n = 11) \qquad (3.5)$$

$$Q_p = 2.668\, A_{mtl}^{0.833} \quad (r^2 = 0.93, n = 11) \qquad (3.6)$$

$$\Omega_S = 0.1261\, E^{1.172} \quad (r^2 = 0.94, n = 11) \qquad (3.7)$$

$$Q_p = 6.083 \times 10^5\, E^{1.062} \quad (r^2 = 0.94, n = 11) \qquad (3.8)$$

These formulae enable tidal discharge and prism to be estimated from rapid and inexpensive measurements of the channel cross-sectional area (A) (measured in the field or from bathymetric charts), and the estuary surface area (E) (e.g., measured off a 1:50,000 topographic map) upstream of the channel cross-sectional area. Similar methods may be applicable to other estuaries.

Hume & Herdendorf (1992) established that for the entrances to barrier enclosed estuaries on the northeast coast of the North Island, there are excellent correlations of spring tidal prism (Ω_S) and peak discharge (Q_p) with inlet throat area (A_{mtl}), as described by the following equations:

$$A_{mtl} = 0.769\, Q^{1.036} \quad (r^2 = 0.97, n = 16) \qquad (3.9)$$

$$A_{mtl} = 1.59 \times 10^{-4}\, \Omega_S^{0.953} \quad (r^2 = 0.98, n = 16) \qquad (3.10)$$

Their findings are similar to those reported by other workers for similar inlets overseas (e.g., O'Brien 1931, 1969; Jarrett 1976). These relationships allow us to estimate tidal prism and discharge for inlet entrances once the throat area has been determined from a chart or by field measurement. Hume & Herdendorf (1987) also established that similar relationships may hold for a wider variety of estuary types, ranging from barrier enclosed lagoons to river mouths and coastal embayments. These equations can be used to estimate tidal prism for a variety of estuary types.

A word of warning when using these methods. Extreme care should be taken to ensure that the data are reduced to common datums and tidal conditions. In estuaries where the main driving force is the semi-diurnal tide, there can be substantial differences between the spring and neap tide ranges (e.g., Manukau Harbour: mean spring range 3.4 m, mean neap range 2.0 m) and therefore the strength of tidal flows. In order to facilitate comparisons between sites, the hydraulic data need to be 'normalised' to a standard situation. The mean spring tide situation is usually chosen because it is under high discharge (spring tide) conditions that channel cross-sections tend to scour and equilibrate with flows. The mean spring tidal prism (Ω_S) can be estimated from the measured tidal prism (Ω) by:

$$\Omega_s = \Omega\,\frac{R_S}{R} \qquad (3.11)$$

where R_S is the mean spring tide range at the Standard Port, and R is the tide range measured at the site at the time of the gauging. This calculation is based on the assumption that the tidal prism is proportional to the tidal range. Of course errors in the 'normalisation' calculation are minimised if the field measurements require little adjustment.

Estimates of tidal prism and discharge by empirical

methods can be accurate to within ±10% of discharges obtained by classical multi-point methods (Christensen & Walker 1969), and this may be quite sufficient for some jobs. At the least they can assist in planning field work by providing a means of evaluating the likely flow conditions.

Hypsometric Method

The hypsometric method, described by Boon (1975), is an elaboration of the method described in the previous section "Bathymetric Charts". It involves developing a simple tidal discharge model from water surface area and tidal height data. For an estuary system closed at one end, the continuity equation expressing discharge Q in a flow cross-section near the mouth can be written as:

$$Q = E\frac{dh}{dt} \qquad (3.12)$$

where Q has units of volume/unit time, E is the free surface area upstream of the cross-section, h is the tidal stage, and t is time. The model assumes that: (1) the channel is frictionless, (2) the free surface is everywhere a level surface, (3) the flow section near the mouth carries all the water entering and leaving the estuary drainage basin, and (4) wind stress and inertial effects are negligible.

Firstly, a surface area-height (hypsometric) relationship is developed for the estuary. The surface area can be obtained from aerial photographs taken at various tidal heights or from a bathymetric chart, and tidal heights recorded at a water level gauge. This allows the tidal prism, or the total volume between any two levels of the tide to be assessed using:

$$\Omega = \int_{t(LW)}^{t(HW)} Q.dt = \int_{h(LW)}^{h(HW)} E.dh \qquad (3.13)$$

Tidal discharge can be predicted at discrete points in time using equation 3.12, providing a suitable expression for the rate of change of tidal height (dh/dt) can be found. During an individual tidal cycle, the tide can be modelled to a first approximation by:

$$h(t) = h_0 + H\cos(\omega t - \phi) \qquad (3.14)$$

where h_0 = mean tide level, H = observed tidal amplitude or semi-range, ω = angular speed $2\pi/T$, (where T = is the semi-diurnal tidal period, 12.42 hours), and ϕ is the angular phase lag with respect to a selected time origin.

Although longer period constituents can be neglected when modelling a single semi-diurnal cycle, there are usually important shallow water effects present in coastal and estuarine waterways that warrant consideration. These effects can be determined by performing spectral analysis on tide level records from the waterway under study, and the additional over-tide terms added to equation 3.14, providing a much improved version of the tidal formula (Boon 1975).

The resulting equations provide the necessary input to an easily applied numerical model of tidal discharge as a function of time, based on the continuity equation 3.12 (see Boon 1975 for details). The models can be used to examine the asymmetry of the tides (which has implications for the flux of materials) and to estimate the tidal discharge and prism for a range of conditions such as neap, average and spring tides.

Chapter 4

FIELD STUDIES

Field data can be obtained by a number of different techniques, supplemented, if necessary, by model simulations (Morris 1983). These options need to be evaluated in terms of efficiency, accuracy and economy, because tidal gaugings are labour intensive and costly exercises (typically NZ$12-20,000). Furthermore gaugings can be difficult to execute because of the large number of people involved, and the weather- and tide-dependent nature of the work. Key decisions when planning a tidal gauging are the spacing of sampling points (both laterally and vertically), in the channel cross-section and the frequency of measurements.

Data Requirements

Surveys of tidal flows and material fluxes involve measuring water level, cross-section bathymetry, current velocity, temperature, salinity, and suspended sediment, over a part, full or several tidal cycles. The survey requirements will of course determine what parameters have to be measured and therefore the measurement strategy. The requirements for various sorts of gaugings are presented in Table 4.1.

Today there is a large variety of equipment and techniques available for making the required measurements. To a great extent the availability of equipment and personnel skills largely govern the method used.

Gauging Techniques

A *conventional tidal gauging* is carried out by making measurements of current velocity at many stations over a channel cross-section, by teams of people using current meters from boats, or from a bridge spanning an estuary. The intensive demands on equipment and personnel of this operation, usually limits such gaugings to a half or full tidal cycle. This type of gauging gives the best and most useful results and therefore is the focus of this handbook. However, there are a couple of alternative approaches that are useful in certain situations and these are summarised below.

The *one-point method*, described by Christensen & Walker (1969) and Mehta *et al.* (1977), involves making continuous velocity measurements at one point in a cross-section, then extrapolating the data to the entire cross-section where the shape and roughness

Table 4.1 Measurement requirements for tidal gaugings.

Survey requirement	Measurements	Field instrument	Laboratory analysis
(n) Discharge vs time and tidal prism	• Velocity (speed and direction)	*	
	• Time and depth and lateral position of velocity measurement	*	
	• Bathymetry of the channel cross-section	*	
	• Water level (time-series)	*	
(o) Suspended sediment & nutrient fluxes	• All above parameters for (a)	*	
	• Concurrent in-situ water samples (filtration/weight determination in the laboratory)	*	*
(p) Salinity & heat flux	• All above parameters for (a)	*	
	• Concurrent in-situ salinity/temperature depth profiles (if salinity variations are small use water sampler and laboratory analysis)	*	*
(q) Tracer fluxes	• All above parameters for (a)	*	
	• Concurrent in-situ dye concentrations using on-board fluorimeter	*	
	• Water samples followed by laboratory analysis for other tracers (e.g., silica)		*

characteristics of the section are known. The method has some advantages over conventional tidal gauging methods in that it is less labour intensive and expensive. Furthermore, it makes it feasible to measure discharge over several tidal cycles, thereby reducing errors due to sea level fluctuations induced by pressure changes or wind-generated forcing, and river discharge. The method is well suited for use in those tidal inlets where the conventional measurements are difficult to make or are unreliable, due to rapid changes in discharge, high current velocities or waves.

The one-point method is applicable only to a non-stratified entrance, because if stratification or a salt wedge is present a point measurement will not be representative of the vertical flow structure. The technique is particularly useful in the lower reaches of estuaries when freshwater inflow is insignificant compared to the tidal flow and the tidal energy is sufficient to cause the flow to be vertically well mixed. Field evidence suggests that in such cases it is not unreasonable to assume that the vertical velocity profiles are logarithmic (Mehta *et al.* 1976) and that an average vertical velocity can be derived from a single point measurement. The bed roughness in general may vary with the low frequency tidal oscillation, because the pattern of near bed flow varies with the tide. However at tidal entrances on sandy shores, which essentially are wide channels in the hydraulic sense, the bed is often "lagged" with shell material and generally remains flat throughout the tidal cycle, exhibiting a relatively constant roughness (Mehta *et al.* 1977).

The one-point method involves installing a recording current meter, or using a direct reading current meter, at some point in an estuarine cross-section to obtain a continuous time-velocity record. This 'at point' measurement is then converted to the discharge through the same section, given the geometry and the bed roughness of the cross-section and the water surface elevation. The *first step* in the calculations involves calibration of the equations in terms of bed roughness based on a single set of cross-sectional velocity data. These data are collected by measuring vertical velocity profiles at selected positions across the channel at a point in time. The (instantaneous) discharge is then computed and the slope of the energy gradient line, tidal elevation, and channel dimensions are used to compute bed roughness. Other data required are waterway maximum depth, area, shape, surface and width; also maximum velocity in the vertical section at the point of maximum depth, and visual observations of the roughness of the bed. The *second step* involves the conversion of the time-velocity (current meter) data to time-discharge data. Details of the method and computer programs are given by Mehta *et al.* (1977) and Christensen & Walker (1969).

In the last decade Acoustic Doppler Current Profilers *(ADCPs)* have become available providing a new tool for tidal gaugings. These state-of-the-art instruments make use of the "Doppler effect" to measure current velocity and direction, and concentrations of particulate matter in the water column (RD Instruments 1989, Simpson & Oltman 1990). ADCP's can divide the water column into over 100 depth increments (or bins), and measure the average velocity in each bin, whereas a conventional current meter measures average current at only one point (the meter). An important feature of ADCP's is that they can measure current profiles from a moving vessel. Therefore, a vessel can motor back and forth across an estuarine cross-section measuring current profiles and computing discharge continuously throughout the section, and throughout the tidal cycle. Only their high cost and, until recently, the lack of commercially available shallow water models, has hindered their widespread application to tidal gaugings.

Selecting a Gauging Site

Tidal gaugings are usually undertaken at constrictions such as an inlet throat, or where a tidal creek links with the main estuary. The reasons for choosing these situations are: (1) the channel is narrow and deep, (2) there is generally only one major channel and flow path, and intertidal flats are minimal, (3) the flows are stronger and well above the threshold of the instrument which enables more accurate measurements to be made, and (4) information on the flows and material fluxes (exchange) between the estuary and coastal waters or between arms of an estuary is often of interest.

In choosing a site for a tidal gauging the information requirements must be weighed against practical factors such as the physical characteristics of the site and availability of equipment and personnel. A visit to the site prior to the gauging is necessary. The amount of boat traffic on the waterway will determine how the gauging is done and the various safety requirements needed. The local harbour master or port authority will be able to advise on some aspects, and approval may be required in certain instances. Access to launching ramps is important and consideration should be given whether to start at high or low tide, darkness or daylight. A low tide inspection of the site is essential, and observations of the flow patterns at peak flow are always useful. Remember, conditions may change dramatically with the state of the tide.

Some considerations important in selecting a gauging cross-section are:

(1) *Alignment of the gauging section* - Ideally the gauging section should be aligned normal to the flow direction at all times. This is particularly important when using current meters from boats, which stream off-station as the direction of tidal flow changes with the state of the tide and with reversals in flow due to ebb and flood tide. In practice, the section is aligned normal to the average direction of the ebb and flood currents. Attention to this aspect is also more important when using current meters which do not measure direction.

(2) *Bathymetry* - Preliminary sounding surveys should be carried out from about 50 m upstream and 50 m downstream of the gauging cross-section, to check

for rock outcrops and sudden falls or rises in bed level. These features will cause undesirable turbulence and changes in direction of flow at the gauging site.

(3) *Channel shape* - Choose a gauging section where the flow is confined to one main channel, and where the course of the channel is relatively straight for approximately 100 m upstream and downstream from the gauging site, so as to avoid changes in water level. Navigation issues must be taken into consideration. Narrow tidal channels are often a main thoroughfare for boat traffic, which poses safety problems, particularly at night, and will dictate the methods used (tag line gaugings are out!)

(4) *Water level gauge location* - Once the *general* location of a gauging site has been determined, a suitable site must be selected nearby for the installation of a temporary tide gauge (if a permanent gauge is not already established). It is important to have the tide gauge close to the gauging cross-section (e.g., within 100 to 150 m) in order to avoid the significant velocity head differences between sites which can occur over short distances near constricted tidal inlets. Obviously, if boat crews are to read tide staff gauges manually, then the gauges must be located close at hand. Where possible, the tide gauge should be sited on the sheltered side of the cross-section. If the channel is particularly wide (e.g., greater than 700 m), or a channel bend cannot be avoided, then it may be necessary to have a tide gauge on both banks of the channel. If tide level readings are possible only some distance from the cross-section, it will be necessary to make time and range corrections to the water level data, calibrated from several manual tide level observations at the cross-section.

Planning the Field Work

The key steps in planning a tidal gauging are presented in Table 4.2.

Tide Levels and Datums

Establishing an accurate water surface reference-level is a basic requirement for tidal gaugings as the cross-section depth soundings must be related to the tide level measurements via some common datum. This can be an arbitrary level, however if practical it is best related to some standard or existing hydrographic or land levelling datum. It is good practice, and often useful in the long run, to reduce the data in terms of the local port Chart Datum or Mean Sea Level.

Table 4.2 Some key steps in planning a tidal gauging.

Timing	Action
Several weeks before gauging	• Field inspection (especially low tide) and selection of the gauging and tide gauge sites
	• Review existing information on the site
	• Pilot in-situ salinity/temperature survey to determine estuary type
	• Liaise with harbour/port authorities on channel use
	• Choose tide and set date and start time
	• Select sampling methods and equipment
	• Organise gauging teams, boats and equipment
One week before gauging	• Install and survey in a temporary tide gauge and staff gauge, establish sounding datum, tie in water level gauge, clean biofouling off any existing staff gauge
	• From sounding chart, estimate number and positions of sampling stations
Previous day	• Carry out detailed echo-sounding of cross-section, finalise positions of sampling stations
	• Briefing session for gauging team
	• Check wind and wave forecast
	• Check equipment (including spares) is operational
Immediately prior to gauging	• Check water level gauge
	• Set-up sampling stations using buoys or tag line
	• Have a practice run

Procedural tips: Where possible, include a spare person and small boat to convey messages, food to boat crews, read the staff gauge, and carry out running repairs to gear; always carry spare instruments and parts in case of malfunctions; snorkelling gear is useful to retrieve equipment lost overboard.

At a particular port, the level of the water at any instant is expressed as a height above a local *datum*. Depths on hydrographic charts are expressed relative to this datum. The datum is defined with reference to permanent bench marks onshore and with respect to nearby tide gauges. *Sounding Datum* is the plane to which soundings are reduced in the course of a hydrographic survey. It is the datum used when compiling the "fair sheet". *Chart Datum* is the datum plane finally adopted for the published chart, and is the level above which tidal predictions and tidal levels are given in both the Tide Tables and on the published charts. It may or may not be the same as the original sounding datum. Chart datum is set at a water level so low that the tide will seldom fall below it. In New Zealand it is usually about 0.3 m (1 foot) below mean low water springs. Chart datum and other important tide levels are illustrated in Figure 4.1 and are described below.

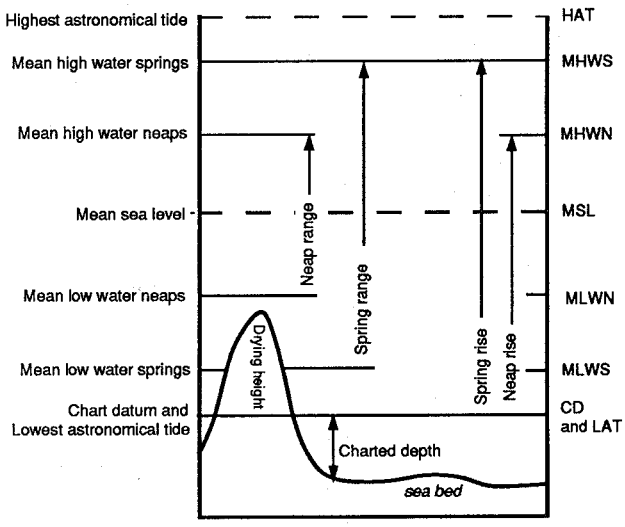

Figure 4.1 Definitions of specific tidal heights, ranges and levels.

Mean Sea Level (MSL) is defined as the arithmetic mean of hourly sea levels over a long period, preferably the metonic lunar cycle of 18.6 years, or the average level that would exist in the absence of tides. MSL values calculated over shorter periods (e.g., 1 month or annual) will vary from the above value due mainly to meteorological effects. *Mean high water springs* (MHWS) and *mean low water springs* (MLWS) are the long-term averages, usually over at least 1 year, of the levels of each successive pair of high waters, and each successive pair of low waters, during that period of about 24 hours in each semi-lunation (approximately every 14 days), when the tide range is greatest. *Mean high water neaps* (MHWN) and *mean low water neaps* (MLWN) are the average of the levels of each successive pair of high waters, and each successive pair of low waters, during that period of about 24 hours in each semi-lunation, when the tide range is least. *Mean spring range* is MHWS - MLWS and *mean neap range* is MHWN - MLWN. *Highest astronomical tide* (HAT) and *lowest astronomical tide* (LAT) are the highest and lowest tidal levels that can be predicted to occur under average meteorological conditions and under any combination of astronomical conditions. Modern chart datums are set at the approximate level of lowest astronomical tide. *Mean tide level* (MTL) is the average of all the successive high and low water levels in a specified period, provided an equal number of HW and LW levels are used. MSL and MTL are different. Whereas MSL can be regarded as a spatially consistent level over a stretch of open coast, MTL varies from place to place, particularly in estuaries, as the tidal response varies. This is because MTL is affected by river flows and the shallow water constituents of the tide, which can vary over quite short distances in estuaries and nearshore areas.

A datum can be established at a site either by transfer from a bench mark, or by establishing an independent datum. Both methods are detailed in "Datums for Hydrographic Surveys - Admiralty Tidal Handbook No. 2" (Hydrographic Department Admiralty 1975), and are described briefly below.

(1) Datums can be transferred from a site which is close to the desired locality by making, at both sites, simultaneous measurements of water level at high and low tide, at which time water surface is assumed to be horizontal. The object of the transfer is to ensure that when the tide falls to datum in one place, it falls to datum at all other points on the survey. The distance over which datums can be transferred with accuracy depends on the tidal conditions. In an estuary the transfer may be possible only over a few kilometres, whereas on the open coast it may be carried out over 15 km or more. The datum can be transferred over longer distances in a series of short steps. To minimise errors, datum transfers should be made between sites with a similar tidal range. The method involves measuring high and low water levels at the two sites over a minimum period of 25 hours (i.e., 3 HW's and 2 LW's), and then calculating true MSL from the observed MTL. The method assumes that the mean levels at the 2 sites are the same and that the tidal ranges are similar. Transfer should be made at or near spring tides because the relative effect of abnormal weather conditions is least when the tidal range is greatest.

(2) An independent datum can be established at a site by making tidal observations or by transferring levels from the land levelling system. MSL can vary in the short-term (2-5 years) by as much as 0.1-0.2 m, particularly during extremes of the Southern Oscillation (El Niño and La Niña) in the South Pacific (Hume *et al.* 1992). In order to get a reliable estimate of MSL it is preferable to calculate it using records of 5 years duration. Over a period of 5 years it is assumed that the value of MSL will differ by less than 10 cm from the average taken over say, 20 years. To establish a sounding datum for a hydrographic survey, MSL may be calculated from a minimum of 25 hourly observations (lunar day). Analysis of a month's records is preferable. Modern surveying equipment has made it

much simpler to transfer levels from the land levelling system. Total station surveying instruments can be used to transfer levels large distances from land bench marks, on say the roading/bridging network, to the tidal gauging site.

Water Level Measurements

The main purpose of water level (stage) measurements is to establish how the flow cross-sectional area varies over the period of the gauging, which is usually a half (6.2 hours) or full (12.4 hours) tidal cycle. In situations where there is a large tidal range, it is important that the water level is measured frequently (every 5-10 min.), because it changes rapidly with time, particularly about mid tide. Water level can be determined by observing a staff gauge (sometimes called a tide board or pole), or by a recording water level gauge. If the water level measurement site is close to the gauging site, a staff gauge can be easily read by boat crews during the gauging. If, however, the staff gauge is less accessible, consideration may be given to installing a recording water level gauge. If this is more practical, use of a staff gauge is still recommended as the recording tide gauge will need to be calibrated and tied in with the surveyed cross-section and level datums. Furthermore, some staff gauge observations during a gauging are a useful back-up in case the recorder fails. A detailed review of levelling techniques for water level gauges is given by Forrester (1983).

Staff gauges

The simplest form of water level gauge is a graduated pole or staff (usually marked in metres, decimetres and centimetres in New Zealand), standing vertically in the water. Installation is comparatively simple if a pier or wharf is available close to the gauging cross-section, although care is needed to ensure that the staff is truly vertical. Where a pier is not available, a length of water pipe can be rammed or jetted (using a high pressure pump and hose attached to the pipe) into a sandy or muddy bed, then the tide board attached to the pipe using adjustable pipe clamps. The clamps enable the tide board to be moved up and down to set the zero on the gauge to a selected datum.

Staff gauges are best installed at spring low water to ensure that they do not go dry at lower stages of the tide. It is also important that the staff gauge is accessible and can be read at all stages of the tide. In situations where there are extensive mud flats flanking the channels this can be difficult, but the problem can be overcome by reading the gauge from shore using a theodolite. Otherwise an observer may have to be stationed by the staff gauge in a small boat. In situations where the tide range is large (the largest tides in New Zealand occur in Tasman Bay and Manukau Harbour, with ranges of 3-4 metres or more), two or more staff gauges can be staggered up the intertidal bank.

Waves and current turbulence about the staff gauge can make the water level difficult to read. Therefore, staff gauges are best installed in areas where the flow is small (e.g., backwaters). The edges of the gauge should be streamlined or sharpened and aligned parallel to the flow to minimise turbulence. To make reading the gauge easier an open ended plastic tube of 1-2 cm diameter can attached to the side of the staff gauge, and the water level in the tube observed. The small opening in the base of the tube effectively dampens the wave motion, enabling a more accurate observation to be taken. The system can be further improved by using a floating ball (van de Ree & Stuip 1984a) or dye inside the tube.

Recording water level gauges

A variety of recording tide gauges are available, either as permanent gauges or readily deployed self-contained instruments. Broad categories of instruments are: a float and counter weight system in a stilling well (vertical chambers), pressure transducers, trapped air diaphragm gauges, bubbler gauges, and ultrasonic sensors. Details of these various types of water level gauges and their accuracy are reviewed by Glen (1979), Forrester (1983), van de Ree & Stuip (1984a) and Rantz *et al.* (1982). When possible, frequent checks should be made during the gauging to ensure the instrument is performing satisfactorily. In our experience, this precaution and the installation of a back-up staff gauge has saved a few tidal gaugings from certain failure and is therefore recommended as a normal procedure.

The most common tide gauges consist of either pressure transducers, fixed at a known level and measuring the pressure exerted by the water above, or devices such as floats in towers that record the level of the water relative to the land. The configuration of these devices may result in the following errors in water levels.

Pressure gauges respond not only to changes in depth, but also to changes in water density. The latter occur during a tidal cycle in estuaries with significant freshwater input, as marine waters at high tide are replaced by more riverine waters at low tide. This effect can be quite pronounced during high river flows and under these situations, pressure gauges will not accurately record the depth of water. Corrections can be made to the record providing salinity and temperature measurements are made during the tidal cycle. If the pressure transducer is not vented to the atmosphere, then the "inverted barometer" correction (see Chapter 2) will also need to be made to the recorded pressure measurements to account for changes in atmospheric pressure.

Stilling well tower structures, used to dampen the effects of currents and wave action, also cause some inaccuracies (Shih & Baer, 1991). Velocity head effects occur if the intake ports for the tower are facing upstream or downstream, or if fast flowing water piles up against the tower itself, thereby elevating the water level immediately above the port. Simple calculations

show that the velocity head $U^2/2g$ (where U = local velocity), can reach 0.2 m if the current speed is 2 m/s. Properly designed and located towers will minimise these errors. A nonlinear interaction between waves and a stilling well intake can also lead to systematic errors in the mean water level (Shih & Baer 1991). The density of water inside and outside the tower changes can differ during the tidal cycle, creating an additional error. At low tide, fresher water surrounds and enters the tower. As the tide rises, the water entering the tower becomes progressively denser (more saline) as more oceanic water enters the estuary. At high tide, the tower will be filled with water that has a mean density somewhere between that of the high tide saline water and the low tide fresh water, while outside the tower the water will be of maximum salinity. If the density of water at high tide is 1025 kg/m^3, and the mean density in the tower 1012 kg/m^3, then the height of the water column outside the tower will be (1025/1012) or 1.013 times that of the outside. This amounts to an error of up to 4 cm for a 3 m tide range.

In addition, errors in water level can arise from badly maintained installations. Siltation and biofouling can partially block the stilling tower intakes and smother pressure transducers, thereby dampening response to water level change. In our experience biofouling is a particularly bad problem in northern New Zealand, where intakes may need cleaning as often as monthly during the summer.

Cross-section Soundings

Accurate sounding of the channel cross-section is extremely important because the discharge and fluxes through an estuary cross-section are computed as the product of mean velocity and channel cross-sectional area.

When the channel cross-section is surveyed by boat and echo sounder, depths are measured relative to the water surface and from a boat which is moving horizontally and vertically (due to wave action). Errors in measurement of apparent depth arise from the technique of measurement itself, in estimating the true location of the sampling point on the bed and in transferring datum levels from the shore to the boat. When sounding by echo sounder under calm sea conditions the best depth accuracy that you can hope to get is generally about $\pm$ 5 cm. Distance can be measured by simply assuming a constant boat speed across the profile. This is easy but gives an inaccurate result. A better technique is to "fix" on the sounding trace the position of known markers (e.g., channel marker buoys) and assume a constant boat speed in between. Best results, however, come from continuously tracking the boats distance from shore with an electronic distance measuring (EDM) device as it runs along a line defined by transit poles, or by continuously tracking the boat's position with a TOTAL STATION- or MICROFIX-type positioning system as the boat runs across the profile.

It is worthwhile surveying the channel profile up to at least MHWS tide level, because spring tide conditions are often needed for various computations, as this is when tidal scour and discharge are greatest.

Current Measurements

Methods and instruments

Current velocity, the parameter which is fundamental to deriving flows, tidal prism and material fluxes, is the most important yet often the most difficult parameter to measure. It is a vector quantity which varies markedly in both magnitude and direction within an estuarine environment.

Current velocity can be measured using floats, drogues or dye patches to track the passage of a water parcel over time. These Lagrangian techniques are simple, give average velocity along the path of travel, and tidal excursion (distance travelled on ebb or flood tide), but are not much use for measuring fluxes past a cross-section.

The average current velocity over the estuary cross-section can be measured by the electromagnetic method, the rising air-float technique and the rating method. The electromagnetic method involves measuring the voltage induced by a current flowing normal to a coaxial cable stretched across the section of interest (Kjerfve 1979 and Forrester 1983). In the rising air-float technique, a perforated air pipe is laid across the channel bed to form multiple sources of air bubbles. The rate of downstream travel of the bubbles is related to the depth-averaged velocity. The use of a stage-discharge rating curve, which has been so successfully applied to rivers, is unsuitable for use in estuaries (Kjerfve 1979 and van de Ree & Stuip 1984b). The main problems are the continuous change in water level throughout a tidal cycle, the likelihood that the times of HW and LW may not coincide with slack tide, the change in flow direction during the slack period, the effects of stratification, and rapid variations in stage as intertidal areas are covered or uncovered.

Current velocity is most commonly measured using current meters from boats or a bridge. Velocity is recorded as a function of time at a fixed position in the water column. These Eulerian methods have proved the most successful and popular by far in estuarine applications. Measurements are taken at regular intervals in time (say every 15-30 mins) over a part or full tidal cycle. They are made at several points or stations along the cross-section and at a number of depth levels at each station. There is a wide choice of meters available, ranging from types commonly used in rivers to those designed specifically for oceanographic work. Current meters are generally categorised as direct reading meters (DRCM) or recording current meters (RCM), the latter are often used in oceanographic investigations. Oceanographic instruments and some DRCM's (e.g., Braystoke propeller meters) have an advantage in that they measure current direction, which is of value because the direction of tidal flow in a

channel can change with the state of the tide. Detailed descriptions of current meter type, operation and care are given in Rantz *et al.* (1982) and Dyer (1979). Sometimes RCMs are suspended in a moored buoy system at a fixed height(s) in the water column e.g., when the one-point method is used. A practical guide to choice of meter, mooring design and analysis of the data for RCM's is given in Bell *et al.* (1988).

The Acoustic Doppler Current Profilers (ADCPs), described previously, can measure current and particulate matter profiles, either from a moving vessel, or from a looking upward position when moored on the sea bed. ADCPs measure currents relative to the ADCP, therefore it is necessary to correct the data for ADCP attitude and motion. It is also necessary to calibrate the signal. What ADCPs lack in precision, they make up for by the huge quantity of data they are able to collect.

In summary, the Eulerian technique seems the best approach for estuarine tidal gaugings, preferably using DRCMs which measure direction. ADCPs are a highly attractive option for gaugings.

Spatial and temporal sampling strategy

Important as good instruments are, the accuracy of the final results will depend more on setting up a good sampling strategy to define the velocity field. A complicating factor in estuaries is the need to describe the vertical velocity profile, particularly where density changes induce vertical circulation. During tidal gaugings velocity should ideally be sampled continuously at a dense network of stations in the cross-section to determine accurate velocity distributions, flows and fluxes. In practice, there is a limit to the number of observations that can be carried out, and so the question arises of how to optimise the sampling in terms of both space and time.

Lateral distribution of sampling stations
In practice the lateral distribution of sampling stations across a cross-section depends on the site characteristics. In this section we examine three tidal gauging case studies to assist with our consideration of the optimum placing of verticals across a gauging section.

Case Study 1 - North Inlet, South Carolina
Kjerfve *et al.* (1981) provides one of the most comprehensive analyses of accuracy and errors due to variations in spatial density of current velocity measurement. Their analysis is based on a very detailed gauging undertaken at North Inlet in South Carolina over *3 tidal cycles*. Here the cross-section is *irregular* in shape, 320 m wide and up to 7 m deep (Fig. 4.2). Sampling occurred simultaneously at *10 stations* every 30 minutes, starting on the hour and half hour, with measurements at 1 meter intervals from surface to bottom. Distances between stations varied from 19 m up to 51 m, with the larger gaps in the deeper main channel, which is likely to be relatively uniform, and narrower gaps where bars or shoulders occurred in the channels.

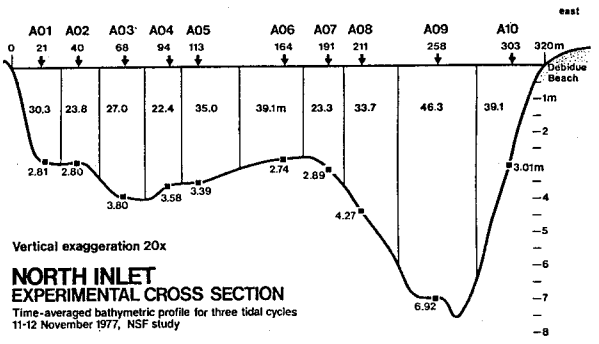

Figure 4.2 The experimental cross-section at mean tide in North Inlet, South Carolina (from Kjerfve & Proehl, 1979) showing: 1) station notation (top row); 2) distance of station in meters from the western bank (second row); 3) distance in metres of each subsection over which measurements at a given station are considered representative (third row); and 4) time-averaged water depths (m) at each station (below the bottom trace).

Kjerfve *et al.* (1981) tested the results and errors for various combinations of fewer lateral velocity measurement stations. A paired t-test was used to distinguish between the sample mean of the full complement of stations, and the sample mean of each of the 29 combinations of the reduced number of stations. As a result 5 cases were rejected on the basis of discharge inaccuracy (i.e., computed t-statistic was in excess of critical t-value), and 4 cases rejected for inaccuracy in the material flux. The rejected cases contained from 1 up to 6 stations, which implies that the particular location of sampling stations in a cross-section is highly critical, not just the number of stations. In this example one of the acceptable cases with only three stations (verticals A02, A06, A09), which were sited in each of the two main channels and on the bar between (Fig. 4.2), resulted in a better representation of the flow than another case where six of the total ten stations were used.

The average percentage error in the tidal prism estimates (0% when all stations were used) was plotted against the number of lateral stations for this particular tidal inlet by Kjerfve *et al.* (1981), and is shown in Fig. 4.3. As expected, the percentage error increases as the number of stations decreases. However, the information gained by increasing the number of stations from 3 to 4 or 5 was minimal. Similarly, very little would have been gained by increasing the number of stations from 6 to 7, 8 or 9.

Case Study 2 - Mangere Inlet, Auckland
A detailed tidal gauging was undertaken from the old Mangere Bridge at the entrance to Mangere Inlet in the Manukau Harbour, New Zealand, for the purpose of assessing the availability of marine cooling water for a proposed thermal power station. Details are given in (Hume 1979c) and the data are summarised in Appendix I.

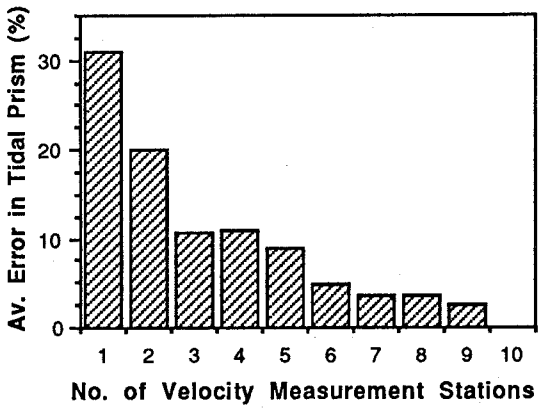

Figure 4.3 The average percentage error in the tidal prism estimates as a function of the number of stations where velocity was measured across a section in North Inlet, South Carolina (from Kjerfve & Proehl 1979).

At the bridge the channel cross-section is of *regular shape*, 234 m wide and 8.6 m deep (Fig. 4.4). Intensive measurements were made from the bridge over a neap *tidal cycle*, using gauging cranes and Gurley current meters, hence the data are free of errors due to boat motion. Velocities were measured at *32 stations* shown in Fig. 4.4, with each gap between bridge piers covered by two verticals, except for the end gaps near the shore, where only one vertical was sampled. Velocities were measured at points 0.1, 0.4, 0.6, 0.9 of the total depth on each vertical (when the water was deep enough to do this), and at approximately 30 minute time intervals throughout the tidal cycle. Water level was measured at 10 minute intervals by a recorder at the site. The cross-section was well described by continuous echo soundings across the section. Current velocity was measured for 40 meter revolutions or 50 seconds, whichever was quicker. In total about 3,300 measurements of current velocity were made. The field measurements were made during low freshwater inflow, and therefore stream inflows had a negligible effect on the records.

These results illustrate three main points:

(1) Substantially reducing the number of verticals (from 32 to a sensible selection of 3) did not result in large differences in the tidal prisms. Apart from option H (ebb tide), the largest variation was only 3.9%. This suggests that the flow through the section is fairly uniform, perhaps due to the regular channel shape and the flow regulation of the bridge piers.

(2) There were some differences in the flood and ebb tidal prism estimates (Table 4.3). The surprisingly good estimate for the flood tide prism using only 3 verticals in option H, contrasts markedly with that for the ebb tide where the prism was 13% less than that calculated using all 32 verticals. Plotting discharge vs time using different numbers of verticals shows this discrepancy, particularly at peak ebb flows (Figure 4.5).

Table 4.3 Estimates of tidal prism for Mangere Inlet after removing various verticals whose locations are given in Fig 4.4. % variations in flood and ebb tidal prism estimates are relative to option A.

Option	No. of verticals	Flood prism ($x10^6$ m^3)	Ebb prism ($x10^6$ m^3)	% variation Flood	Ebb
A All verticals	32	6.993	6.738	0.0	0.0
B Remove end verticals 1 & 32	30	7.099	6.736	+1.5	-0.02
C Remove 3 verticals at each end	26	7.268	6.796	+3.9	+0.9
D Remove all verticals in alternate pier gaps (i.e., 2, 3; 6, 7; ...; 30, 31)	16	6.873	6.753	-1.7	+0.2
E Remove all even Nos. except No. 32	17	6.738	6.720	-3.6	-0.3
F Remove all odd Nos. except No. 1	17	7.212	6.752	+3.1	+0.2
G Leave only 3 verticals (5, 17, 28) to cover left, right sides & centre	3	6.968	6.606	-0.4	-2.0
H Leave only 3 verticals (4, 16, 29) to cover left, right sides & centre	3	6.872	5.850	-1.7	-13.2

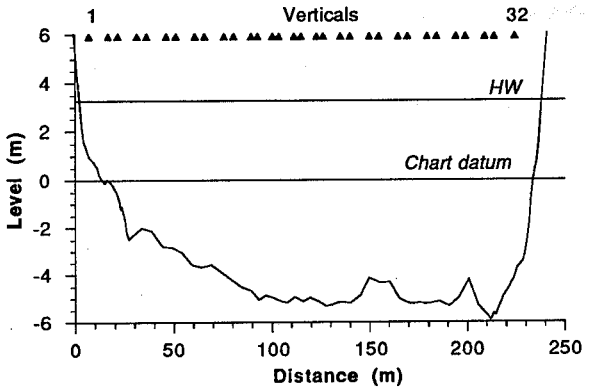

Figure 4.4 Channel cross-section at Mangere Inlet showing location of the 32 measurement stations (verticals) across the section.

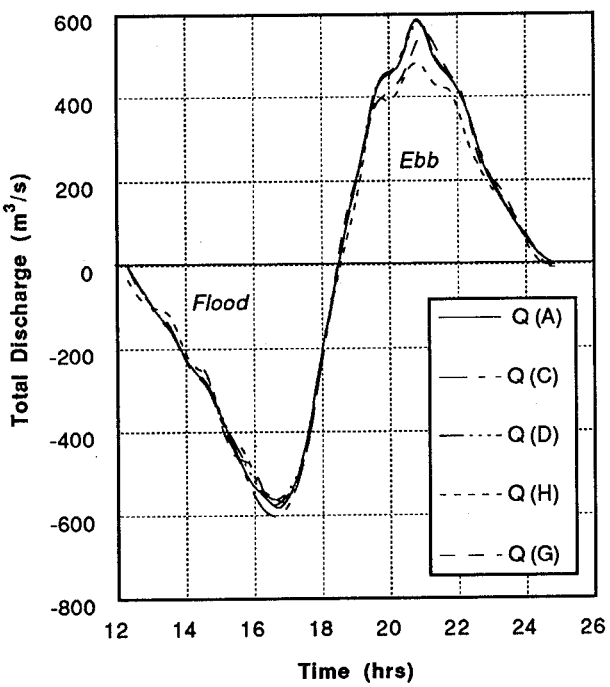

Figure 4.5 Time variation in estimated total discharge through the Mangere Inlet channel for a selection of combinations of verticals (measurement stations) detailed in Table 4.3. A = 32 verticals; C = 26 verticals with the 3 at each end removed; D = 16 verticals with all verticals in alternate pier gaps removed; H = 3 verticals to cover left, right and centre; G = 3 different verticals to cover left, right and centre.

We recently reanalysed the Mangere dataset, using the TIGA program for tidal gauging analysis (described in Chapter 5), to investigate the effect of varying the spatial density and number of measurement stations on tidal discharge and prism. The results are summarised in Table 4.3.

The reason for this effect can be seen in Figure 4.6, which is a plot of the tidally-averaged (or net) velocity at each vertical over a full tidal cycle. The selection of verticals 4, 16, 29 (Option H) meant no net ebb velocity sites were included in the calculations, and hence the ebb tide prism estimate was considerably reduced. In comparison the other '3 vertical' option (G), using adjacent verticals 5, 17, and 28, included a mixture of ebb and flood net velocities and therefore resulted in a more accurate estimate. This result emphasises the need to have a reasonable coverage of verticals across the section, even where the channel appears to be regular, to account for the different flow patterns between the flood and ebb tides.

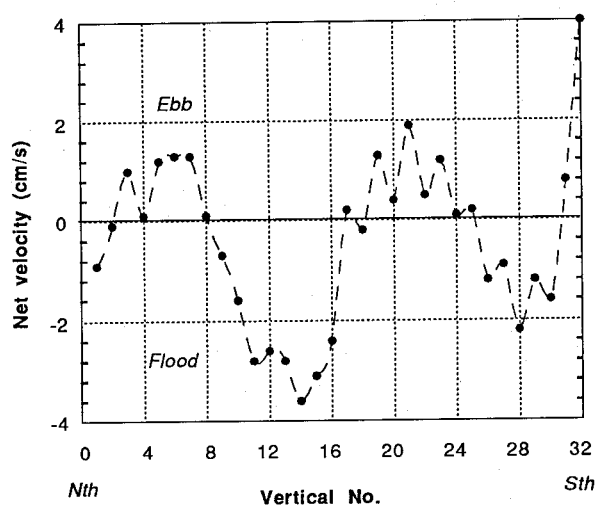

Figure 4.6 Plot of the tidally-averaged velocity (or net or residual velocity) at each vertical over a full tidal cycle across the Mangere Inlet channel. Note the -ve values represent flood tide velocities and the +ve values ebb tide velocities. The x-axis is not to scale.

(3) The importance of having verticals at the extreme ends of the cross-section are indicated by the overestimate in flood tide prism that results when these verticals are left out (e.g., option C +3.9% in Table 4.3). This is also shown in Fig. 4.5 by the "overshoot" at the peak discharge on the flood tide, where most of the 'error' would have been generated. For less regular shaped sections, the placement of verticals at the extremities will take on an even greater significance, as shown in the next case study.

Case Study 3 - Parerau River, Kaipara Harbour

A gauging undertaken at the Parerau River, a tidal creek in the Matakohe River arm of the northern Kaipara Harbour (McLachlan 1981) to provide data for the design of a roading causeway. At the site the channel cross-section is of *irregular shape*, and about 80% of the 260 m wide section is *intertidal* (Fig. 4.7). Here the extensive intertidal muds, vegetated with mangroves up to 3 m high in places, make access to, and measurements at, the site difficult from a practical

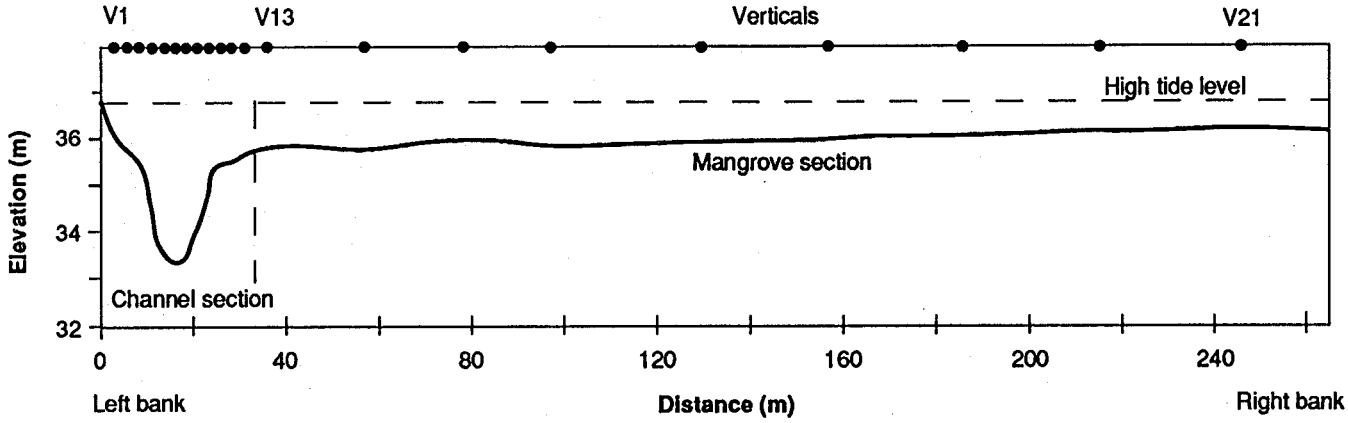

Figure 4.7 Channel cross-section at Matakohe showing location of measurement stations (verticals).

point of view, and special characteristics of the hydrology need to be anticipated. The tidal gauging at this site involved a standard tag wire gauging from boats in the channel section, supplemented by wading the shallow "mangrove" section. Velocities were measured at *21 stations*, with 12 verticals concentrated in the main flow path, and 9 in the mangroves (Fig. 4.7). Details are given in McLachlan (1981).

On the day of the gauging the spring tidal range was about 3 m. Only the ebb tide flow was gauged and it lasted about 5 hours. The velocity measurements demonstrate that the tidal currents through the mangrove section are very weak (<0.05 m/s), and that they only persist for the first 1.75 hours of the ebb tide (Fig. 4.8).

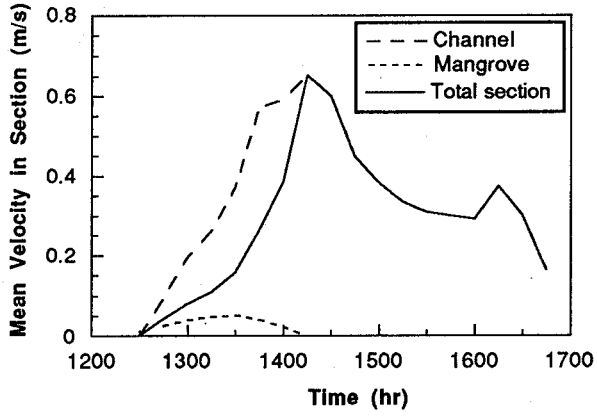

Figure 4.8 Variation of mean velocity in section through time for an ebb spring tide at Matakohe Estuary.

In comparison flow in the channel section is much faster, peaking at 0.65 m/s about 1.75 hours after HW, or about the time the tidal flats have drained and when the flow first becomes confined to the channel section. There is also a minor peak in velocity some 4 hours after HW. A plot of discharge vs time (Fig. 4.9) shows that flow through the cross-section peaks at 27 m^3/s and that the total volume passing through the section on the ebb tide, is 163,800 m^3. A comparison of Figures 4.8 and 4.9 highlights the fact that although currents are very weak in the shallow mangrove section, and flow for a short time only, the large cross-sectional area means that the mangrove section delivers a substantial amount (14%) of the total ebb flow volume. In fact, in the first 1.75 hours of the ebb tide, 22% of the total ebb volume passed through the intertidal section.

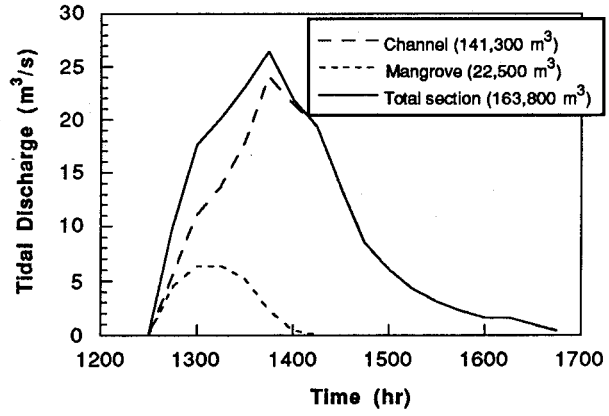

Figure 4.9 Variation of tidal discharge through time for an ebb spring tide at Matakohe Estuary.

Summary

While the choice of lateral distribution of sampling stations must be made on a case-by-case basis, the results from the gaugings described above, and other experience, permit some general principles and recommendations to be made as follows:

(1) In some cases, a reasonable estimate of tidal prism can be obtained from only a few measurement stations (at least 3 for regular-shaped narrow cross-sections). However, in channel cross-sections that are irregular in shape it is critical that the verticals are strategically placed to minimise errors. Furthermore, even in sections that are regular in shape there must be sufficient measurements such that the flow differences between ebb and flood tides are accounted for.

(2) Experience has shown that in estuaries, where the cross-section is generally wide and shallow, it is better to sample the channel cross-section at

numerous stations (or verticals) along the cross-section, rather than make intensive measurements at only a few verticals (van de Ree & Stuip 1984b). Plotting and examining the estuary cross-section on a non-exaggerated scale (Fig. 4.10) highlights this fact, and will assist in optimising the sampling network.

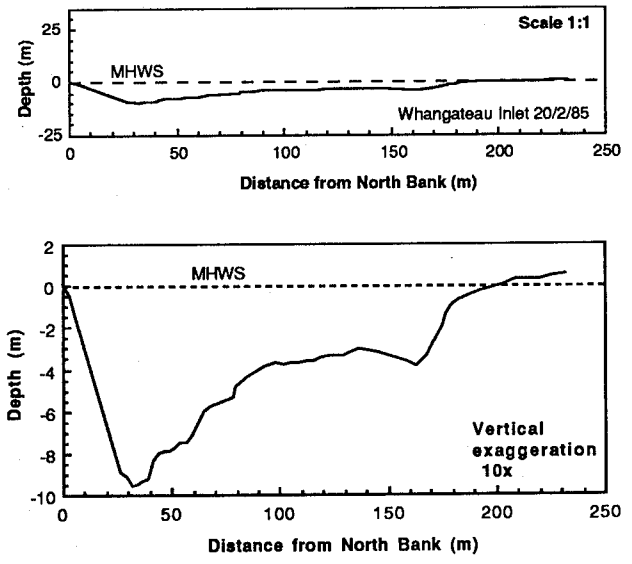

Figure 4.10 Estuary cross-section at Whangateau inlet comparing plots at normal scale with the more commonly presented vertically exaggerated scales, which shows that the depth of the estuary is generally only a fraction of the total width.

(3) In general for narrow and deep cross sections, fewer lateral stations will usually be required for flux computations (Kjerfve *et al.* 1981), although it may be wise to measure the velocity at more points in the vertical profile.
(4) Sampling stations should be placed at intervals across the section to sample the main channel (where most of the flow occurs), the sides of the main channel, the secondary channels or flood and ebb dominated channels and above any shallow bars separating the channels. Intervals between stations may be irregular if necessary to sample change points along the section.
(5) Placement of verticals at the ends of the section is important, even if they dry out at low tide, particularly in irregular shaped channels.
(6) In situations where there are extensive intertidal areas an attempt should be made to quantify flow over the tidal flats, which will peak perhaps only an hour or two after the HW, and where the current velocities may be very weak.

The method finally used to calculate discharges and fluxes also has a influence on the positioning of the velocity sampling stations (see Chapter 5).

Measurement of vertical velocity profiles
A current meter measures velocity at a point where the velocity is not constant but fluctuates due to turbulence induced by eddies of various lengths. The water velocity can be reduced to the sum of two components: an *average* component (deterministic) and a high frequency *stochastic* component. In most instances, a measurement time of 50 seconds or more is required to average out the influence of the stochastic component.

The mean velocity in a vertical is generally obtained by one of two methods. In the *multi-point method* the mean velocity is approximated by making velocity observations at several fractions of the total depth, that have been established by previous experiment to represent an estimate of the depth-averaged velocity. In the *vertical velocity curve method* velocities are measured at several points in the vertical and a mean is derived by mathematically fitting a curve to the data. The multi-point method assumes a logarithmic velocity profile, and uses measurements at a few selected relative depths on the profile to determine a mean velocity by calculating a simple arithmetic average.

The multi-point method is widely used in river gauging surveys, where the mean velocity is the average of observations made in each vertical at 0.2 D and 0.8 D of the depth D *below* the surface (the two-point method), or at 0.1 D, 0.4 D, 0.6 D and 0.9 D (the four-point method), and 0.6 D (the one-point or six-tenths method) for shallow waters where a single observation is used as the mean velocity (Rantz *et al.* 1982).

The vertical velocity curve method involves interpolation and is discussed by Rantz *et al.* (1982), Kjerfve (1979) and van de Ree & Stuip (1984b). The latter describe an arrangement of measuring points in a vertical (Fig. 4.11) found to be satisfactory, based on the experience of the Rijkswaterstaat in tidal regions of The Netherlands. To minimise errors, introduced by the need to extrapolate the velocity curve to the surface and to the bed, it is desirable to make measurements as close to the bed and water surface as possible.

In estuaries, the vertical velocity profile often follows a logarithmic profile, described by:

$$\frac{u-\bar{u}}{u_*} = \frac{1}{k} \log_e\left(e\,\frac{z}{D}\right) \;:\; z>z_0 \qquad (4.1)$$

where u = velocity at depth z, and u = $\bar{u}$ at z = D/e (=0.37D) above the bed, z_0 = bed roughness height, e = 2.7183, u_* = shear velocity, and k = Von Karman constant (= 0.4). Dyer (1970), however, points out that some profiles are best described by other formulations. For example a power law relationship such as:

$$\frac{u}{u_1} = \left(\frac{z}{z_1}\right)^{1/p} \qquad (4.2)$$

where u_1 is the velocity at reference height z_1, and p is normally considered to be between 7 and 10, may be more appropriate. Alternatively, a compound profile

comprising two different logarithmic slopes separated by a shear layer may sometimes be better.

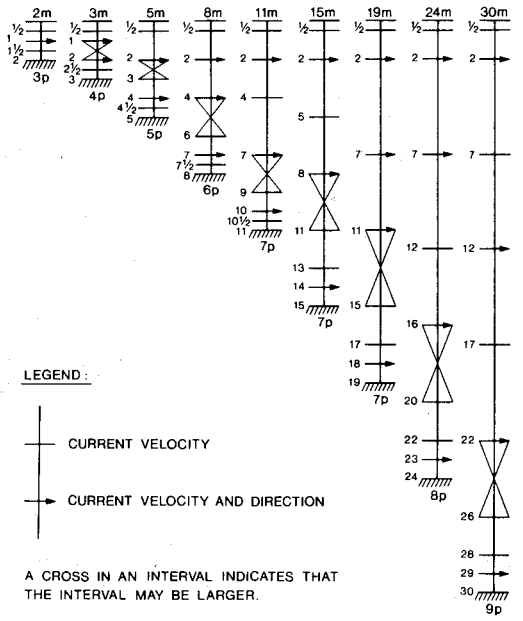

Figure 4.11 Arrangement of velocity measuring points in a vertical based on the experience in tidal regions by the Rijkswaterstaat in The Netherlands (from van de Ree & Stuip 1984b). The data show that for a water depth of 15m, for instance, the measurement points are not equi-spaced, velocity should be measured at 7 points in the vertical, and that both current velocity and direction should be determined at least 3 of these points.

In very shallow waters (say less than 1m depth) it is usually only practical to measure velocity at one point in the vertical, although this does depend to some extent on the type of current meter being used and the depth that the sounding weight assembly hangs below the meter. In deeper waters it is advisable to make at least three velocity observations for each vertical so as to enable a velocity profile to be interpolated (and extrapolated) between the bed and the water surface.

Caution is required when calculating mean velocities using the multi-point method in case the velocity profile is not logarithmic. Christensen (1990) presents a useful multi-point method (Table 4.4) which gives the relative depth levels for a given number of measurement points in a vertical. Importantly, the change in the velocity between neighbouring point in such a vertical profile ($\Delta u = u_i - u_{i+1}$) will be a *constant* if the velocity profile is logarithmic. This method can therefore be used to provide an immediate field check of the logarithmic assumption for the velocity profile.

For sediment studies, it is normal to have one of the velocity measurements observed at 1m above the bed. This measurement can then be readily related to the threshold of sediment motion or shear stress on the bed.

The estimated tidal prisms will vary depending on whether the mean velocity has been obtained by the multi-point method or the vertical velocity curve method. For the Mangere Inlet case, using the different methods results in differences in the flood and ebb prism estimates of 4.8% and 5.3% respectively (Table 4.5).

Experience has shown that the vertical velocity curve method is likely to be more reliable, particularly in cases where the velocity distribution does not follow a uniform logarithmic velocity profile over the depth e.g., where marked velocity fluctuations occur in the vertical, and during tide changes.

Sampling rate

The question of temporal sampling rate has received considerably more attention than that of the lateral sampling system. As tidal currents largely dominate the current velocity regime in an estuary, it is necessary to sample a number of times over the semi-diurnal tide cycle (period approximately 12.4 hours) to define adequately the cyclic velocity variation. It is generally recognised that 1.5 hours (8 samples per tide cycle) is the longest acceptable interval between measurements (Kjerfve *et al.* 1981). Generally, half-hour intervals (25 samples per tide cycle) are the optimum, although this may vary for practical reasons such as the availability of boats, instruments and personnel. It is also important to carry out a few extra measurements over the half-hour before and after the start and finish of the tide cycle to cover the period of slack tide, and thus fix the times when the velocity changes direction.

Starting time and duration of measurements

As most tidal gaugings employ only direct reading instruments, either one (12-15 hours) or two (25 hours) tidal cycles may be the maximum practical limit. The shortest meaningful duration is a half tidal cycle (approx. 6.5 hours). If net or tidally-averaged velocities are required, Kjerfve (1975) recommends a *constant* sampling rate and suggests that measurements begin around either high or low water, when currents are minimal. This will serve to minimise possible averaging errors due misinterpreting the duration of the tidal cycle period, which can vary depending on tide type, river flow, meteorological effects etc. For example, two tidal gaugings executed at the Tairua inlet for spring and neap tides yielded tidal cycles of 12.1 and 12.5 hours respectively (Hume *et al.* 1986c).

In our experience starting a gauging around high water is easiest because the phase lag or time difference between HW and slack water is generally shorter than for LW. Launching boats and setting out buoys or taglines to mark sampling stations (often deployed immediately before a gauging to minimise navigation interference) are also more easily accomplished at high water. A start time in daylight is also recommended as it enables a routine to be established before nightfall.

Table 4.4 Relative location of measurement points *below* water surface, starting at either 0.1 or 0.2 of the depth (after Christensen 1990).

Number of Measurement Points Starting 0.1 D iD	n = 1	n = 2	n = 3	n = 4	n = 5	n = 6	n = 7	n = 8	n = 9
(1)	0.632	0.100	0.100	0.100	0.100	0.100	0.100	0.100	0.100
(2)	-	0.850	0.632	0.504	0.425	0.371	0.332	0.303	0.280
(3)	-	-	0.850	0.727	0.632	0.560	0.504	0.460	0.425
(4)	-	-	-	0.850	0.765	0.692	0.632	0.582	0.540
(5)	-	-	-	-	0.850	0.785	0.727	0.676	0.632
(6)	-	-	-	-	-	0.850	0.797	0.749	0.706
(7)	-	-	-	-	-	-	0.850	0.806	0.765
(8)	-	-	-	-	-	-	-	0.850	0.812
(9)	-	-	-	-	-	-	-	-	0.850
Starting 0.2 D									
(1)	0.632	0.200	0.200	0.200	0.200	0.200	0.200	0.200	0.200
(2)	-	0.830	0.632	0.523	0.458	0.414	0.383	0.360	0.340
(3)	-	-	0.830	0.716	0.632	0.570	0.523	0.487	0.458
(4)	-	-	-	0.830	0.750	0.685	0.632	0.589	0.553
(5)	-	-	-	-	0.830	0.770	0.716	0.670	0.632
(6)	-	-	-	-	-	0.830	0.780	0.736	0.697
(7)	-	-	-	-	-	-	0.830	0.789	0.750
(8)	-	-	-	-	-	-	-	0.830	0.795
(9)	-	-	-	-	-	-	-	-	0.830

Nevertheless there can sometimes be an advantage in a night gauging, when the wind is less and the sea calmer than during the day. If anchored buoys are used to mark stations in shallow estuaries, then the lines should be shortened and lengthened as necessary during the falling and rising tides to minimise boat swing on the mooring. Boat swing can change the depth of the water at the measurement station and also result in swing of the current meter and therefore errors in velocity measurement.

Table 4.5 Comparison of estimates of tidal prism for Mangere Inlet made using the mean velocity obtained by the multi-point method versus the vertical velocity curve method (piece-wise log-fit profiles using TIGA, see next chapter).

Method	Flood tide ($x10^6$ m^3)	Ebb tide ($x10^6$ m^3)
Multi-point mean	6.656	6.382
Vertical velocity curve mean	6.993	6.738

Determining Material Fluxes

A different strategy is required to determine the flux of materials (solutes or suspended matter) than that for estimating the flux of water mass (or water discharge).

If salinity is being sampled in partially-mixed or stratified estuaries, it may be necessary to sample the vertical salinity profile at more depth levels than the velocity profile, particularly where the halocline occurs. Conversely, sampling may be less intensive where a depth layer is well-mixed with near constant salinity values.

The velocity profile depths may also be unsuitable as sampling points for other solute or particulate material concentrations. For suspended sediment fluxes, the coarser fraction is concentrated in the bottom one to two metre layer (McCave 1979), and therefore suspended sediment sampling should be biased towards the bottom layers. When measuring the flux of particulate matter, sampling should be more intensive when current velocities are greatest, because the sediment transport varies approximately as the 3rd power of the current velocity, and a threshold velocity must be exceeded before sediment movement occurs. Sediment transport varies laterally across channels, particularly in the vicinity of an estuary mouth. Strong flows and sediment transport are common around the tips of sand spits on the incoming tide. Close examination of bathymetric charts or aerial photographs taken at low tide will indicate whether flood and ebb dominated channels exist. If they do, then it may be necessary to concentrate sampling in the flood channel during the flood tide and in the ebb channel on the ebb tide to get a more representative sample of material fluxes.

For nutrient or other solute fluxes, an overriding constraint is often the limited number of laboratory

analyses which can be performed. Therefore, only the surface and mid-depth (or bottom) layers should be sampled and, if concentrations are likely to be relatively uniform across the section, samples could be reduced to every alternate station.

Carrying Out the Measurements

For each tidal gauging the following information should be recorded:

- Name and location of the measurement site
- Exact location of the site (map reference and physical description)
- Name of authority conducting the measurements
- Names of persons making the measurements
- Date
- Number of verticals
- Horizontal distance of the vertical profiles from the zero point
- Method of measurement (current meter, cable or rod suspension, floats, dye)
- Instrument details (meter type, number, rating table number)
- Exact beginning and end time of the gauging
- Tide type and ranges
- Special comments (e.g., disturbances from boat traffic, meter damage, time of tide reversals)
- Water levels every 5-10 minutes
- Tide gauge datum

For the point measurements:

- Number of individual vertical (V1, V2, V3.....etc)
- Total water depth at the vertical (m)
- Number of observation points in the vertical profile, and fraction of water depth (0.2, 0.8.... etc)
- Depth (m) of each observation point below the water surface
- Time of measurement (hrs, Standard Time or Daylight Time)
- The current meter revolutions (revs), duration of measurement time (secs), and current direction (note whether current is flowing 'to' or 'from')
- Water temperature and salinity (if required)
- Water sample numbers (if required)

In addition the following may be required:

- Details on the weather (wind, air temperature, rain, atmospheric pressure)
- Reference tide gauge or recorder
- Size of catchment area and river inflow estimate

An example of a form for recording these details is presented in Appendix II. It is important that on each page of the measurement records that the name of the site and the date should be entered, along with the page number.

Chapter 5

DATA PROCESSING AND FLOW COMPUTATION

Pre-Processing Tidal Gauging Data

No matter how sophisticated the analysis methods are, good results are dependent on good input data. This is particularly true as data interpolation and extrapolation are an integral part of most tidal gauging analysis techniques. Data interpolation and extrapolation are necessary because of the unavoidable sparseness of the measurement points in the cross-section, both laterally and vertically, and also in time (sampling intervals being typically every half-hour). Therefore, the error in the computed tidal prism or flux is compounded not only by actual measurement errors (e.g., current meter, boat movement, tide levels etc), but also by errors inherent in the computational methods used to derive the cross-section and time-series estimates of flow and material fluxes.

Regardless of how the data were obtained and entered into a computer file, it is essential that a thorough check for errors be made before any analysis begins. The data check should look at the following items.

Cross-section bathymetry and water level

Bathymetry

- Check the direction which the cross-section soundings were run (e.g., east to west or vice versa), and from this determine that left and right banks are correctly noted on the sounding traces.

- Ensure bed levels were surveyed through the intertidal areas, up to at least the maximum water level attained during the gauging.

Water level

- Check that the water level data has been reduced to the same datum as the cross-section reference datum.

- Plot the water level time-series to check for any obvious errors. Note that seiching, a natural process, can occur under certain conditions in estuaries or harbours, producing secondary short period (e.g., 10 to 60 minutes) water level oscillations.

- Look for any timing drift errors for a recorded water level time-series.

Current velocity

Time

- Measurements on the data file for each station should be sequential in time. If the gauging period moves into the next day, the time format may need to take this into account for some computer programs e.g., 0100 hrs on the second day could be entered as 2500 hrs.
- Check that the time base is consistent throughout i.e., NZ Standard Time (NZST) or NZ Daylight Time (NZDT), including the water level time-series.

Speed

- Ensure the meters have been recently calibrated and that the correct calibration coefficients are entered.
- Check that the speed readings (either revolutions or actual speed) for each depth in any one vertical are consistent. Speed generally increases in magnitude towards the surface (not a necessary condition for most analysis procedures). Any large variations in speed between adjacent points in a vertical should be investigated. Large variations in the vertical can throw the interpolation/extrapolation routine into disarray or bias the mean velocity computed where the multi-point averaging technique is used.
- Check that the speed has the correct sign (usually positive for ebb and negative for flood tides) if no directions were measured. It is usually necessary to measure direction when the estuary is wide, or has a complex bathymetry or shape (e.g., flood and ebb tide dominated channels).
- A common fault in many gaugings (often due to a late start) is the lack of velocity and time data defining the slack water periods. If no measurements are possible at the start or finish, then at least the time when the current direction changed should be entered, with an assumed zero or low velocity. This then constrains any extrapolation in time that may be required from the first or last velocity measurement.

Direction

- Check whether directions are in *Magnetic* or *True North* format. If the former, then the Magnetic North declination angle will need to be added (usually during the initial data manipulation phase). The declination angle can be readily obtained from Navy or Admiralty Charts of the area. Also check whether the directions are in the usual oceanographic convention (i.e., direction current is flowing to) or vice versa.

Depths

- Depths of point velocity measurements are most often measured in metres *from the water surface,* but sometimes from the bed. Check that all the depth values are in a consistent reference frame e.g., from the water surface (particularly where a combination of boat and wading gauging is used).

Solutes

Time (as above)

Concentration/value

- As above for speed, the measured values in any one vertical should be consistent e.g., it is very rare that the salinity decreases with depth below the surface, unless there is a nearby outfall discharge.
- Each field instrument should be calibrated before and checked during and after the gauging if possible, to correct for drift, and the solute readings adjusted accordingly.

Depths

- As above, ensuring same reference system is used for both water velocity and solutes.

Suspended sediment

Time (as above)

Concentration/value

- As above for speed, the measured values in any one vertical should be consistent. Suspended sediment concentrations will generally increase with depth below the surface, being highest immediately above the bed.

Depths

- As above, ensuring same reference system is used for both water velocity and sediment.

While these checks may seem tedious and time-consuming, they will ensure that avoidable errors (e.g., transcribing errors and inconsistencies) are minimised, producing the most reliable results within the accuracy of the methods used to measure and analyse the data.

Data Processing and Analysis Programs

With the pre-processing checks complete, the raw data is in a standard format and ready to be processed. The processing can be done by hand (i.e., calculator or graphical method), or more easily by a set of computer analysis programs, based on the methods outlined in this Chapter and Chapter 6. There are a few comprehensive analysis packages available, which have been specifically designed for tidal gauging analyses. Examples of such packages are discussed in detail by Kjerfve (1979) and Bell & Burton (1986), the former containing the FORTRAN source code.

Programs designed by Kjerfve (1979) have been adapted and extended to produce a generalised FORTRAN tidal gauging analysis package called TIGA (Tidal Gauging Analysis). TIGA runs on a VAX system and is described in detail by Bell & Burton (1986). It handles water velocity , salinity and temperature data. As an example of the type of analysis routines required for a tidal gauging, the processing programs of TIGA are:

SECTWL An input routine for entering and processing both cross-section bed levels and tide level data which are then reduced to the same reference datum. Data can be entered either from a disk file or keyed in via the terminal.

PROCESS An input routine for entering vertical profile measurements of velocity, temperature and salinity with preliminary processing of the data to:
- sort data into blocks for each station or site across the section
- compute speed from rotor revolutions
- correct for NZ Daylight Time
- add on Magnetic North declination to current direction
- intercept input errors, such as depths and times out of sequence.

PROFILE Computes vertical profiles of velocity, salinity and temperature in 0.1D increments based on the program of Kjerfve (1979).

FLUX Computes depth-averaged values and fluxes for velocity, salinity and temperature, using vertical profiles from PROFILE. Residual or net velocities and fluxes are also calculated, together with cumulative discharge volumes, material effluxes and tidal prism.

The TIDEDA system (Rodgers & Thompson, 1991) is widely used in New Zealand and overseas for river gaugings and it is possible to use this package to process some of the data e.g., compute depth averaged velocities, and generate plots.

It is assumed in the discussion below that the measurement technique employed is based on Eulerian measurements made from a bridge or boats at several verticals in a cross-section.

Computation of Vertical Velocity Profiles

Current velocity and depth are measured at finite points between the bottom and the water surface. These points may be more or less regularly spaced. As mentioned in Chapter 4 (Current Measurements), there are two main methods for determining the mean or depth-averaged velocity for each profile. In the *multi-point method*, the mean velocity is approximated by making velocity observations at several fractions of the total depth, that have been established by previous experiment to represent an estimate of the depth-averaged velocity (see Walker 1988, for a general two-point method). As an example, where the three-point method (0.2D, 0.6D, 0.8D) was followed during the gauging, the mean velocity can be estimated by the arithmetic average $\overline{U} = (U_{0.2D} + U_{0.6D} + U_{0.8D})/3$. The multi-point method assumes the velocity profile is always a single logarithmic relationship with depth, which is not always the case, unless established prior to, or during, the gauging by several intensively sampled vertical velocity profiles. In the *vertical velocity curve method*, a mean is derived by mathematically or graphically fitting a vertical profile curve through the measured velocities at various depths and integrating over the depth. The graphical fitting technique and the subsequent computation of the mean velocity are described in DVWK (1990).

To standardise the data analysis, it is desirable to

interpolate the shape of each vertical profile and then read off the data values at regularly spaced intervals (see discussion in Kjerfve 1979). The data points used in the analysis are therefore interpolated data, not the measured values. This procedure is likely to be more accurate than using the simple averaging approach of the multi-point method.

Interpolation of the actual measured points in the vertical profile allows more flexibility as the type of profile may change, especially during tide reversals when oppositely directed flows often exist between the surface and bottom layers. For various reasons, material concentrations are not always sampled or measured at the same depths as velocity. Therefore when computing material fluxes it becomes essential to use an interpolated profile to match both velocity and material concentration/values at common depth levels. The method of making velocity measurements at *fixed depths* below the water surface (e.g., 0.5, 1.0, 1.5 m ....etc) is not generally recommended, particularly for situations where the tidal range is a significant fraction of the total depth.

Interpolation methods

The most favoured approach to defining estuarine vertical profiles is to use non-dimensional depths. This was first used by Bowden (1963) on the Mersey and further developed as a general method by Kjerfve (1975, 1979). It enables the water level variation throughout a tidal gauging to be accounted for, and enables a rational procedure to be adopted for computing time-averaged or net velocity profiles, flow discharges and material fluxes.

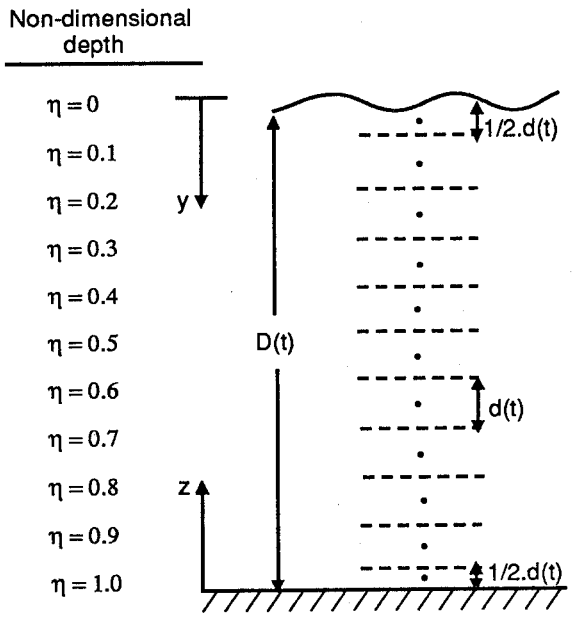

Key: • = computed velocity U(η,t)

Figure 5.1 Non-dimensional depth notation and vertical reference frames.

At any station, let the instantaneous water depth be D(t). A non-dimensional ratio can be defined:

$$\eta = \frac{y}{D(t)} \qquad (5.1)$$

where y = the distance *below* the instantaneous water surface, y = 0. Therefore at all times the water surface is represented by $\eta = 0$ and the bed by $\eta = 1$ as shown in Figure 5.1.

A unique vertical velocity profile at each sampling time can be interpolated or plotted from the measured velocity data using piece-wise curve fitting procedures, such as cubic spline algorithms. The computed velocity profile can then be represented by velocities at equally spaced depth levels e.g., every one-tenth of the depth from the surface to the bottom. The derived velocity at the surface ($\eta = 0$) would be denoted by $U(\eta_0, t)$ while at the bottom ($\eta = 1$) the velocity would be $U(\eta_{10}, t)$.

Therefore to obtain the depth-averaged velocity at any time t, the equi-spaced interpolated velocities, $U(\eta, t)$, are averaged as follows:

$$\bar{U}(t) = \frac{1}{10}\left\{ \frac{1}{2}U(\eta_0,t) + \sum_{j=1}^{9} U(\eta_j,t) + \frac{1}{2}U(\eta_{10},t) \right\} \qquad (5.2)$$

with a weighting of 0.5 given to the surface and bottom velocities, as $U(\eta_0, t)$ and $U(\eta_{10}, t)$ are only representative over half a depth increment (see Figure 5.1). In some schemes such as the one described in Kjerfve (1979), the bottom segment velocity, $U(\eta_{10}, t)$, is assumed to be zero.

Turning back to the vertical interpolation-extrapolation procedure, the velocity profiles can be obtained either graphically or numerically from the finite number of measured points. The latter method is preferred to reduce both the time taken and the risk of errors. The procedure adopted by Kjerfve (1979) was to fit a curve through the measured data using a cubic spline interpolation procedure (e.g., as given by Pennington 1970). With N depth measurements for any one profile, the spline technique requires the determination of N-1 piece-wise continuous third order polynomials which describe N-1 curved segments, assuming the curvature is constant where the segments join. Problems from excessive curvature can arise when the profiles are extrapolated to the surface and the bottom from the nearest measured point. To minimise any errors introduced by the extrapolation, Kjerfve (1979) suggested it is desirable to make respective measurements as close to the surface as possible and less than 1 metre above the bed. Further, Kjerfve (1979) fitted to the bottom flow zone (up to 1 metre above the bed) the well-known logarithmic profile

described by Dyer (1970):

$$U(z) = \frac{u_*}{k} \log_e\left(\frac{z}{z_0}\right) \qquad (5.3)$$

where z = distance *above* the bed (Fig. 5.1) and the other variables are defined in equation 4.1.

However, some shortcomings were found with the above cubic spline/logarithmic boundary profile procedure. Firstly, estuaries in New Zealand tend to be relatively shallow; a significant number of verticals are sampled in depths of around 1 metre, and they may not necessarily fit the "universal" logarithmic boundary layer profile (equation 5.3). Secondly, marked departures in *measured* velocity from a uniform or consistent profile causes unrealistic oscillations to develop in the cubic spline fit and hence inaccurate extrapolations to the surface.

An improved and more physically realisable procedure is possible, using piece-wise logarithmic splines between the measured data points. This serves to dampen rather than magnify perturbations in fitting piece-wise curves in the upper layers, and enables a full depth logarithmic profile to arise out of the computation if actual measurements adhere to a single logarithmic profile. Finally, the universal boundary layer logarithmic profile is easily incorporated at the bottom, as a separate piece, with the bed velocity being set at a small distance z_0 above the bed (or $y = D(t) - z_0$ below the surface), rather than zero at the bed, which is not possible with a logarithmic profile. This boundary layer profile can be fitted *below* the deepest measured velocity.

The development of the logarithmic piece-wise fitting procedure based on a similar equation to (5.3) is presented in Appendix III.

These extra refinements, necessary to extrapolate from the measured data, introduce some errors in the computation of fluxes and mean velocities, which highlights the need to make measurements reasonably close to the surface and the bed. A few examples of the resulting piece-wise logarithmic fit to measured velocity data are shown in Figure 5.2.

The interpolated vertical profiles for other parameters such as velocity, direction, salinity and temperature can be computed using the same method (cubic spline routine), as described by Kjerfve (1979). One refinement of this method (Bell & Burton 1986) is the use of the maximum salinity encountered during the tidal gauging (usually the open coast salinity), which is used to constrain the cubic spline fit of the salinity profile to that value near the bed and thereby prevent excessive oscillations in salinity. This problem frequently arises below the halocline, where the waters are well-mixed and where the salinity readings differ by only a few decimal places or so.

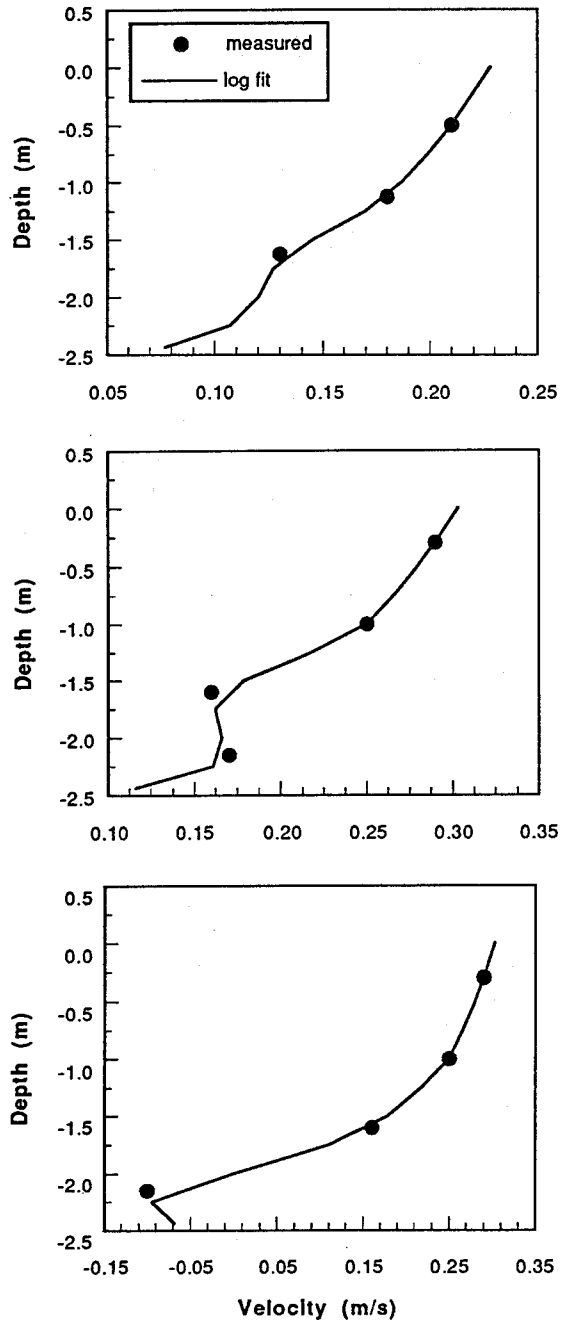

Figure 5.2 A few examples of piece-wise logarithmic interpolation to measured velocity data from a gauging at Tairua. These examples demonstrate the robustness of the method and its ability to handle various types of real or actual velocity profiles.

By using the interpolation techniques described above it is possible to estimate data values at the *same* dimensionless depth level η_j in each profile for each parameter measured.

Computation of Tidal Discharge and Prism

The discharge or water flow rate through an estuarine cross-section is calculated from the measurements or interpolated values of velocity and depth along with the horizontal distance between measurement sites.

The total discharge Q through a cross-section S of area A at a specific time, t, can be expressed by a double (or surface) integral:

$$Q(t) = \int_S\int U(x,y) \cdot dA \qquad (5.4)$$

where U(x,y) is the instantaneous velocity component normal to the section and the integral covers the entire wetted area of section S in small areal increments dA.

This double integral is approximated in river hydrology by summing the incremental flow rates q_i calculated from the mean velocity over the vertical profile and total depth at each measurement station (i = 1, 2... M), which applies over a representative width Δb_i of the sub-section. However, using this "river" approach for tidal gaugings has problems because the flow rate is continually changing due to the tide. Firstly, all measurement sites across the section should ideally be sampled simultaneously, but this is seldom achievable. To overcome this the flow-duration curves must be interpolated at the same regular time intervals for each *sub-section* over the gauging period before being combined to form the total flow-duration curve for the cross-section. Secondly, the intensity of sampling sites across the section is generally more limited to ensure each station is sampled regularly. To overcome this it is best to use the continuous bed profile (echo sounded depth trace) rather than relying on the depths at each vertical (or sampling station).

The tidal prism, or the *total* volume of water which flows through the section on either the flood or ebb tide, is defined as:

$$\Omega = \int_{T_0}^{T_1} Q(t) \cdot dt \qquad (5.5)$$

where $t = T_0, T_1$, define successive *slack water* times when the mean cross-section flow reverses direction.

Methods for incorporating the above refinements for tidal flows into reliable estimates of total cross-section flow and tidal prism are discussed below.

Computation of sub-section discharge

Several methods for estimating the water flow q_i through a sub-section of the total cross-section are described below and illustrated in Figure 5.3.

- *Depth-velocity integration method* - (Fig. 5.3) where the area under each velocity-depth curve across a section is determined by numerical or graphical integration to yield flows (q_v) per unit width at each vertical. The second stage of the computation is to determine the area under the fitted curve qv versus the distance across the section, again by numerical and graphical integration. The waters edge is assumed to have $q_v = 0$. Further details are given in DVWK (1990).

- *Mean-section method* - (Fig. 5.3) where the mean is taken of the two average vertical velocities at adjacent sampling stations i and i+1 and is then applied to the whole sub-section area *between* the sampling stations i.e.:

$$q_i = \frac{\bar{U}_i(t) + \bar{U}_{i+1}(t)}{2} \cdot \left\{ \frac{D_i(t) + D_{i+1}(t)}{2} \right\} \cdot \Delta b_i \qquad (5.6)$$

The area can also be integrated from sounding data in a similar manner to equation (5.8) between x_i and x_{i+1} ($= x_i + \Delta b_i$). Usually the instantaneous shore wetline at either side of the cross-section is assumed to be a sampling station with a velocity of zero.

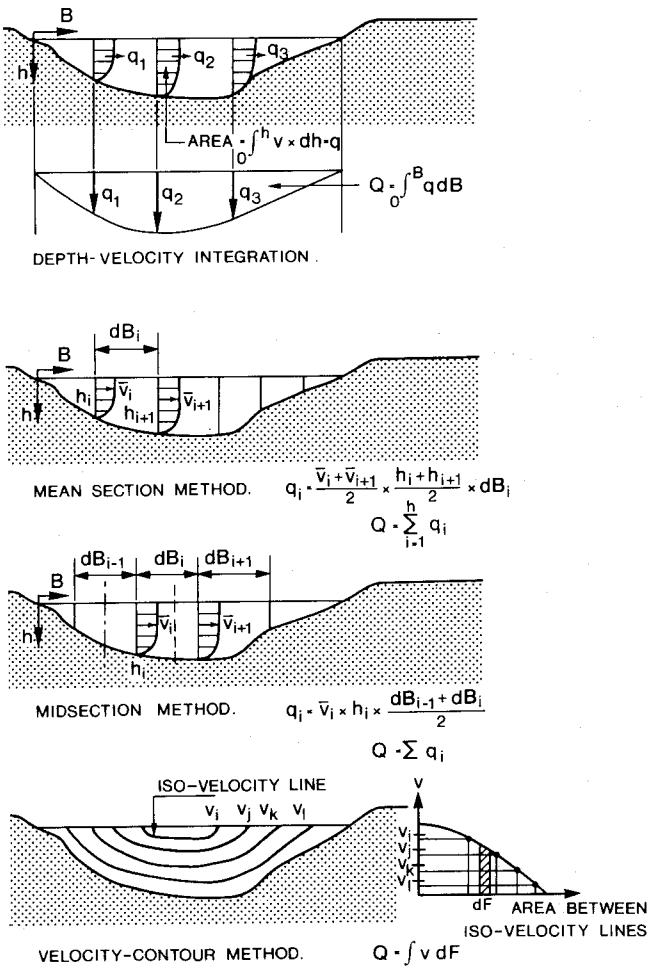

Figure 5.3 Four methods for computing tidal flow through a cross-section (from van de Ree & Stuip 1984b).

- *Mid-section method* - (Fig. 5.3) where the average vertical velocity measured at a sampling station is assumed to represent the mean velocity over a sub-section, which extends laterally from half the distance to the preceding station to half the distance to the next (as shown in Fig. 5.4). At time t the

flow rate (m^3/s) through the sub-section i is estimated by:

$$q_i = \bar{U}_i(t) \cdot D_i(t) \cdot \left\{ \frac{\Delta b_{i-1} + \Delta b_i}{2} \right\} \qquad (5.7)$$

where Δb_i = the distance between station i and i + 1

etc. and the average vertical velocity $\bar{U}$ is obtained from equation 5.2 or the multi-point velocity method. To include the refinement of using the sounding data, the sub-section area can be integrated or summed over finer distance intervals (Fig. 5.4) such that:

$$q_i = \bar{U}_i(t) \cdot \int_{x_i - 0.5\Delta b_{i-1}}^{x_i + 0.5\Delta b_i} D(x,t) \cdot dx \qquad (5.8)$$

where x is the distance across the sounded section and the depth D varies with x and t.
The first and last sub-section are extended to the instantaneous shore wetline applying at time t (Fig. 5.4).

In both the above methods, the total flow Q(t) at time t is the sum of the sub-section flows q_i.

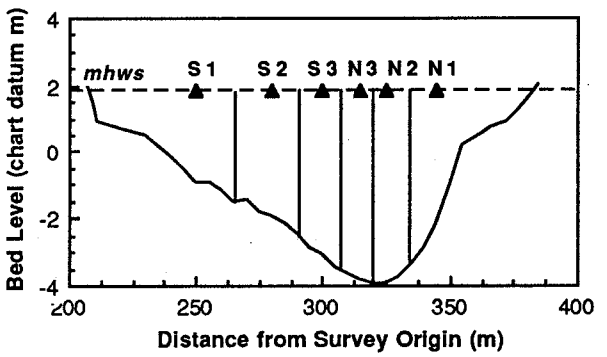

Figure 5.4 Example of subsections used in the mid-section velocity-area computation.

- *Ratio interpolation method* - was developed in 1981 for rivers where circumstances such as unsteady flow or navigation intensity enable only a few vertical sites to be sampled. The ratio interpolation method assumes that the ratio

$$\frac{\bar{U}_i(t)}{\sqrt{D_i(t)}} \approx \text{const} \qquad (5.9)$$

is nearly constant for a channel cross-section, having a similar form to a Froude number $U/\sqrt{gh}$, implying that the ratio of kinetic to potential energy is a constant. To compute the discharge, the cross-section is divided into an arbitrary number of equal-width sub-sections (e.g., 50, 100). The average vertical velocity for each sub-section is then determined by assuming the ratio in equation 5.9 varies linearly between measured verticals, and is constant between the bank and the nearest vertical. The method also assumes the channel cross-section has been accurately sounded using echo or weight soundings. Comparisons of this discharge computation technique with the mid-section method have been carried out for river sections by Fulford & Sauer (1986) and Bohman & Carswell (1986). As yet, it is untested on estuarine cross-sections and may be applicable only where channel sections are uniform with a regular lateral velocity distribution. It probably should not be applied in channels with shallow side banks (e.g., extensive inter-tidal areas) or irregular bathymetry unless sufficient stations are measured in these areas.

- *Velocity-contour method* - (Fig. 5.3) described in van de Ree & Stuip (1984b), where contours of equal velocity (isovels) in the entire cross-section are determined from the interpolated vertical velocity data $U(\eta_j, x)$ at a given time t. A function can be computed of isovel velocity versus area between isovels ΔF and the total flow through the cross-section is:

$$Q(t) = \int U \cdot dF \qquad (5.10)$$

In *summary*, the method used to calculate the flow rate influences the final accuracy of the results. Also, the location of sampling stations may need to be different depending on the method adopted, especially if the cross-section is irregular. Studies by Young (1950) and Hipolito & Loureiro (1988) conclude that the mid-section method is simpler to compute and is a slightly more accurate technique than the mean-section method. The ratio interpolation method and the velocity-contour method are not widely used for tidal gaugings.

Interpolation of Sub-sectional Discharge Time-series

Once the time sequences of sub-section flows q_i (t) at sites i measured at various times t throughout the gauging have been computed, sub-section flow-duration curves (e.g., Figure 5.5) can be interpolated. The sub-section flows at a particular time t_n, can then be combined to compute the total cross-section flow $Q(t_n)$. This order is necessary because vertical sites are seldom sampled all at the same time. Also, the measured velocities are seldom all perpendicular to the cross-section alignment. Both these aspects need to be standardised before computing the total flow Q.

A useful computation technique to interpolate, all the mean velocity, sub-section flow area and discharge time-series, is to perform piece-wise parabolic curve fitting to successive groups of three measured values over the gauging period. For example (Bell & Burton 1986), carry out the parabolic interpolation at intervals of Δt = 5 minutes, using a parabola of the form:

$$q_i(t) = a_1t^2 + b_1t + c_1 \qquad (5.11)$$

where a_1, b_1, c_1, are coefficients computed from three successive sub-section discharge measurements $q_i(t_1)$, $q_i(t_2)$, and $q_i(t_3)$.

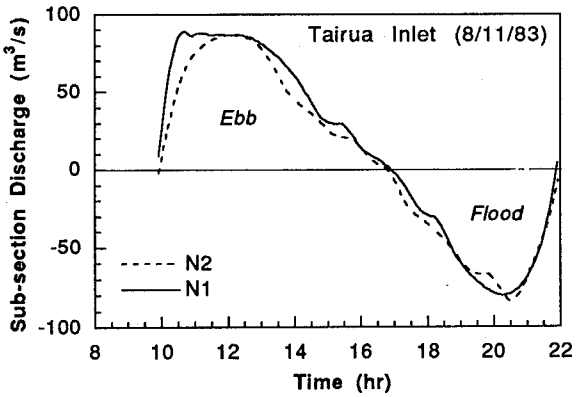

Figure 5.5 Interpolated flow-duration curves, q_i vs t, for two sub-sections (N2 and S2) at Tairua Inlet.

When $t > t_3$, another set of coefficients a_2, b_2, c_2 are computed from the set of sub-section discharges at $t = t_2, t_3, t_4$ and so on. When an initial measurement is not made around the slack water (U = 0) time, then extrapolation back through time (or forward) from the nearest velocity measurement is required. This can lead to significant errors, particularly if there is a long time interval to the nearest measured value. In order to eliminate extrapolation errors, measurements of velocity around slack water should be made at both the start and finish of the tidal gauging, even if velocities are very low. In this case it is the time of slack water that is important. The other problem which can lead to errors in the interpolation technique is a long time interval between successive measurements, particularly if the interval is greater than one hour.

For any estuarine tidal gauging, every effort should be made to measure the direction of the flow as well as the speed. The velocity, being a vector quantity can then be resolved into two orthogonal components (Fig. 5.6), with U_v perpendicular to the cross-section and V_v parallel to the cross-section alignment. To arrive at the flow q_i through the sub-section, only the perpendicular velocity component (U_v) should be included in the computation of the flow-duration curve (Fig. 5.5) before interpolation. The usual convention for the velocity components is to consider the ebb flow (outgoing tide) to be positive, with the flood tide negative and the lateral velocity (V_v) to be positive towards the right bank when looking in the direction of ebb tide flow.

Computation of total flow and tidal prism

It is now a simple matter to construct a flow time-series for the whole cross-section by summing the m interpolated sub-section flows $q_i(t_n)$ such that at $t_n = n.\Delta t$:

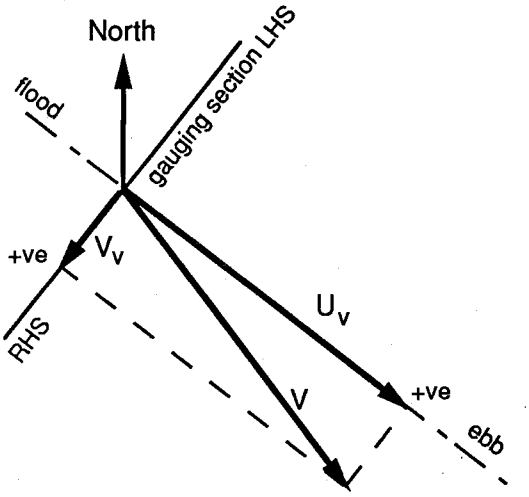

Figure 5.6 Velocity, being a vector quantity, can be resolved into two orthogonal components, with U_v, perpendicular to the cross-section and V_v parallel to the cross-section alignment.

$$Q_n = \sum_{i=1}^{m} q_i(t_n) \qquad (5.12)$$

where n = 1, 2,... N being the number of time-interpolated flow values at a constant time increment Δt, m = the number of sub-sections, and q_i is directed at right angles to the cross-section line.

The tidal prism Ω or cumulative flow through the total cross-section can be estimated over the half-tide period from equation 5.5 by the summation:

$$\Omega = \sum_{n=2}^{n=N_1} \frac{1}{2}(Q_n + Q_{n-1}).\Delta t = \Delta t \left[\frac{Q_1}{2} + Q_2 + Q_3 + ... + \frac{Q_{N_1}}{2} \right] \qquad (5.13)$$

where $N_1.\Delta t$ is the time closest to the next slack tide $t = T_1$ when Q changes sign. Note that n=1 should correspond closely to the time of the initial slack water. The summation can also be continued from then until the next slack tide when $t = N_2.\Delta t$, to yield the tidal prism on the reverse tide. There may be a difference between the ebb and the flood tidal prisms for any one tidal cycle (see Table 4.3). This can be attributed to several factors including net freshwater runoff, differences in successive HW levels (e.g., the diurnal inequality) or changes during the gauging due to non-tidal water level effects, such as rapid changes in atmospheric pressure.

Chapter 6

COMPUTATION OF MATERIAL FLUXES AND TIDALLY-AVERAGED QUANTITIES

When computing material fluxes of various dissolved solutes or suspended particulates the quantity measured is a concentration, say in units of mass per mass of estuarine water. Therefore the mass fluxes are derived in terms of mass per unit time after multiplying concentrations by the sub-section water flow rate and the water density.

In general, following Kjerfve (1979), the material flux f_i (in kg/s) at time t through a sub-section i of area a_i (m^2) is computed by:

$$f_i = \overline{\rho_i(\eta,t)\, c_i(\eta,t)\, U_i(\eta,t)} \cdot a_i(t) \qquad (6.1)$$

assuming that the concentration of a constituent, $c(\eta,t)$ in (kg/kg) has been interpolated for depth intervals $\Delta\eta$ from surface to the bed along with velocity $U(\eta,t)$ and water density $\rho(\eta,t)$ in kg/m^3. The overbar in the above equation indicates the vertical average of the multiplied quantity underneath. The density may vary significantly with depth and with time throughout the tidal cycle. For this reason any surveys requiring estimates of material fluxes should include both salinity and temperature profiles to enable water density to be computed, unless the density is known to be relatively uniform in the cross-section. The interpolated velocity values $U(\eta,t)$ should be the component U_v perpendicular to the cross-section line (Fig. 5.6).

It is important to note that the product $\rho_i.c_i.U_i$ in (6.1) is *first* computed at each depth level η *before* being vertically averaged in a similar manner to equation 5.2, replacing U by (ρ.c.U). A single product $\bar{\rho}_i.\bar{c}_i.\bar{U}_i$ using only the individual vertically-averaged values does *not* give the correct result.

With m stations in a cross-section, the total flux F_n at time t_n in (kg/s) is computed in a similar way to equation 5.12, by substituting the sub-section fluxes f_i in lieu of q_i. The total material tidal prism, or export/import mass, is computed from equation 5.13 with the total material fluxes F_n in lieu of Q_n, which are simply water mass fluxes.

Methods for computing the total and net (or residual) material fluxes are outlined below. In all computations care is required to ensure that consistent SI units are used.

Total Transport

Salt flux

The concentration of salts in marine waters is represented by the salinity S, which on the Practical Salinity Scale (as measured by conductivity) is given in units of 10^{-3} salt mass/mass of seawater i.e. a salinity S = 35 corresponds to a concentration $C(\eta,t) = 35 \times 10^{-3}$ kg/kg for calculation purposes. A salinometer is used to measure both conductivity and temperature and salinity can then be computed from these measurements.

The density of estuarine water $\rho(\eta,t)$ is dependent on salinity (S), temperature (θ) and water pressure, although the latter has a negligible effect for shallow coastal waters.

Look-up tables or formulae to calculate density as a function of temperature and salinity can be found in many texts e.g., Fischer *et al.* (1979), Kjerfve (1979), and Pond & Pickard (1983). A comprehensive computer program, based on the full 1980 equation-of-state for seawater (Pond 1983, p. 310), which computes a density anomaly (σ) is available in UNESCO (1983). Oceanographers are primarily interested in small variations in density and therefore have established a convention whereby:

$$\sigma = \rho - 1000 \ (kg/m^3) \qquad (6.2)$$

Thus for a density of 1026.95 kg/m^3 (S = 35; θ = 10°C), then the density anomaly σ = 26.95 kg/m^3. The density anomaly for some values of temperature and salinity are given in Table 6.1 which can be used for checking the correct use of formulae and computer programs.

Normally in estuarine surveys, the accuracy required for the water density value is less than is necessary for oceanic surveys where the salinity range is small. As a simpler alternative, if temperatures lie in the range 8 - 20°C, an approximation to the density anomaly can be computed using:

$$\sigma \cong \sigma_0 + k_\theta \cdot S \quad (kg/m^3) \qquad (6.3)$$

where σ_0 is the density anomaly at S = 0 (freshwater), (listed in Appendix A of Fischer *et al.* 1979), and k_θ is a coefficient depending on temperature. For a typical range of estuarine temperatures $8° \le \theta \le 20°C$, k_θ can be expressed as:

$$k_\theta = 0.798 - 0.002\,\theta \qquad (6.4)$$

Table 6.1 Reference values of the density anomaly (σ) in units of kg/m^3. (Based on 1980 equation-of-state for seawater for S > 2.0 and Fischer *et al.* (1979) for S = 0.)

Salinity S	Temperature θ (°C)		
	10°	15°	20°
0	-0.274	-0.875	-1.772
30	23.051	22.122	20.954
32	24.611	23.661	22.476
35	26.952	25.973	24.763

Equations 6.3 & 6.4 will yield estimates of σ with an accuracy of at worst $\pm$ 0.04 kg/m^3 which is more than adequate for most estuarine applications. (Note: larger errors will result if temperatures outside the above range are used). To obtain the actual density, ρ, simply add 1000 kg/m^3 to the density anomaly.

The ρ.S.U product yield results in units of kg/s/m^2, which, after vertical-averaging and using equation 6.1, produce fluxes f_i in kg/s.

Other solutes or particulates (e.g., nutrients, dye, suspended sediment)

Once the vertical profile concentrations $c(\eta,t)$ are known from interpolation of measured values, the flux computation is carried out using equation 6.1 in a similar manner to the salt flux calculation. The only difference is that concentrations of other constituents are often expressed in units of mass per unit volume e.g. mg/l. Table 6.2 lists the various concentration units in use and their equivalent mass/unit volume form. Note that all these conversions are approximate since they depend on fluid density. If concentrations are expressed in these units related to a unit *volume* of estuarine water, then it is necessary to leave out the water density $\rho(\eta,t)$ in the cross-product of equation 6.1.

Table 6.2 Equivalent concentration units.

ppt (parts per thousand)	≡	g/l or mg/l x 10^{-3}
ppm (parts per million)	≡	mg/l
ppb (parts per billion)	≡	µg/l
µg-atoms/l	=	µg/l ÷ atomic weight
µM or µmol/l	=	µg/l ÷ molecular weight
µg/l	≡	mg/m^3
mg/l	≡	g/m^3

Temperature

While temperature is often measured as an auxiliary to computing salinity and water density, it can also be used to estimate the heat flux through the section. The specific heat of seawater c_p (Joules/kg - °C) is defined to be the heat in Joules required to raise the temperature of 1 kg of seawater by 1°C at a constant pressure. The specific heat (c_p) increases with temperature and decreases with salinity. A detailed procedure for calculating $c_p(S,\theta)$ can be found in UNESCO (1983) and Millero *et al.* (1973).

To compute the heat flux f_i in Joules/s, the following equation is used:

$$f_i = \overline{\rho_i(\eta,t)\, c_{pi}(\eta,t)\, \theta_i(\eta,t)\, U_i(\eta,t)} \cdot a_i(t) \qquad (6.5)$$

Computation of total fluxes

In a similar manner to summing the flow rates for m sub-sections, the total cross-section flux F_n at time t_n is

$$F_n = \sum_{i=1}^{m} f_i(t_n) \qquad (6.6)$$

The above computation of flux gives an instantaneous value over the cross-section, which in itself is of little use. Flux calculations need to be made over one or more tidal cycles to assist with an understanding of overall mass balance and material circulation. The average flux per tide cycle, called the net or residual flux, is obtained by integrating the instantaneous flux values over the tidal cycle, for all the sub-sections as well as the total cross-section. These computations are discussed in the next section.

Net or Residual Water Flow and Material Flux

Often when the water or material flux at a section or point is averaged or summed over the tidal cycle, taking into account the sign of the flow direction (+ = ebb; - = flood), the result will be a relatively small, but non-zero value (see Fig. 4.6). This is called the residual, tidally-averaged or net quantity. The circulation of water within an estuary is frequently characterised by strong tidal oscillations on which are superimposed residual water circulations. These can be generated by non-linear interactions between the bathymetry and the tidal flow, protruding headlands, density gradients, wind stress and freshwater run-off to the estuary (Uncles & Jordan 1979). Complex interactions between the tide, residual flow and material concentrations/gradients will also lead to variations in the residual fluxes for different materials during the same tide. For example, the presence of high concentrations of suspended sediment near the bed may occur in the bottom layers which have

a different net flow direction to the surface layers.

However the net (time-averaged) value is not as straight-forward as it may seem, particularly for net velocities at different levels in a vertical profile. The reason for the difficulty in deriving net velocity profiles is that in estuaries the water depth at each vertical changes appreciably over a tidal cycle (Kjerfve 1975). The methods outlined below are designed to overcome this difficulty using the interpolated values at the η depth levels. These methods apply only to the analysis of *full* tidal cycle gaugings.

Net water velocities and flows

The interpolated velocity values $U_i(\eta,t)$ at each non-dimensional depth level η for each time t, in a sub-section i are the basic data used in the following analysis.

The net velocity, denoted <U>, at each η level over a full tidal cycle of T hours is given by integrating $U_i(\eta,t)$ (preserving the sign of the flow direction):

$$\langle U_i(\eta)\rangle = \frac{1}{T}\int_0^T U_i(\eta,t)\,dt \qquad (6.7)$$

which for constant time increments n.Δt can be approximated by:

$$\langle U(\eta_j)\rangle = \frac{1}{N}\left\{\frac{1}{2}U(\eta_j,t_0) + \sum_{n=1}^{N-1} U(\eta_j,t_n) + \frac{1}{2}U(\eta_j,t_N)\right\} \qquad (6.8)$$

This is then repeated for each depth level j = 0, 1, 2 ... 10 and each vertical. The first and last velocities at t_0 and t_N (the start and end of the tide cycle) are weighted by a factor 0.5, as these end values are representative only of half the time increment between time-interpolated values

Equation 6.8 can be used to calculate the net or residual values of both velocity components, U_v, and V_v, normal and parallel to the cross-section, at each of the non-dimensional depth-levels. An example of the net velocity U_v component plotted against non-dimensional depth η is shown in Figure 6.1a.

The net *depth-averaged* velocity components for each sub-section i = 1, .., m can also be calculated in a similar way by:

$$\langle \bar{U}_i\rangle = \frac{1}{N}\left\{\frac{1}{2}\bar{U}_i(t_0) + \sum_{n=1}^{N-1} \bar{U}_i(t_n) + \frac{1}{2}\bar{U}_i(t_N)\right\} \qquad (6.9)$$

Other residual values usually computed for each sub-section i are the net discharge $\langle q_i\rangle$, net depth $\langle D_i\rangle$ and net area $\langle a_i\rangle$. These are obtained by substituting the relevant parameter in equation 6.9 in lieu of the depth-averaged velocity. As an example the distribution of the net depth-averaged velocity across the section for a neap tide gauging at Tairua is shown in Figure (6.1b).

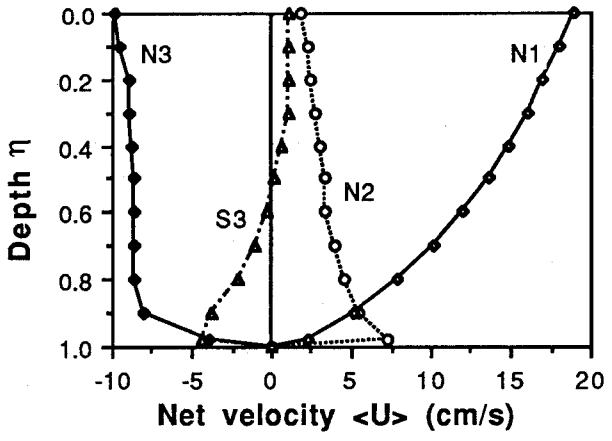

Figure 6.1a A selection of net velocity <U(η)> at various non-dimensional depths at four verticals (N1, N2, N3, S3) for a neap tide gauging at the inlet to Tairua Estuary.

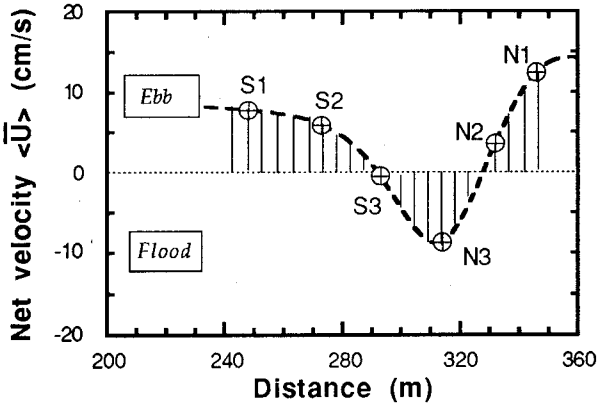

Figure 6.1b Lateral distribution of net depth-averaged velocity from a neap tide gauging at the inlet to Tairua Estuary.

This graph again (see also Figure 4.6) demonstrates the lateral variability in overall flows, with the channel sides being ebb-dominant, and the central portion flood-dominant in this case.

The *total* net cross-section discharge would again be given by a summation of the m sub-sections, such that

$$\langle Q\rangle = \sum_{i=1}^{m} \langle q_i\rangle \qquad (6.10)$$

This value can then be compared with the average freshwater run-off rate during the gauging.

Net material fluxes and concentrations

In a similar manner to the computations performed in the previous section, the net concentration of a material $<c_i(\eta)>$ over a tidal cycle of T hours at each non-dimensional depth η in sub-section i is given by:

$$<c_i(\eta)> = \frac{1}{T}\int_0^T c_i(\eta,t)\,dt \qquad (6.11)$$

This equation can be approximated using equation 6.8, substituting c for U, from the time-interpolated values of $c_i(\eta,t_n)$ at constant time intervals. Examples of net salinity $<S(\eta)>$ vertical profiles at three stations from a tidal gauging are shown in Figure 6.2. The surface layers, as expected, show less saline waters than those near the bed. In turn, these net salinity values at *each* depth level can be averaged over the vertical profile (using equation 5.2 with the net values in lieu of $U(\eta,t)$) to arrive at a depth-averaged net salinity. Net salinity values are useful for ascertaining the degree of mixing or stratification that is occurring in the estuary. These can be determined by using the circulation-stratification diagram in Hansen & Rattray (1966).

Similarly to equation 6.10, the net material flux $<f_i>$ in each sub-section i can be computed, then summed over all m sub-sections to derive the total net cross-sectional flux. For nutrients, where an appreciable difference occurs between the oceanic and river concentrations, there will be a relatively large total net flux towards the lower concentration zone. The total net salt flux should, on the other hand, indicate a small net loss or gain of salt for any one tidal cycle, provided river flows and meteorological conditions are reasonably steady.

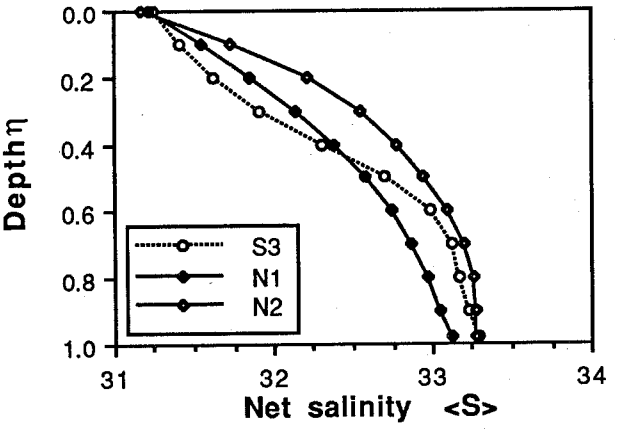

Figure 6.2 A selection of net salinity $<S(\eta)>$ at various non-dimensional depths at three verticals (N1, N2, S3) for a neap tide gauging at the inlet to Tairua Estuary.

Chapter 7

RESULT PRESENTATION AND DATA STORAGE

Tidal gaugings are expensive exercises that can generate a large amount of data. In our experience uses for the data are often found long after the gauging is done, and for purposes never envisaged at the time of the gauging. To optimise the use of the data, and facilitate data retrieval, it is important that the information be clearly presented and filed, soon after the job. Gauging cards (the raw data) should be checked for completeness, plans or computer plots summarising the data should be drawn and a table summarising key results compiled. Ideally all results should be filed in an in-house report.

Graphical Presentation of Data

Examples of the various ways of plotting data are illustrated in Appendix I with results from a gauging at Mangere Inlet, Auckland. These show:

(1) Locality plan and cross-section (Sheet 1) - Sketch of the locality and channel cross-section, noting important survey or water level datums (e.g., MHWS and chart datum), survey coordinates, positions of measurement stations (verticals), obstructions in the flow path (e.g., piers), left and right banks.
(2) Tide level (Sheet 2) - A water level versus time plot with datums. Note: asymmetry reflects shallow water effects or freshwater input.
(3) Cross-section area versus time (Sheet 2) - Useful for interpreting effects in very shallow situations and where the channel is an irregular shape (see Parerau River example in Chapter 4).
(4) Depth-averaged velocity versus time plots for the individual verticals (Sheets 3 & 4) - From these plots it is possible to tell at what point in the channel the greatest velocities occur, how the velocities vary throughout the tidal cycle, and how the ebb tide velocities compare with those of the flood tide. The plots are also useful for visually determining whether there is an ebb or flood tide dominance in any of the channels across the section, and when slack water occurred at various points in the cross-section.
(5) Isovel plots of velocity (Sheets 5 & 6) - These show a "snapshot" of the velocity distribution throughout the section at a particular point in time. They are useful for illustrating the main flow paths in the section at various stages of the tide.
(6) Stage versus velocity plots for the individual verticals (e.g., Fig. 2.3 and sheet 7) - These describe how the current velocity varies with tide level (stage). In particular, one can determine diurnal inequality between successive tides, at what level of tide the highest velocities occur, and whether or not slack water coincides with low tide. Comparing the areas under the flood and ebb tide curves gives an indication of the direction and magnitude of the net velocity.
(7) Cross-section mean velocity in section versus time plots (Sheet 8).
(8) Discharge versus time plot (Sheet 9) - This enables a direct comparison of flood and ebb tide flow characteristics, including the value of peak discharge, the time when it occurs, and the degree of asymmetry in the flood and ebb flows (important in flux determinations). Note that the total area under the flood tide, or ebb tide (less freshwater inflow), portion of the graph is the tidal prism (tidal volume).

Similar plots can be produced for other parameters such as temperature and salinity.

For estuarine flux studies, it's desirable to illustrate spatial variability in the cross-section by graphing isopleths of averaged or net quantities for the tidal cycle. However, unlike an instantaneous isopleth plot (e.g., Sheets 5 & 6), this is not a trivial matter where the tidal range is an appreciable fraction of the water depth at MTL, because the use of the mean cross-sectional area will not properly conserve net discharge and net material fluxes. Kjerfve & Seim (1984) present an area weighted technique for constructing isopleth plots of net velocity, material concentration, or flux.

Summary Table

In our experience a one page summary table of the key parameters determined by the gauging is always useful, particularly at a later date. This table can be prepared with a minimum of effort. It can include such things as date of gauging, the organisation that undertook the work, map reference of site, section bearing, freshwater inflow, drainage basin area, estuary area above gauging site, inlet throat depth and area, tide range, tide duration, mean maximum current velocity, mean velocity in section, peak discharge, and tidal prism. An example of such a table is given in Appendix I.

The In-house Report

An in-house report is a good way to file tidal gauging data permanently, and should be used in addition to storage on a computer system. The report can include information on gauging location, personnel involved, field methods and data analysis methods, surveying and sounding logs, photographs, and it can tabulate and graph the various parameters collected (e.g., raw cross-section and velocity data). Data may also be included on a floppy disc in a pocket in the report. The summary discussed above should be included. No attempt need be made to interpret the data, although it may be appropriate to make comments on features of the data relevant to their correct interpretation and use.

The value of the report is that the data are easy to file, reference and retrieve (and sell) at a later date.

NOTATION

Symbols and abbreviations used in this manual are defined in the following list:

a_i	area of a sub-section of the cross-section
A	cross-section area
A_{mtl}	cross-section area below mean tide level
c, C	concentration
C_k	log-spline fit constant
c_p	specific heat of seawater
d	contour bed level; segment depth between non-dimensional η levels
D	instantaneous total water depth
DRCM	direct reading current meter
e	exponential constant (= 2.71828)
E	estuary surface area (horizontal plane) at various tidal and bed levels
EDM	electronic distance measurement survey instrument
f_i	material flux through a sub-section
F	total material flux through cross-section
h	tidal stage level
H	tidal constituent amplitude or semi-range
HW	high water
k	Von Karman constant (= 0.4)
k_θ	constant for computing density anomaly σ
LW	low water
mb	millibar - measurement of atmospheric pressure
M	number of measurement sites across the section
M_2, M_4	lunar semi-diurnal and quarter-diurnal tidal constituents respectively
MHWN	mean high water neap tide level
MLWN	mean low water neap tide level
MHWS	mean high water spring tide level
MLWS	mean low water spring tide level
MSL	mean sea level on open coast
MTL	mean tide level
n	number of data points for correlation test
N	number of measurements in each vertical profile
N	number of time-interpolated values
p	inverse power exponent for velocity profile relationship (equation 5.2)
q_i	flow through sub-section
q_v	flow per unit width at a specific vertical
Q	flow through cross-section
Q_{max}	maximum flow through cross-section
Q_p	peak flow through cross-section
r	correlation coefficient
R	tidal range between successive HW and LW
R_e	tidal exchange ratio
R_s	mean spring tidal range
RCM	recording current meter
S	salinity, cross-section
S_2	solar semi-diurnal tide constituent
t	time
T	tidal cycle period (approx. 12.4 hours)
T_0, T_1	successive slack water times
u	velocity
u_*	shear velocity
$\overline{U}$, $\overline{u}$	vertically-averaged velocity
U	interpolated velocity at η levels
U_{mean}	mean tidal speed (irrespective of direction)

U_v	velocity component perpendicular to cross section
V	measured velocity values
V_v	velocity component parallel to the cross section
x	horizontal distance along the cross-section
y	vertical depth from water surface
z	vertical distance up from the bed
z_0	bed roughness height
η	non-dimensional depth in vertical profile (= y/D)
θ	temperature
μ	micro- (10^{-6})
π	pi (= 3.14159)
ρ	water density (kg/m^3)
σ	water density anomaly = (ρ - 1000)
σ_0	freshwater density anomaly
ϕ	angular phase lag
ω	angular speed = ($2\pi/T$)
Δb	horizontal distance between successive measurement sites
ΔF	area between contours on an isovel plot
Δt	constant increment of time for time-interpolation
Ω	tidal prism volume (m^3)
Ω_{ebb}	ebb tidal prism (total outflowing volume)
Ω_{flood}	flood tidal prism (total inflowing volume)
Ω_s	spring tidal prism
< >	net or residual quantity averaged over a tidal cycle
–	vertically- or depth-averaged quantity

REFERENCES

Anderson, P. W. 1977: Bibliography of scientific studies of the Wairau lagoons and surrounding coastal region, South Island, New Zealand. *New Zealand Oceanographic Institute miscellaneous publication 81.* 16 p.

Agnew, R. 1966: Storm tides in the Tasman Sea. *New Zealand journal of geology and geophysics 9:* 239-242.

Bardsley, E. 1976: The natural history of Kaipara Harbour: a bibliography. *New Zealand Oceanographic Institute miscellaneous publication 79.* 54 p.

Bell, R. G. 1982: Contour map digitizing package. Water Quality Centre report 82/16. DSIR, Hamilton. 10 p.

Bell, R. G.; Burton, J. H. 1986: A system of computer programs for the analysis of tidal gauging data (TIGA). Water Quality Centre report 86/20. DSIR, Hamilton. 24 p.

Bell, R. G.; Oldman, J. W.; Hume, T. M. 1988: A handbook on the use of moored current meters in coastal waters. *Water and soil miscellaneous publication 117.* Ministry of Works and Development, Wellington. 64 p.

Bohman, L. R.; Carswell, W. J. 1986: A preliminary evaluation of a discharge computation technique that uses a small number of velocity observations. In: *Selected papers in the hydrologic sciences 1986.* US Geological Survey water-supply paper 2290: 145-154.

Boon, J. D. 1975: Tidal discharge asymmetry in a salt marsh drainage system. *Limnology and oceanography 20:* 71-80.

Bowden, K. F. 1963: The mixing processes in a tidal estuary. *International journal of air and water pollution 7:* 343-356.

Christensen, B. A. 1990: Discussion of "General two-point method for determining velocity in open channel" by J. F. Walker. *Journal of hydraulic research, ASCE, 116:* 295-297.

Christensen, B. A.; Walker, H. E. 1969: Rapid discharge measurement in tidal inlets. In: *Proceedings of civil engineering in the oceans - II,* Miami Beach, Florida, ASCE, pp 743-761.

DVWK 1990: *Manual for water level gauging and discharge measurements.* DVWK Guidelines for water management 301. German Association for Water resources and Land Improvement (DVWK). Verlag Paul Parey, Hamburg. 258 p.

Day, J. H. 1981: The nature, origin and classification of estuaries. In: Day, J.H. (ed). *Estuarine ecology: with particular reference to South Africa.* A. A. Balkema, Rotterdam, pp. 1-6.

Druery, B. M.; Dyson, A. R.; Greentree, G. S. 1983: *Fundamentals of tidal propagation in estuaries.* In: Proceedings of 6th Australasian Conference on Coastal and Ocean Engineering, Gold Coast. Institution of Engineers, Australia, pp. 187-193.

Dyer, K. R. 1970: Current velocity profiles in a tidal channel. *Geophysical journal of the Royal Astronomical Society 22:* 153-61.

Dyer, K. R. 1973: *Estuaries - A physical introduction.* John Wiley & Sons, London. 140 p.

Dyer, K. R. (ed.) 1979: *Estuarine hydrography and sedimentation.* Cambridge University Press, Cambridge. 230 p.

Estcourt, I. N. 1976: Bibliography of scientific studies of New Zealand mainland estuaries, inlets, lagoons, harbours and fiords. *New Zealand Oceanographic Institute miscellaneous publication 75.* 40 p.

Fischer, H. B.; List, E. J.; Koh, R. C. Y.; Imberger, J.; Brooks, N. H. 1979: *Mixing in inland and coastal waters.* Academic Press, New York. 483 p.

Forrester, W. D. 1983: *Canadian tidal manual.* Department of Fisheries and Oceans, Canadian Hydrographic Service, Ottawa. 138 p.

Freestone, H. J. 1978: A short summary of tidal gauging results and techniques in Bay of Plenty surveys between 1966 and 1978. Hydrology Centre report, Ministry of Works and Development, Hamilton. 22 p.

Fulford, J. M.; Sauer, V. B. 1986: *Comparison of velocity interpolation methods for computing open-channel discharge.* In: Selected papers in the hydrologic sciences 1986. US Geological Survey water-supply paper 2290: 139-144.

Glen, N. C. 1979: Tidal measurement. In: Dyer, K.R. (ed.) *Estuarine hydrography and sedimentation.* Cambridge University Press, Cambridge, pp 19-40.

Godin, G. 1972: *The analysis of tides.* Liverpool University Press, Liverpool. 264 p.

Hansen, D. V.; Rattray, M. Jr. 1966: New dimensions in estuary classification. *Limnology and oceanography 11:* 319-326.

Heath, R. A. 1977: Phase distribution of tidal constituents around New Zealand. *New Zealand journal of marine and freshwater research 11:* 383-392.

Heath, R. A. 1979: Significance of storm surges in the New Zealand coast. *New Zealand journal of geology and geophysics 22:* 259-256.

Heath, R. A. 1981: Tidal asymmetry on the New Zealand coast and its implications for the net transport of sediment. *New Zealand journal of geology and geophysics 24:* 361-372.

Heath, R. A. 1985: A review of the physical oceanography of the seas around New Zealand - 1982. *New Zealand journal of marine and freshwater research 19:* 79-124.

Hipólito, J. N.; Loureiro, J. M. 1988: Analysis of some velocity-area methods for calculating open channel flow. *Hydrological sciences - Journal 33:* 311-320.

Hulsing, H.; Smith, W.; Cobb, E. D. 1966: Velocity-head coefficients in open channels. US Geological Survey water-supply paper 1869-C. 7 p.

Hume, T. M. 1979a: Tidal observations in Tamaki inlet, Waitemata Harbour. Water and Soil Division report, Ministry of Works and Development, Auckland. 20 p.

Hume, T. M. 1979b: Factors contributing to coastal erosion on the east coast of Northland during July 1978. Water and Soil Division report, Ministry of Works and Development, Auckland. 25 p.

Hume, T. M. 1979c: Aspects of the hydrology of the Mangere Inlet - Wairopa Channel area, northeastern Manukau Harbour. Water and Soil Division report, Ministry of Works and Development, Auckland. 62 p.

Hume, T. M. 1984: Bibliography of hydrological and sedimentological studies in the Manukau and Waitemata Harbours, Auckland. *Water and soil miscellaneous publication 71.* Ministry of Works and Development, Wellington. 56 p.

Hume, T. M. 1991: Empirical stability relationships for estuarine waterways and equations for stable channel design. *Journal of coastal research 7:* 1097-1112.

Hume, T. M.; Harris, T. F. W. 1981: Bibliography of oceanography and sedimentology for the Northland-Auckland coast. *Water and soil miscellaneous publication 28.* Ministry of Works and Development, Wellington. 63 p.

Hume, T. M.; Williams, B. L. 1981: Aspects of hydrology of the Wairau Estuary. Water Quality Centre report 81/16. DSIR, Hamilton. 46 p.

Hume, T. M.; Herdendorf, C. E.; Burton, J. H. 1986a: Tidal gaugings at three Northland inlets : Whananaki, Ngunguru, Pataua. Water Quality Centre report. 86/12.

Hume, T. M.; Herdendorf, C. E.; Burton, J. H. 1986b: Tidal gaugings at three Auckland inlets : Mangawhai, Whangateau, Puhoi. Water Quality Centre report 86/13.

Hume, T. M.; Herdendorf, C. E., Burton, J. H.; Bell, R.G. 1986c: Tidal gaugings at three Coromandel inlets: Whangapoua, Tairua, Whangamata. Water Quality Centre report 86/10.

Hume, T. M.; Herdendorf, C. E. 1987: Tidal inlet stability : proceedings of workshop. *Water and soil miscellaneous publication 108.* Ministry of Works and Development, Wellington. 80 p.

Hume, T. M.; Herdendorf, C. E. 1988: A geomorphic classification of estuaries and its application to coastal resource management - A New Zealand example. *Journal of ocean and shoreline management 11:* 249-274.

Hume, T. M.; Roper, D. S.; Cooke, J.; Langham, N.; Burke, E. 1990: Environmental impact statement: motorway realignment through Ahuriri Estuary, Napier. Water Quality Centre consultancy report 8069. DSIR, Hamilton. 120 p.

Hume, T. M.; Bell, R. G.; de Lange, W. P.; Healy, T. R.; Hicks, D. M.; Kirk, R. M. 1992: Coastal oceanography and sedimentology in New Zealand, 1967-1991. *New Zealand journal of marine and freshwater research 26:* 1-36.

Hume, T. M.; Herdendorf, C. E. 1992: Factors controlling tidal inlet characteristics on low drift coasts. *Journal of coastal research 8:* 355-375.

Hutchison, G. E. 1975: *A treatise on limnology.* Vol. 1. John Wiley and Sons, N.Y. 166 p.

Hydrographic Department Admiralty 1975: *Datums for hydrographic surveys.* Admiralty handbook no. 2. N.P. 122(2). Hydrographic Department Admiralty, Taunton, Somerset. 38 p.

Jarrett, J. T. 1976: Tidal prism-inlet area relationships. GITI report No. 3, U.S. Army Corps of Engineers, Waterways Experiment Station, Vicksburg, Mississippi. 54 p.

Johnston, R. M. S. 1980: Interim physical data report on the Upper Waitemata Harbour estuary. Water Quality Centre report 80/6. DSIR, Hamilton. 192 p.

Kingston Reynolds Thom & Allardice 1986: Maketu Estuary. Stage I Report. report to Bay of Plenty Catchment Commission. 128 p.

Kjerfve, B. 1975: Velocity averaging in estuaries characterised by a large tidal range to depth ratio. *Estuarine and coastal marine science 3:* 311-323.

Kjerfve, B. 1979: Measurement and analysis of water current, temperature, salinity and density. In: Dyer, K.R. (ed.) *Estuarine hydrography and sedimentation.* Cambridge University Press, Cambridge, pp. 186-226.

Kjerfve, B. (ed.) 1988: *Hydrodynamics of estuaries.* 2 volumes. CRC Press, Florida. 163 p. and 125 p.

Kjerfve, B.; Proehl, J. A. 1979: Velocity variability in a cross-section of a well-mixed estuary. *Journal of marine research 37:* 409-418.

Kjerfve, B.; Seim, H. E. 1984: Construction of net isopleth plots in cross-sections of tidal estuaries. *Journal of marine research 42:* 503-508.

Kjerfve, B.; Stevenson, L. H.; Proehl, J. A.; Chrzanowski, T. H.; Kitchens, W. M. 1981: Estimation of material fluxes in an estuarine cross-section: A critical analysis of spatial measurement density and errors. *Limnology and oceanography 26:* 325-335.

Maling, D. H. 1989: *Measurements from maps - principles and methods of cartometry.* Pergamon Press, Oxford. 577 p.

McCave, I. N. 1979: Suspended sediment. In: Dyer, K.R. (ed.) *Estuarine hydrography and sedimentation.* Cambridge University Press, Cambridge, pp. 131-185.

McDowell, D. M.; O'Connor, B. A. 1977: *Hydraulic behaviour of estuaries.* Macmillan Press Ltd., London. 292 p.

McLay, C. L. 1976: An inventory of the status and origin of NZ estuarine systems. *Proceedings of the New Zealand Ecological Society 23:* 8-26.

McLachlan, M. J. 1981: Report of ebb tide gauging of the Matakohe estuary at the Matakohe and Parerau rivers , Upper Kaipara Harbour. Water and Soil Division report, Ministry of Works and Development, Auckland. 16 p.

Mehta, A. J. ; Byrne, R. J. ; DeAlteris, J. T. 1976: Measurement of bed friction in tidal inlets. In: Proceedings 15th Conference on Coastal and Ocean Engineering, Honolulu, Hawaii. ASCE, pp. 261-268.

Mehta, A. J. ; Hayter, E. J. ; Christensen, B. A. 1977: A generalised point-velocity method for discharge computations in tidal waterways. In: *Hydraulics in the coastal zone*, Proceedings of 25th annual Hydraulics Division Specialty Conference, Texas. ASCE. pp. 1701-1720.

Millero, F. J.; Perron, G.; Desnoyers, J. E. 1973: The heat capacity of seawater solutions from 5 to 35°C and 0.5 to 22 °/oo chlorinity. *Journal of geophysical research 78:* 4499-4507.

Morris, A. W. (ed.) 1983: *Practical procedures for estuarine studies.* Institute for Marine Environmental Research, Natural Environment Research Council, Plymouth. 262 p.

NZ Nautical Almanac (published annually): Government Printing Office , Wellington.

O'Brien, M. P. 1931: Estuary tidal prisms related to entrance area. *Civil engineering 1:* 738-739.

O'Brien, M. P. 1969: Equilibrium flow areas of tidal inlets on sandy coasts. *Proceedings ASCE Journal, Waterways Harbours and Coastal Engineering Division 95 (WW1):* 43-52.

Officer, C. B. 1976: *Physical oceanography of estuaries (and associated coastal waters).* John Wiley & Sons, New York. 465 p.

Pennington, R. H. 1970: *Introductory computer methods and numerical analysis.* 2nd ed. Collier-Macmillan Ltd, London. 497 p.

Pond, S. ; Pickard, G. L. 1983: *Introductory dynamical oceanography.* 2nd ed. Pergamon Press, Oxford. 329 p.

Pritchard, D. W. 1967: Observations of circulation in coastal plain estuaries. In: Lauff, G. H. (ed.) *Estuaries.* Publication 83, American Association for the Advancement of Science, Washington D.C., pp. 37-44.

Pugh, D. T. 1987: *Tides, surges and mean sea-level.* John Wiley & Sons, Chichester. 472 p.

Rantz, S. E. et al. 1982: *Measurement and computation of streamflow:* Vol. 1 - Measurement of stage and discharge. US Geological Survey water-supply paper 2175. 284 p.

RD Instruments 1989: Acoustic Doppler current profilers. Principles of operation: a practical primer. RD Instruments, San Diego. 36 p.

Rodgers, M.W.; Thompson, S.M. 1991: TIDEDA reference manual. Publication No. 24, Hydrology Centre, National Institute of Water & Atmospheric Research, Christchurch

Shih, H.H.; Baer, L. 1991: Some errors in tide measurement caused by dynamic environment. In: Parker, B.B. (ed.) *Tidal hydrodynamics.* John Wiley & Sons Inc., New York, pp. 641-671.

Simpson, M. R.; Oltman, R. N. 1990: An acoustic Doppler discharge-measurement system. In: Proceedings of 1990 National Conference of Hydraulic Engineering, Volume 2. ASCE, New York, pp 903-908.

Smith, N. P. 1985: The decomposition and simulation of the longitudinal circulation in a coastal lagoon. *Estuarine, coastal and shelf science 21:* 623-632.

Thompson, R. M. C. 1981: A bibliography of the major ports and harbours of New Zealand. *New Zealand Oceanographic Institute miscellaneous publication 93.* 60 p.

Uncles, R. J.; Jordan, M. B. 1979: Residual fluxes of water and salt at two stations in the Severn estuary. *Estuarine coastal and marine science 9:* 287-302.

UNESCO 1983: Algorithms for computation of fundamental properties of seawater. UNESCO technical papers in marine science 44. 52 p.

van de Ree, W.; Stuip, J. 1984a: Measurement of stage. In: *The closure of tidal basins.* Delft University Press, Delft, The Netherlands, pp. 137-145.

van de Ree, W.; Stuip, J. 1984b: Measurement of current. In: *The closure of tidal basins.* Delft University Press, Delft, The Netherlands. pp. 155-167.

Walker, J. F. 1988: General two-point method for determining velocity in open channel. *Journal of hydraulic engineering 114:* 801-805.

Weisberg, R. H. 1976: A note on estuarine mean flow estimation. *Journal of marine research 34:* 387-394.

Young, K. B. 1950: A comparative study of mean-section and mid-section methods for computation of discharge measurements. US Geological Survey open-file report. 52 p. Cited in Rantz *et al.* (1982).

Appendix I

MANGERE INLET GAUGING DATA
&
TIDAL GAUGING SUMMARY SHEET

Location	**Mangere Inlet at Old Mangere Bridge**
Map reference	R11/695727
Organisation	Water & Soil Division, Ministry of Works and Development, Auckland
Date	5 June 1978

Catchment Characteristics			
Land area	3446 ha		
Estuary area above site	660 ha		
Tide range (mean spring/neap)	3.42 to 1.98 m		
Water way characteristics (at MTL)			
Width	234 m		
Max. depth	8.6 m		
Area	1469 m^2		
Gauging data			
Freshwater inflow (average)	0.47 m^3/s		
Tide state	Neap (flood and ebb)		
	Flood	Ebb	
Tide range	2.18	2.05	m
Tide duration	6.50	6.00	hr
Max. at point velocity	0.53	0.63	m/s
Max. depth-averaged velocity for any vertical	0.47	0.49	m/s
Max. velocity averaged over cross-section	0.35	0.36	m/s
Max. discharge	536	560	m^3/s
Tidal prism (volume)	6,656,000	6,382,000	m^3

Notes:
1. Other parameters determined - salinity and temperature.
2. Method - from bridge, crane and Gurley meters.
3. Measurement density - 32 verticals; 0.1, 0.4, 0.6, 0.9 at points.
4. Purpose of work - power station cooling water intake design.

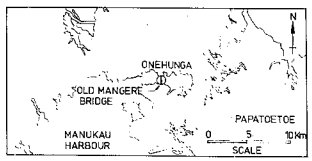

LOCALITY PLAN

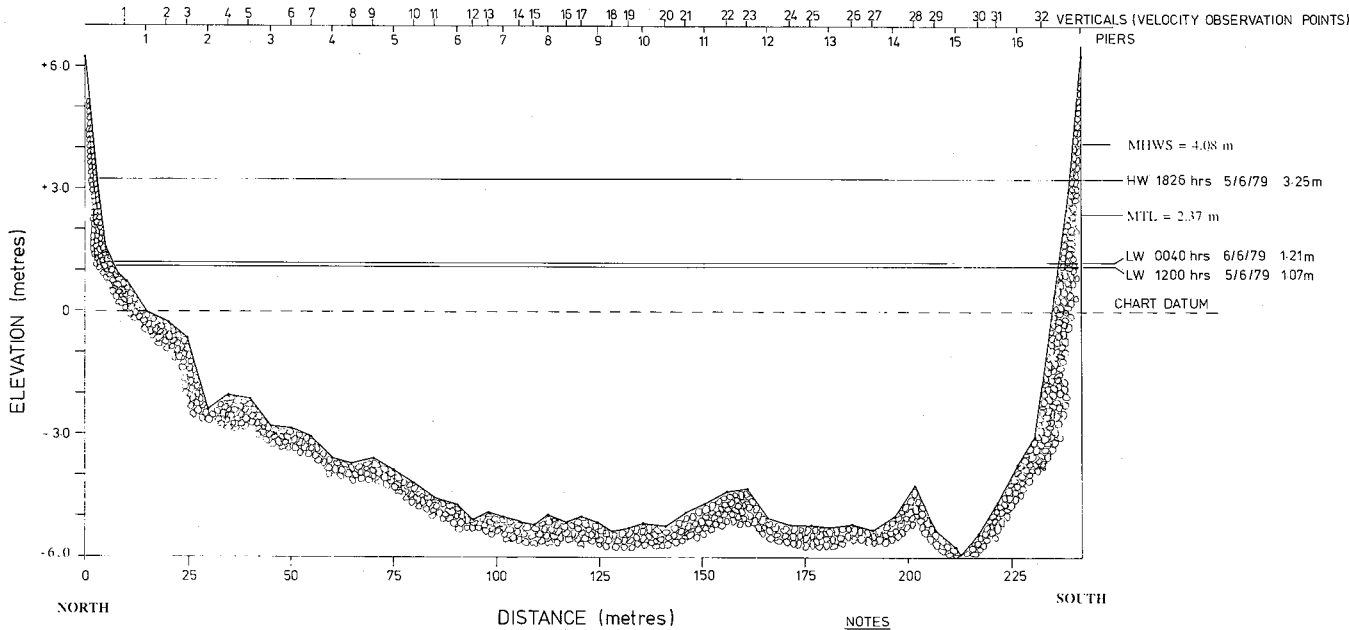

NOTES

1. ELEVATIONS IN TERMS OF AHB DATUM. (0 = zero on Onehunga tide gauge)
2. DEPTH MEASUREMENTS MADE BY TAKING LINE SOUNDINGS FROM BRIDGE ON 5.6.79.
3. DISTANCE 0 = CENTRE OF PILE CAP AT NORTHERN END OF OLD MANGERE BRIDGE.

AMENDMENTS	BY	APPD.	DATE

	BY	CHECKED	DATE
DRAWN	S.Thompson		10/79

A. W. GIBSON, DIRECTOR OF WATER & SOIL
APPROVED:

Ministry of Works and Development
CIVIL ENGINEERING AUCKLAND
WATER AND SOIL
N.C. McLEOD Commissioner

AUCKLAND COMBINED CYCLE POWER STATIONS
TIDAL GAUGING - NEAP TIDE
MANGERE INLET AT OLD MANGERE BRIDGE
LOCALITY PLAN AND CROSS SECTION

ORIGINAL SCALES

Sheet 1 of 9

FILE

JOB	CODE	SHEET	REVISION

Whole numbers = mm
Decimalised expressions = m
unless indicated otherwise

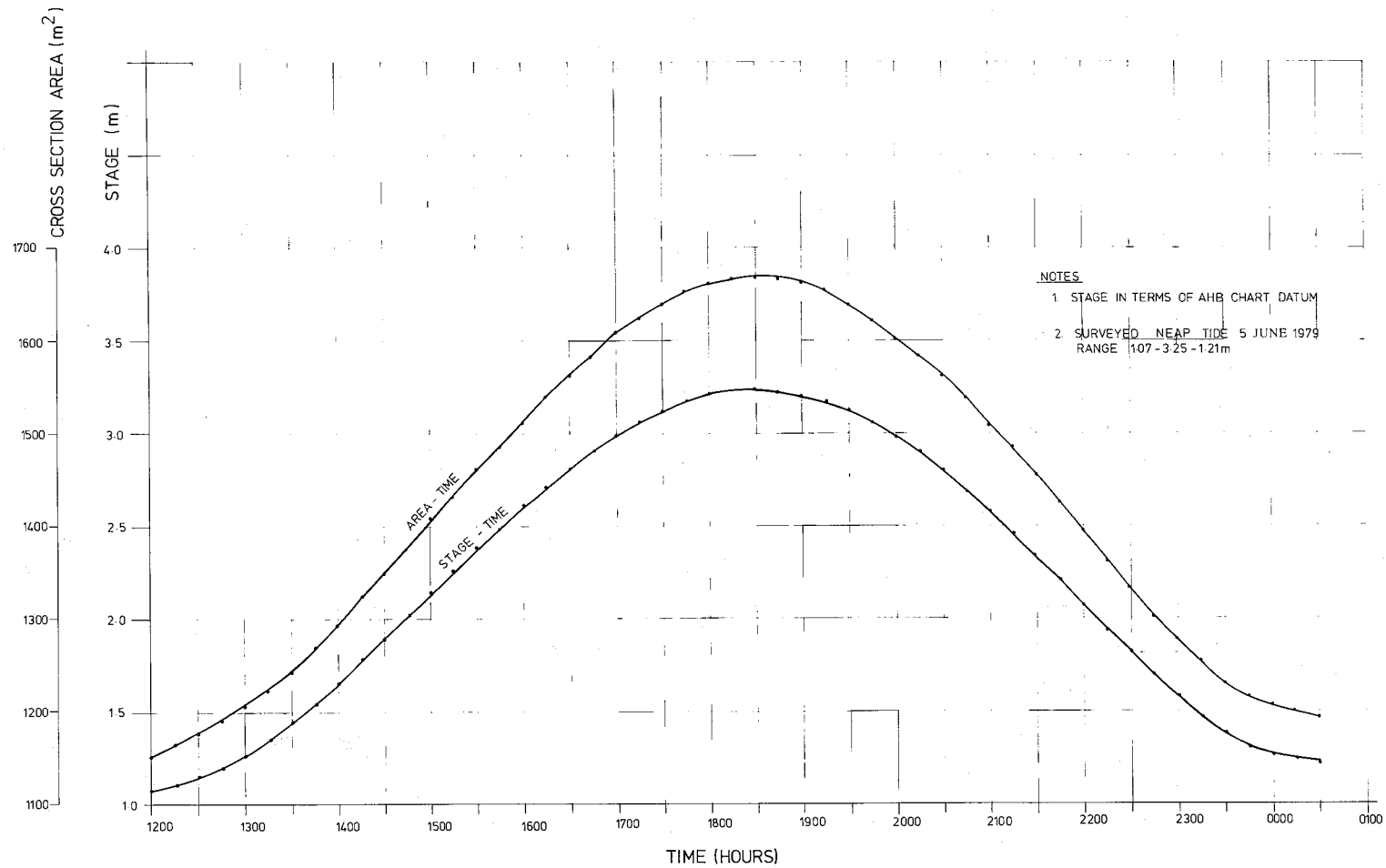

AMENDMENTS	BY	APPD.	DATE

	BY	CHECKED	DATE
DRAWN	S.Thompson		10/79

A. W. GIBSON
DIRECTOR OF
WATER & SOIL

APPROVED:

Ministry of Works and Development
CIVIL ENGINEERING
AUCKLAND
WATER AND SOIL
N.C. McLEOD Commissioner

AUCKLAND COMBINED CYCLE POWER STATIONS
TIDAL GAUGING

MANGERE INLET AT OLD MANGERE BRIDGE
STAGE, AREA VERSUS TIME PLOTS

ORIGINAL SCALES

FILE

Sheet 2 of 9

JOB | CODE | SHEET | REVISION

Whole numbers = mm
Decimalised expressions = m
unless indicated otherwise

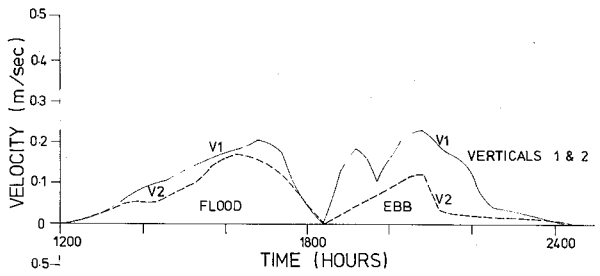

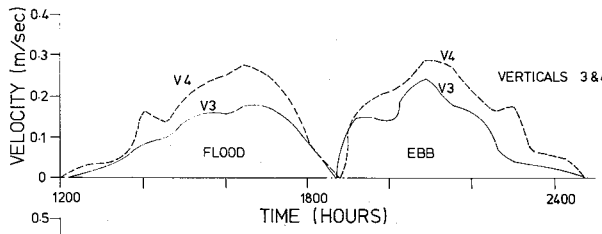

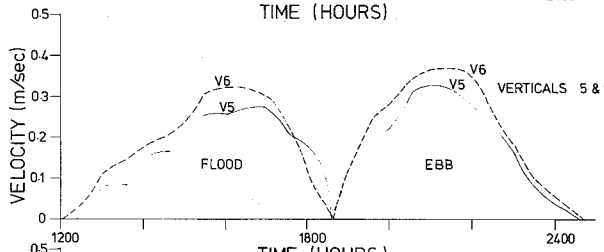

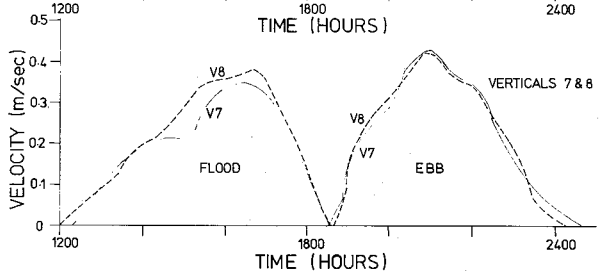

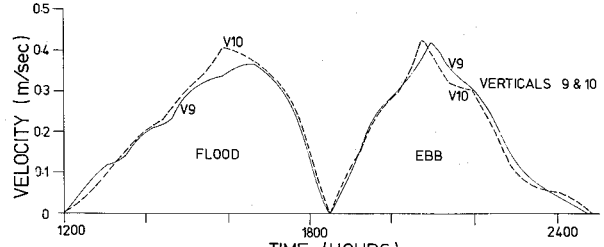

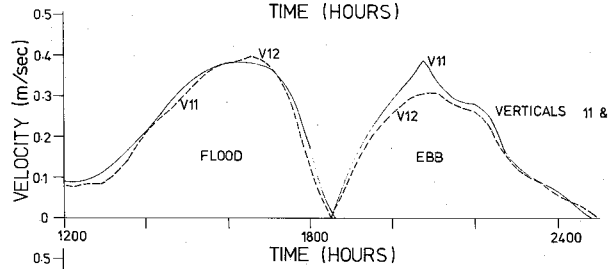

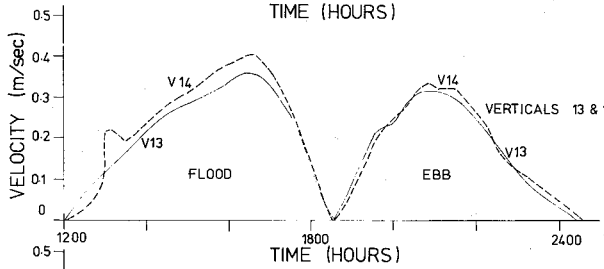

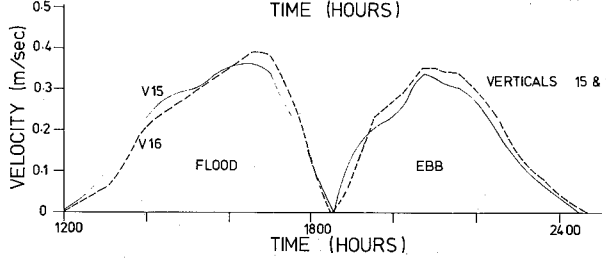

SURVEYED NEAP TIDE
5 JUNE 1979

	BY	CHECKED	DATE
DRAWN	J. Thompson		11/79

A. W. GIBSON
DIRECTOR OF
WATER & SOIL

APPROVED:

Ministry of Works and Development
CIVIL ENGINEERING
AUCKLAND
WATER AND SOIL
N.C. McLEOD Commissioner

AUCKLAND COMBINED CYCLE POWER STATIONS
NORTH EASTERN MANUKAU HARBOUR

MANGERE INLET AT OLD MANGERE BRIDGE
MEAN VELOCITY VERSUS TIME PLOTS

ORIGINAL SCALES
FILE
Sheet 3 of 9
JOB | CODE | SHEET | REVISION

AMENDMENTS	BY	APPD.	DATE

Whole numbers ± mm
Decimalised expressions ± m
unless indicated otherwise

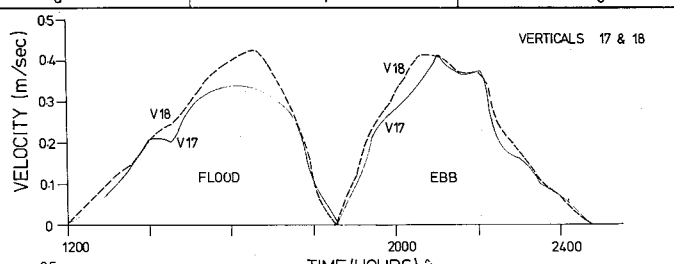

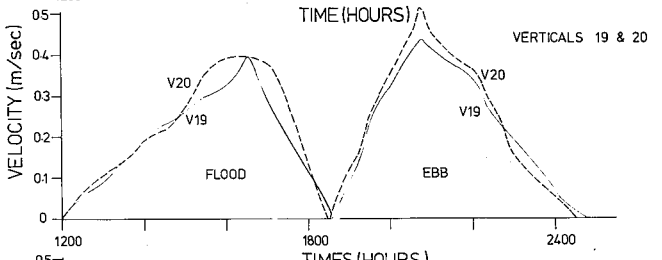

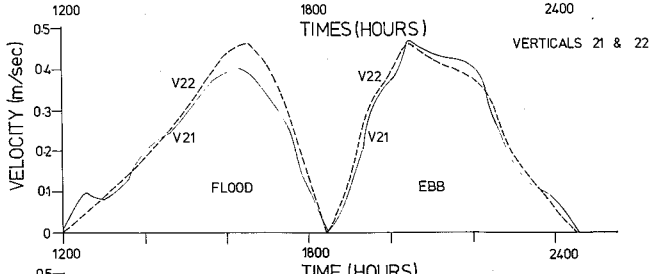

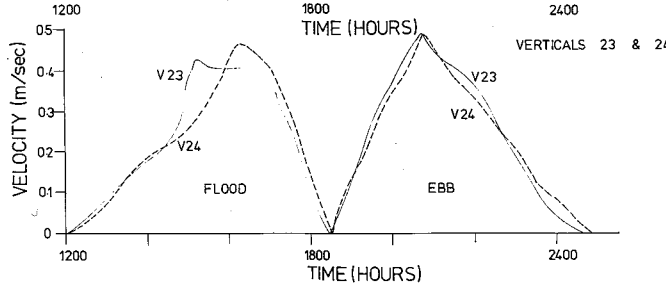

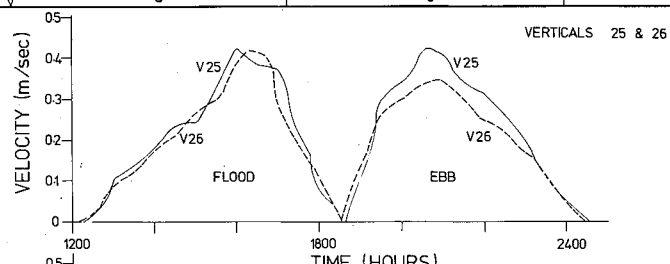

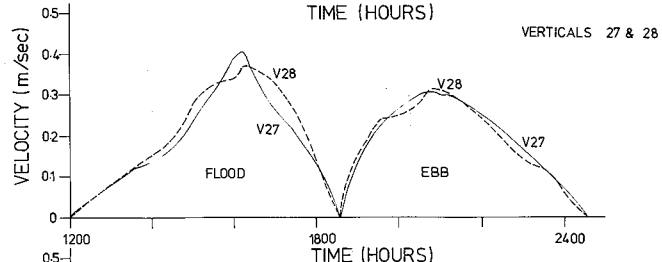

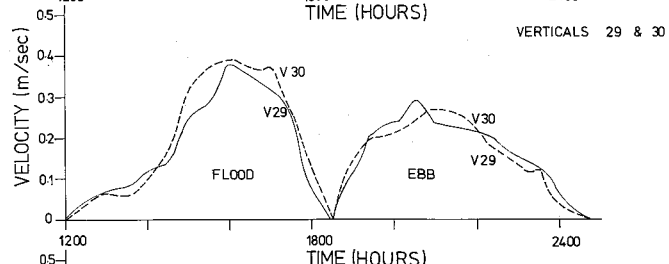

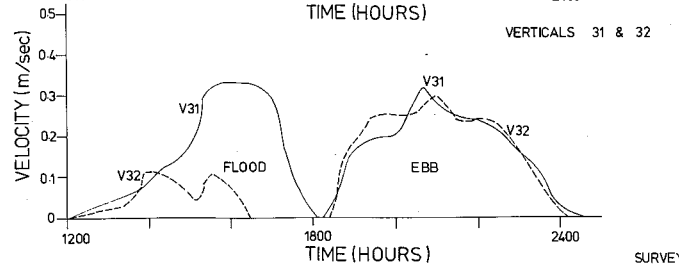

SURVEYED NEAP TIDE
5 June 1979.

	BY	CHECKED	DATE
DRAWN	S.Thompson		11/79

AMENDMENTS | BY | APPD. | DATE

A. W. GIBSON
DIRECTOR OF
WATER & SOIL

APPROVED:

Ministry of Works and Development
CIVIL ENGINEERING
AUCKLAND
WATER AND SOIL
N.C. McLEOD Commissioner

AUCKLAND COMBINED CYCLE POWER STATIONS
NORTH EASTERN MANUKAU HARBOUR

MANGERE INLET AT OLD MANGERE BRIDGE
MEAN VELOCITY VERSUS TIME PLOTS

ORIGINAL SCALES | FILE

Sheet 4 of 9

JOB | CODE | SHEET | REVISION

Whole numbers = mm
Decimalised expressions = m
unless indicated otherwise

LOCAL OR TRACING No

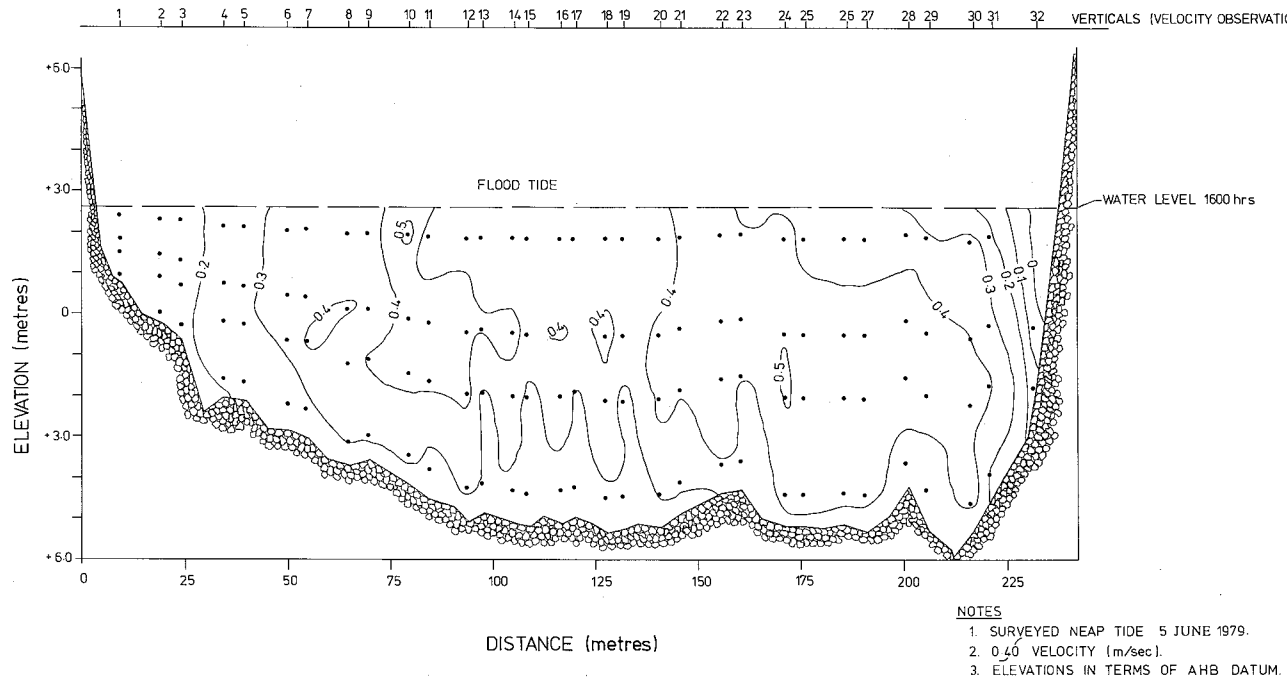

NOTES

1. SURVEYED NEAP TIDE 5 JUNE 1979.
2. 0.40 VELOCITY (m/sec).
3. ELEVATIONS IN TERMS OF AHB DATUM.
4. DISTANCE 0 = CENTRE OF PILE CAP AT NORTHERN END OF OLD MANGERE BRIDGE.

	BY	CHECKED	DATE
DRAWN	S.Thompson		10/79

A. W. GIBSON
DIRECTOR OF WATER & SOIL
APPROVED:

Ministry of Works and Development
CIVIL ENGINEERING AUCKLAND
WATER AND SOIL
N.C McLEOD Commissioner

AUCKLAND COMBINED CYCLE POWER STATIONS
TIDAL GAUGING

MANGERE INLET AT OLD MANGERE BRIDGE
VELOCITY DISTRIBUTION IN SECTION AT 1600 hours

ORIGINAL SCALES | FILE

Sheet 5 of 9

JOB | CODE | SHEET | REVISION

AMENDMENTS | BY | APPD | DATE

LOCAL OR TRACING No

ORIGINAL SIZE A1

482-A1

Whole numbers = mm
Decimalised expressions = m

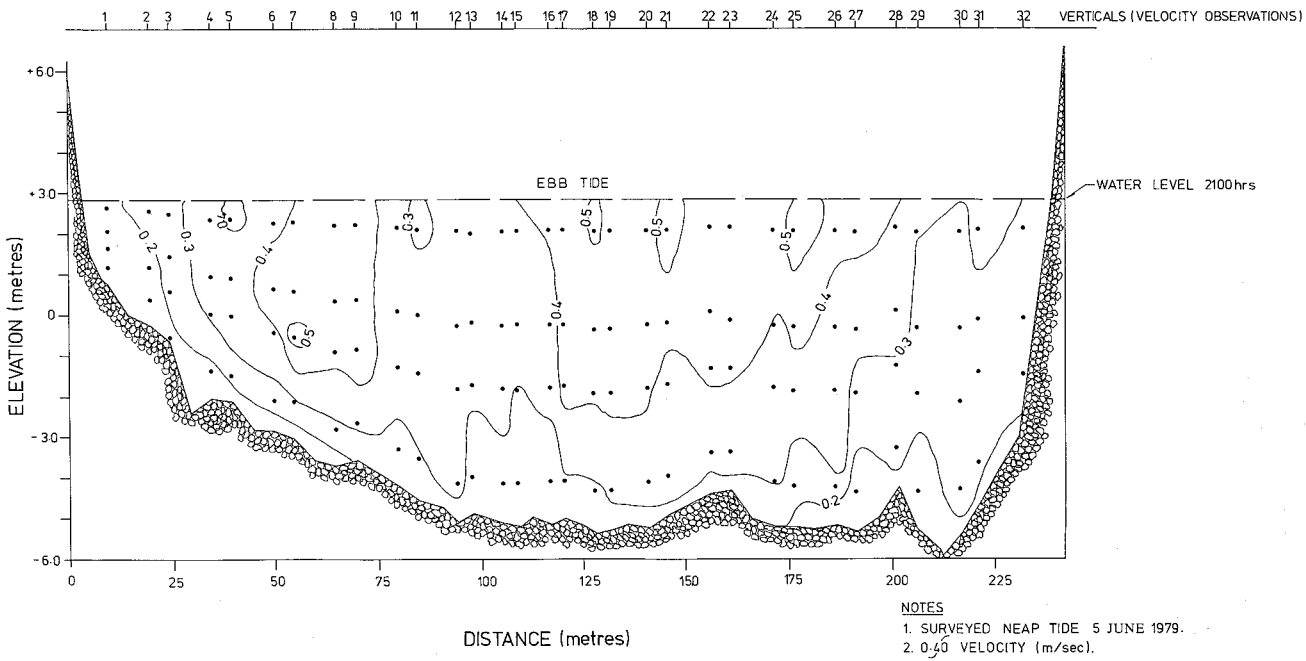

NOTES

1. SURVEYED NEAP TIDE 5 JUNE 1979.
2. 0.40 VELOCITY (m/sec).
3. ELEVATIONS IN TERMS OF AHB DATUM.
4. DISTANCE 0 = CENTRE OF PILE CAP AT NORTHERN END OF OLD MANGERE BRIDGE.

AMENDMENTS	BY	APPD.	DATE	DRAWN S.Thompson	CHECKED	DATE 10/79	A. W. GIBSON DIRECTOR OF WATER & SOIL
							APPROVED:

Ministry of Works and Development
CIVIL ENGINEERING AUCKLAND
WATER AND SOIL
N.C. McLEOD Commissioner

AUCKLAND COMBINED CYCLE POWER STATIONS
TIDAL GAUGING
MANGERE INLET AT OLD MANGERE BRIDGE
VELOCITY DISTRIBUTION IN SECTION AT 2100 hours

ORIGINAL SCALES
Sheet 6 of 9
FILE
JOB | CODE | SHEET | REVISION

LOCAL ON TRACING No

Whole numbers = mm
Decimalised expressions = m
unless indicated otherwise

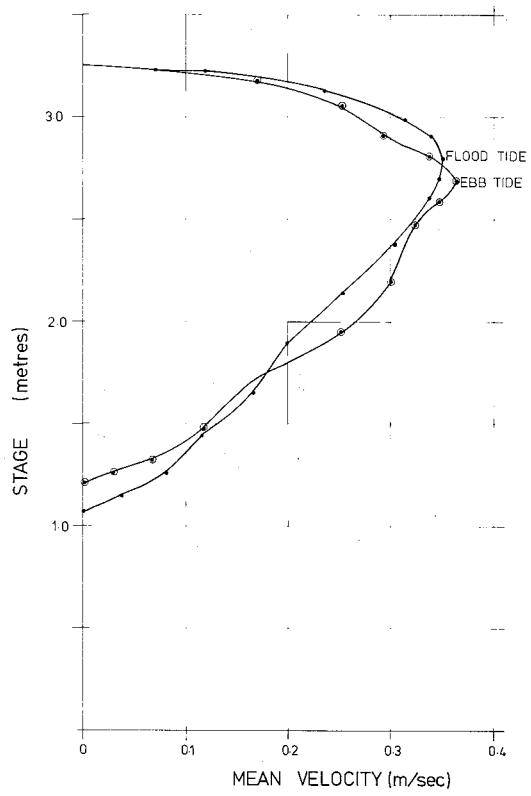

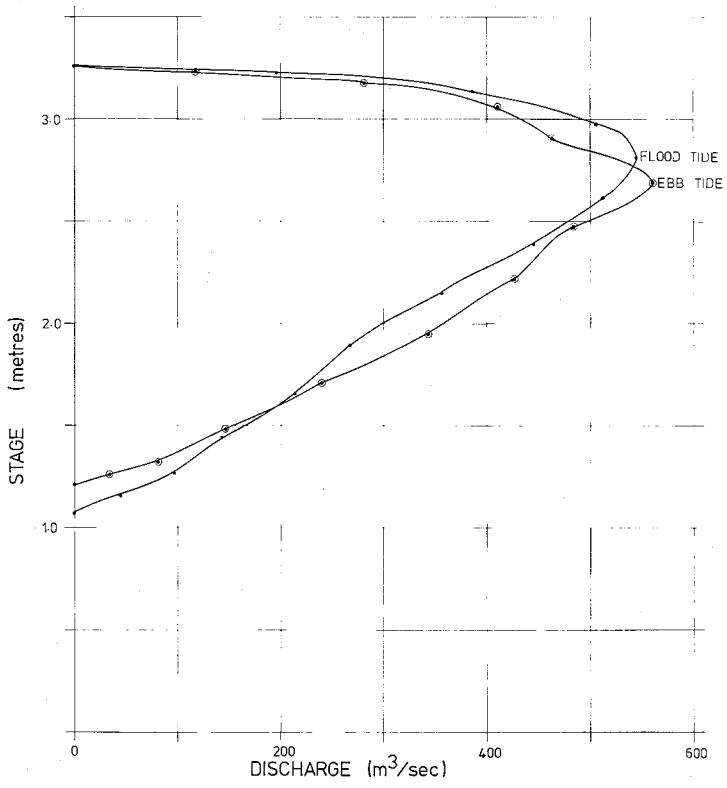

SURVEYED NEAP TIDE 5-6-79

AMENDMENTS	BY	APPD	DATE
LOCAL OFFICE TRACING No			

	BY	CHECKED	DATE
DRAWN	S.Thompson		11/79

APPROVED

Ministry of Works and Development
CIVIL ENGINEERING
AUCKLAND
WATER & SOIL
N.C McLEOD Commissioner

AUCKLAND COMBINED CYCLE POWER STATIONS
NORTH EASTERN MANUKAU HARBOUR

MANGERE INLET AT OLD MANGERE BRIDGE
STAGE VERSUS MEAN VELOCITY PLOTS

ORIGINAL SCALES	FILE
Sheet 7 of 9	
JOB / CODE / SHEET / REVISION	

Whole numbers = mm
Decimalised expressions = m
unless indicated otherwise

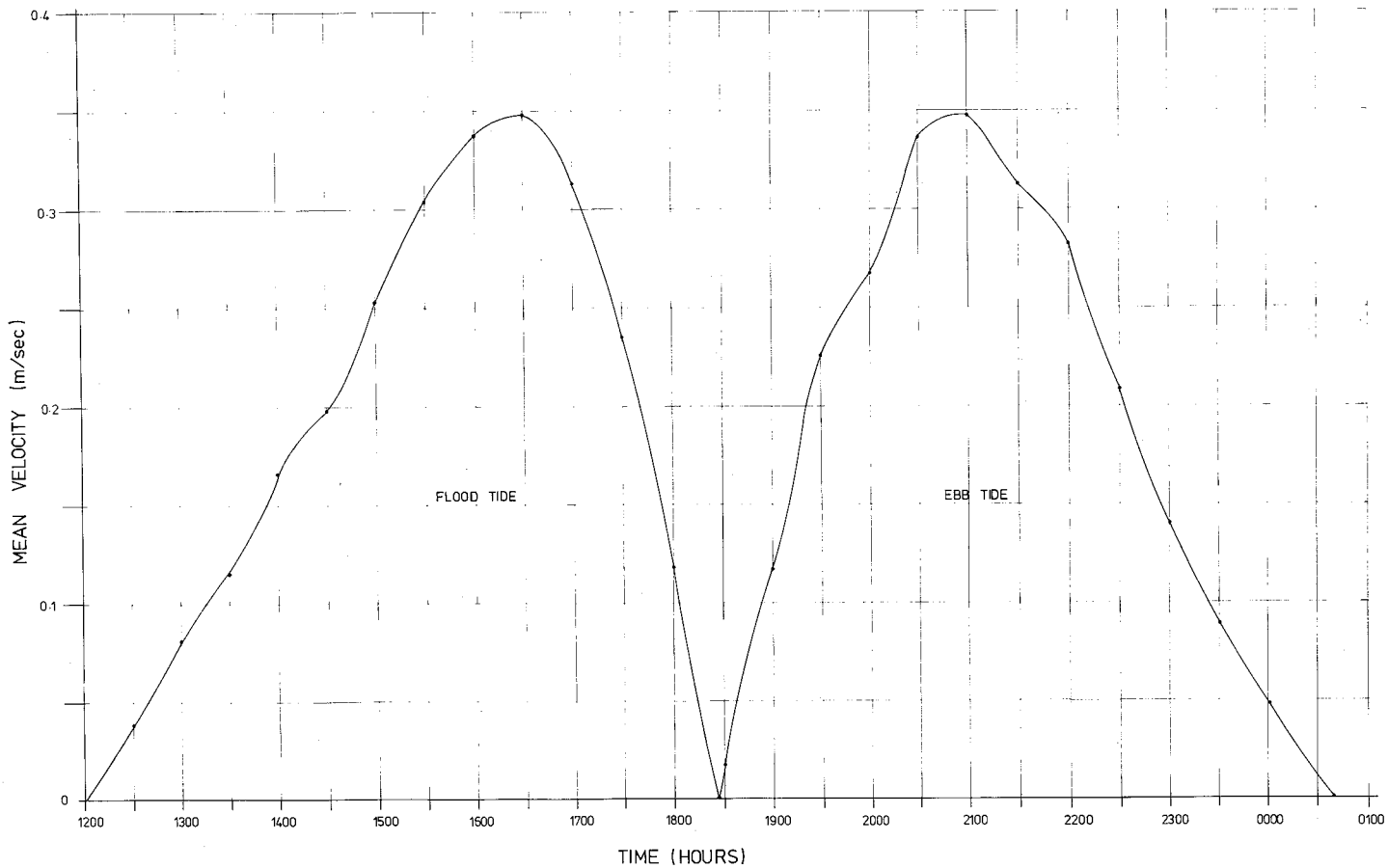

SURVEYED NEAP TIDE 5.6.79

	BY	CHECKED	DATE
DRAWN	S.J.Thompson		9/79

AMENDMENTS | BY | APPD. | DATE

A. W. GIBSON
DIRECTOR OF
WATER & SOIL

APPROVED:

Ministry of Works and Development
CIVIL ENGINEERING
AUCKLAND
WATER AND SOIL
N.C. McLEOD Commissioner

AUCKLAND COMBINED CYCLE POWER STATIONS
TIDAL GAUGING

MANGERE INLET AT OLD MANGERE BRIDGE
MEAN VELOCITY VERSUS TIME PLOT

ORIGINAL SCALES | FILE
Sheet 8 of 9
JOB | CODE | SHEET | REVISION

Whole numbers = mm
Decimalised expressions = m
unless indicated otherwise

LOCAL OH TRACING No

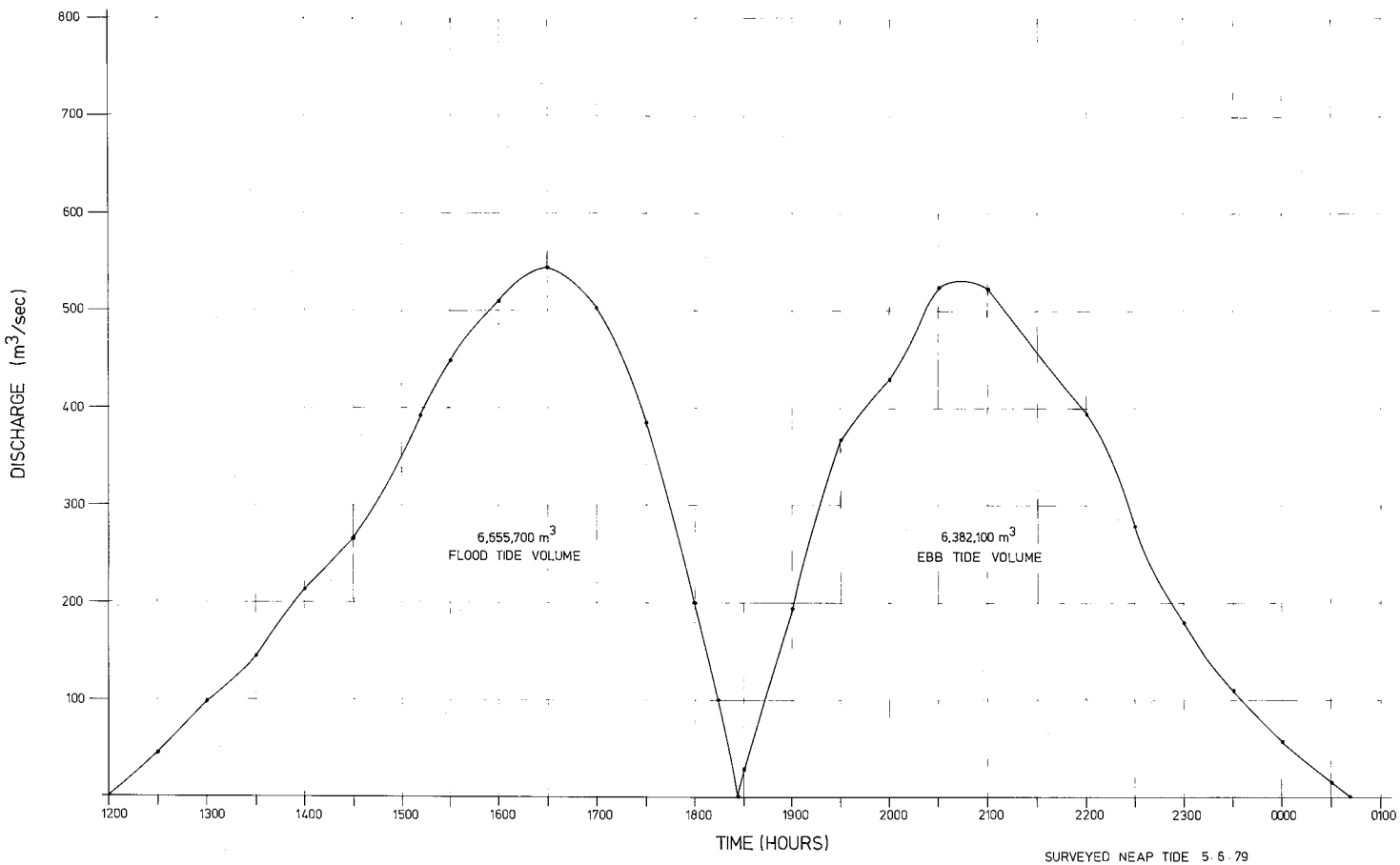

SURVEYED NEAP TIDE 5.6.79

	BY	CHECKED	DATE
DRAWN	S.Thompson		9/79

A. W. GIBSON
DIRECTOR OF
WATER & SOIL

APPROVED:

Ministry of Works and Development
CIVIL ENGINEERING
AUCKLAND
WATER AND SOIL
N.C. McLEOD Commissioner

AUCKLAND COMBINED CYCLE POWER STATIONS
TIDAL GAUGING - NEAP TIDE

MANGERE INLET AT OLD MANGERE BRIDGE
DISCHARGE VERSUS TIME PLOT

ORIGINAL SCALES

Sheet 9 of 9

FILE

JOB | CODE | SHEET | REVISION

AMENDMENTS	BY	APPD.	DATE

LOCAL OR TRACING No

Whole numbers = mm
Decimalised expressions = m
unless indicated otherwise

Appendix II

FORM FOR RECORDING TIDAL GAUGING FIELD MEASUREMENTS

NIWAR - Tidal Gauging No. : **Page** **of**

Site:

Observers:

Date:

Meter:

Time: DST or NZST

Rating table no.:

Vert. no.	Obs. depth (m)	Method of obs.	Depth of obs. (m)	Time of meas. (hrs)	Revs	Count time (secs)	Velocity at point (m/s)	Current direction (degrees)	Comments

Appendix III

A LOGARITHMIC PIECE-WISE FITTING PROCEDURE FOR FITTING VELOCITY PROFILES BETWEEN MEASURED DATA POINTS

For a sequence of N *actual* velocity measurements, denoted V_k (k=1, N), at various increasing dimensionless depths *below the water surface*, η_k (k= 1, N) where $\eta_k < \eta_{k+1}$, the coefficient C_k characterising the constant slope of each logarithmic spline between adjacent data points is:

$$C_k = \frac{V(\eta_k) - V(\eta_{k+1})}{\log_e [\,(1-\eta_k) / (1-\eta_{k+1})\,]} \qquad \text{(III.1)}$$

The coefficient C_k will be positive if $V(\eta_{k+1}) < V(\eta_k)$ i.e., where velocities decrease towards the bed as normally occurs. To derive *interpolated* values of velocities at constant depth increments, $U(\eta_j)$; j = 0, 10, where $\eta_k < \eta_j \leq \eta_{k+1}$, the piece-wise logarithmic spline yields:

$$U(\eta_j) = V(\eta_k) - C_k \log_e \left\{ \frac{1-\eta_k}{1-\eta_j} \right\} \qquad \text{(III.2)}$$

Similarly, equation III.2 can be modified to yield *extrapolated* velocity values up to the water surface (η = 0.0), when $\eta_j < \eta_{k=1}$, to give:

$$U(\eta_j) = V(\eta_{k=1}) - C_1 \log_e \left\{ \frac{1-\eta_{k=1}}{1-\eta_j} \right\} \qquad \text{(III.3)}$$

Two options can be used for extrapolating beyond the deepest velocity measurement to the bed. The last logarithmic spline, characterised by C_{N-1}, can be extrapolated, (using equation III.2), to the bottom, set in this case at η_j = 0.975, rather than at the bed (as in Fig. 5.1), to yield a more representative velocity for the bottom half-segment. However if the slope is too large (such that $C_{N-1} > V_N$) then for total water depths D(t) of less than 1 metre, the extrapolated slope can be amended to yield a bottom layer velocity, centred at η_j = 0.975 of:

$$U(\eta_{j=10}) = K \cdot \frac{\eta_{k=N}}{0.975} \cdot V(\eta_{k=N}) \qquad \text{(III.4)}$$

where K = 0.8, which is derived from velocity coefficients for the near-bottom layers of the standard vertical velocity curve of Hulsing *et al.* (1966). For total water depths of D(t) ≥ 1 metre, equation 5.3 is applied to the boundary layer below the deepest measured velocity. For the last extrapolated velocity at $\eta_{j=10}$, equation 5.3 is integrated over the interval z = z_0 to z = 0.05D(t), resulting in a local *mean* velocity in the near-bed depth segment.

Published in 1993 by:
Water Quality Centre, Ecosystems Division, National Institute of Water and Atmospheric Research - NIWAR
PO Box 11-115, Hamilton, New Zealand.